BIO-INSPIRED APPROACH TO EARLY-STAGE STRUCTURAL FORM FINDING

IVAN AVDIĆ

MSc Architecture, Urbanism and Building sciences | Building Technology

BIO-INSPIRED APPROACH TO EARLY STAGE STRUCTURAL FORM FINDING

Ivan Avdić | 4749472

Master Thesis Committee:

dr. ir. Pirouz Nourian | Architectural Engineering + Technology, Design Informatics

dr. ir. Matthijs Langelaar | Faculty 3mE, Precision and Microsystems Engineering (PME)

Master's Thesis
P4 report | 09.2019

Delft University of Technology

Faculty of Architecture and the Built Environment

Foreword

In the context where the building industry is transitioning towards a more sustainable future, the way we design and build our structures becomes a burning question. Thus, graduation from the Building Technology track gives an opportunity to research and exercise novel approaches to such challenges. I would like to contribute to this discourse of sustainable building and construction by drawing inspiration from the way such functional challenges have been solved by nature.

I embarked on the journey of doing this research wishing to learn from nature about the way we, as humans, can design things better. At the center of this notion was the belief that, having the advantage of 3.8 billion years to test what works and what doesn't, nature was able to develop solutions for many of the challenges we are trying to solve today. Hence, I strongly believe that biomimicry is the way forward, and that there is much more to discover than to invent.

As an architect, I have continuously been amazed and baffled by how nature produces structures whose forms are seemingly perfectly tailored to the functions they perform. Why aren't all leaves and all the trees the same shape and size? Why do some animals have claws, some paws, some talons and some hooves? And how can such a tiny ant carry 20 times his own weight? I knew the answer to better design was hiding there.

However, a true wakeup call came only after reading Janine Benyus's seminal book Biomimicry, Innovation Inspired by Nature, and the profound understanding of just how lifechanging of an endeavor taking nature as a design teacher can be.

I hope this research, and the work presented withing it, will inspire and encourage anyone who has set out to design something to stop and look around. Maybe the solution has been there all along, right under their feet.

01. RESEARCH FRAMEWORK

"In all that time [3.8 bilion years since the first bacteria], life has learned to fly, circumnavigate the globe, live in the depths of the ocean and atop the highest peaks, craft miracle materials, light up the night, lasso the sun's energy, and build a self-reflective brain. Collectively, organisms have managed to turn rock and sea into life-friendly home, with steady temperatures and smoothly percolating cycles. In short, living things have done everything we want to do, without guzzling fossil fuel, polluting the planet, or mortgaging their future. What better modoels could there be". (Benyus, 2009, p.3)

1.1 Introduction

The following section of the report provides an overview of the research. It illustrates its framework, the motivation behind it, and the methods used in relation to the formulated problem and research questions derived from it. The section also delineates the boundaries of the research focusing it primarily on the topics of architectural design, computational design and structural mechanics.

1.2 Background and Necessity

A snapshot of the world's population, provided every year by the United Nations, shows that there is currently 7.5 billion people living on Earth. Slighly more than half (55%) live in highly urbanised areas, and that percentage is projected to rise to 70% by the year 2050 (UN, 2017). The built environment is replacing the former 'natural' environment as our 'normal' surrounding.

In such state of affairs designing our built environment to accommodate this expansion is of paramount importance. How can we mitigate the negative consequences of such growth to our environment as a whole? The impact of the building industry (and architecture with it) has thus far been manifold, the most pressing of which are the irreversible destruction of biodiversity, overexploitation of raw materials, extensive use of unsustainable energy, production of waste, and the emission of harmful substances into soil, water and air.

Having realized the repercussions, the building industry is making a transition to a 'more sustainable future'. But what does that entail and how do we make sure that the decisions we make today will ensure a successful transition? Will the incremental improvements in technology be enough or is there a necessity for a paradigm shift in the way we think, design and construct our environment.

Taking inspiration from Buckminster Fuller's mission statement "To make the world work for a hundred percent of humanity, in the shortest possible time, through spontaneous cooperation, without ecological offense and disadvantage of anyone" (Fuller, 1969), Michael Pawlyn (2016) suggests three cornerstones of a succesful leap to a more sustainable future of our cities:

- achieving radical increases in resource efficiency
- transitioning from a fossil-fuel driven to a solar driven economy
- transforming from a linear, wasteful way of using resources to a fully circular model in which nothing is considered "waste" but everything is a resource.

This research will mainly problematize the first objective, the basis of which will be elaborated throughout this research report.

1.3 Research Context and Scope

Context:

The work presented here is part of an academic research project, performed towards the purpose of attaining a graduate degree Master of Science, Architecture, Urbanism and Building Sciences (Building Technology Track). This thesis is mainly targeted towards fellow students and researchers working in the areas of computational architectural design, particularly those interested in bio-inspired approaches.

The reported research primarily dwells between the fields of Design Informatics and Structural Mechanics, and is thus essentially concerned with developing methods for establishing structurally sound designs. This contextualises the research on the building scale level, mainly focusing on it's functional aspects. However, the research also adresses the areas of architectural design, morphology, and aesthetics.

Scope:

The given scope of the project serves to outline the boundaries of this research and the expected deliverables at the end of it. The following statements outline the scope of this research and the anticipated results:

- Making a case (manifesto) for biomimetic design
- Creating a computational model that simulates the natural process of uniform stress distribution in bones and trees with a satisfactory accuracy.
- Developing a valid method for structural topology optimisation that successfuly solves the problem of reducing material usage for several TOY problems:
    - 2D & 3D simply supported beam with a point load;
    - 2D & 3D cantilever beam with a point load;
    - a 3D volume supported in it's corner points;
- Successfuly applying the method with the purpose of form finding the design of a double storey mono-material structure
- Creating a simple tool in the form of Grasshopper script to be freely used and further developed.

1.4 Problem Statement

The way we are erecting our buildings today has not changed much in the last 50 years. The process taken towards the design and construction of a skyscraper today is not so much different from the way the Seagram building was built. This is primarily due to the fact that design problems are inherently multidimensional and that we as humans are incapable of understanding and comprehending such spaces beyond three dimensions

What is meant by this is that a design of a building includes not only its physical manifestation in three dimensions but also a plethora of other aspects which need to be taken into consideration such as environmental aspects of the project (thermal comfort, acoustics, lighting...), social aspects (people's wellbeing withing the building, mobility, security, space perception...) and economic considerations (feasibility, construction sequence, choice of contractors, resource management etc.). All of these dimensions of a design can be seen as its 'degrees of freedom' which define a vast realm of possible final designs (Nagy 2017).

Since a single human designer can not think about such a multidimensional problem holistically, we tend to break it down into a series of smaller problems with the aim to limit the design space to a dimensionality which we can understand.

In practical terms this means that we end up looking at buildings in a reductionist manner as a sum of their parts: the structure, the envelope, the roof, the foundation the climate system etc. which we consider and design individually. Inherently, we educate architects that the structure of a building is merely something which serves the purpose of supporting its formal appearance, and something to be concealed. We are looking at Firmitas (durability), Utilitas (function), and Venustas (beauty)(Vitruvius & Morgan 1960) as three separate, competing architectural features.

The author argues the fact that nature knows no such divisions. In Frei Otto's words (1985) "Form and structure come into being by way of a common developmental process, depending on physical and chemical laws". Designs in nature represent holistic approaches to a an environmental response. Thus the final form is inherently the optimal structure (firmitas), performing the intended function (utilitas), and with inherent beauty (venustas).

The question arises: What if we as human designers were able to design structures in the same way nature does: by using only the materials and energy we need, and perfectly fitting form to function? Rather then designing a building, can we discover its design?

Contemplating over Michelangelo's words in which "Every block of stone has a statue inside it, and it is the task of the sculptor to discover it", one can't help but

give thought to the question: Does every volume of space have a perfectly befitting form, and it is the task of the architect to discover it?

Among various approachs, the method of Topology Optimization (TO) has emerged as valid approach to finding a more befitting form for various elements of the building. However the method is currently emplyed as an end stage solution to optimize certain elements of the design like beams, columns, slabs or walls.

With the proliferation of computational design tools, architects have been able to take more integrative design approaches, which allowed designers to transition towards the idea of form finding, in which the design's performance is consolidated not merely into an evaluative discourse but into its generative stage (Naboni & Paoletti, 2018).

Thus the general objective of this research is to investigate how a nature inspired approach to TO can be applied towards the morphogenesis of a building's structural design and be used as an early-stage design guidance. It is worthwile stressing the fact that the method of TO is considered not merely for its use in material optimization, but also with respect to its potential of creating novel architectural formal expressions. This research will thus advocate for a bio-inspired, performance driven approach to structural topology optimization of an architectural design.

This is to be done from an emerging standpoint that lays in the junction between biology, architecture, structural mechanics, and computation.

For the purposes of validating the proposed method, a model of

The objective is to study the organism's growth and behavior, and translate it into a digital model, which would later be used to "grow" a simple mono-material house. Even though a seeming disparity between these two concepts may seem evident, this research will try to illustrate how intertwined the notion of growing and building can be.

1.4.1 Research Problems

The following section adresses several sub problems, arising from previous problem statement.

Problem: In similar fashion that we have been designing buildings for the past half a century, we have also been designing the elements they are built with. From around 1800, engineers have been able to determine the sizes and shapes of structural elements - beams, columns, roofs, foundations - based on structural mechanics. That resulted in that we now have a variety of 'ideal', prescribed shapes for such structural elements, which reflect the structural mechanics used to determine them. The likes of such are arches in the form of catenaries or parabolas,

or truesses whose members only carry compressive or tensile forces, and which are precisely sized in their cross sections according to the forces they carry (Knippers et al. 2016).

Furthermore, in order to manufacture better performing structures, engineers often rely on the synthesis of new alloys, new ceramics, new plastics and composites made possible by extremely high temperatures, high pressures and strong chemical treatments. This “heat, beat and treat” method, as Benyus (2009) calls it, has become the modus operandi in the way we design everything.

Nature, on the other hand can not afford to follow this strategy. Imaginative by necessity, nature follows a different paradigm in which “material is expensive, but form is cheap” (Vincent, 1997, pp.36) and designs its structures through a slow process of iterative refinement i.e. evolution. Such an approach inevitably results in durable and resource efficient structures that are perfectly tailored to meet the challenges imposed on them by their surroundings.

Proposition: Advancements in high-speed computers and computational design tools (CAD) have allowed for the introduction of Structural optimisation as a method to achieve the best performance of a structure with the minimal amount of material that befits the unique external constraints such as loads and supports. This research advocates for the use of structural optimisation technology as a way of reaching the previously mentioned increase in resource efficiency, and decrease environemntal impact, while at the same time proposing novel formal and aesthetic possibilities.

Problem: Even though Structural Topology Optimisation proves to be a promising technology for better design of buildings and structures, it's practical applications have mostly been limited to the aerospace, automotive and medical industry, due to higher demands on weight saving (Baalen, 2017). Another possible reason for the lack of topologically optimised building structures may be due to the fact that such large scale structures have additional, non quantifiable requirements imposed on them other than structural soundness, such aesthetic appeal. Furthermore, TO structures tend to have a high degree of geometric complexity, leading to manufacturability difficulties, which may have hindered their application on larger scales. Additionally, current commercially available tools for topology optimization are predominantly focused on small scale applications, which alongside the requirements for numerical inputs might have detered their use by architects and designers.

Proposition: There is a space for proliferation of large scale topologically optimised structures. Several examples of TO structures made with isotropic material such as concrete give clues about the possibilities and limitations of such endeavors. Reflecting on the notion of geometric complexity of such proposals, new advancements in manufactoring technologies such as large scale additive

manufacturing, pave the way towards a future where complexity of designs is becoming less of a limiting factor.

1.4.2 Design Problems

As was previously noted, current commercially available software for topology optimization require special environments and 3rd party software, which are not integrated into the current commonly used tools and workflows of architects. This became one of the reasons which prompted the creation of a tool within the Rhino – Grasshopper environment, being a go-to program for not only architects but also designers from various industries.

In addition, one of the reasons for the lack of proliferation of topology optimization wihin the design process could be the high degree of mathematical complexity of TO aproaches, which may have detered architects from using them. Therefore, one of the design tasks of this research is the implementation of a heuristic method which would be intuitive and understandable for the designer.

Lastly, the most commonly used TO software (presented in a later chapter) seldom produce a discretized (vector) output and require additional post processing to be prepared for later manipulation or manufacturing. The intent with the tool proposed by this thesis is the creation of a vectorized result in all steps of the process which the designer can edit and customize.

1.5 Research Objectives

The main objective of this research is to propose a methodology for a nature-inspired Structural Topology Optimisation. The proposed method is aimed at contributing to material savings, sound structural performance and a different aesthetic of architecture. The ultimate aim is to manifest this method in the form of an intuitive, freely accesible tool, which would be integrated into the computational design workflow of architects. Towards achieving these goals, several sub-objectives are introduced:

- Creatinga design methodology which brings biological postulates of uniform stress distribution to the problem of Structural Topology Optimisation.

- Developing a valid method for structural topology optimisation that successfuly solves the problem of mass minimization for a 2D & 3D problems.

- Defining the most suitable type of architecture as a case study to perform the topology optimisation.

- Successfuly applying the method to a 3D design of a double story mono-material building.

-Evaluate the output of the topology optimised design with respect to it's structural requirements and compare it with a well established TO method.

- Determine the implications such an approach would have on the functional and aesthetic aspects of the building.

- Creating a simple tool in the form of a script for Grasshopper to be freely used and further developed.

- Assure that the designer has sufficient control over the tool to influence the output through intuitive control over the input parameters (the design space, design objectives, and constraints).

1.6 Research Question

How can an approach inspired by bone mineralization and tree growth be taken towards topologicaly optimizing the form of a building, while considering its spatial configuration?

Several research sub-questions arise from the main one:

- What characterizes a bio-inspired approach?

- Why would such an approach be more beneficial than conventional ones?

- What kind of architectural design problems is such a method applicable to?

-What are the implications of using topology optimization on functional and aesthetic aspects of the design

- Is a topologically optimised design inherently the best ?

- Where does such a method fit within the workflow of an architect or designer?

- How do bone mineralization and tree growth relate to topology optimization?

1.7 Limits and Constraints of the research

Limits:

The following statements portray the self-imposed limitations in the methods and tools used towards the achievement of the abovementioned objectives of the research. Accordingly, the following topics fall withing the scope of this research:

– Computer Aided Architectural Design

– Structural Topology Optimisation

– Structural Mechanics

– Finite Element Analysis (FEM)

In contrast, the following topics and terms are related to this research to a limited extent, and as such fall out of the scope of this work:

– Building Information Modelling (BIM)

– Bionics
– Non-conventional Computing
– Optimization of Architectural Layouts
– Graph Optimisation
– Multi-objective Topology Optimisation
- Schools of thought in Design Methodology

Constraints:

- The research does not aim to create with a faster algorithm for a standard TO problem but rather solving an architectural design problem with TO.

- The Structural Topology Optimisation will be performed within Rhino6 and Grasshopper software packages

- The material taken for all the TOY problems and the final problem is an idealized isotropic material with the same behavior in tension and compression

- The structural loads and safety factors for both the beam (TOY problem) and the house will be based on Eurocode standards.

- The loadcases to which these structures will be subjected to are simplifications of the actual loads, so as to avoid complex computational analysis.

- The part of the research which deals with the manufacturability of the designs falls outside the scope of this research and will be covered only on a theoretical basis.

1.8 Position within related research fields

This research relies on the successful intersection of various scientific disciplines. Aside from being an architectural design problem and thusby concerning the field of architecture, the topic requires the disciplines of structural mechanics and computer science to be integrated. In addition, limited venturing into the area of biology was necessary for the proper abstraction of the proposed method. Within these four major disciplines, the topics of biomimetic and computational design with numerical structural simulation become central. In specific, the thesis focuses on the integration structural computational design of buildings.

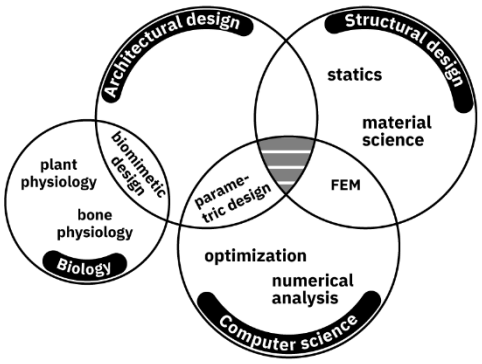

Figure 1. Position of this thesis withing related fields of research.

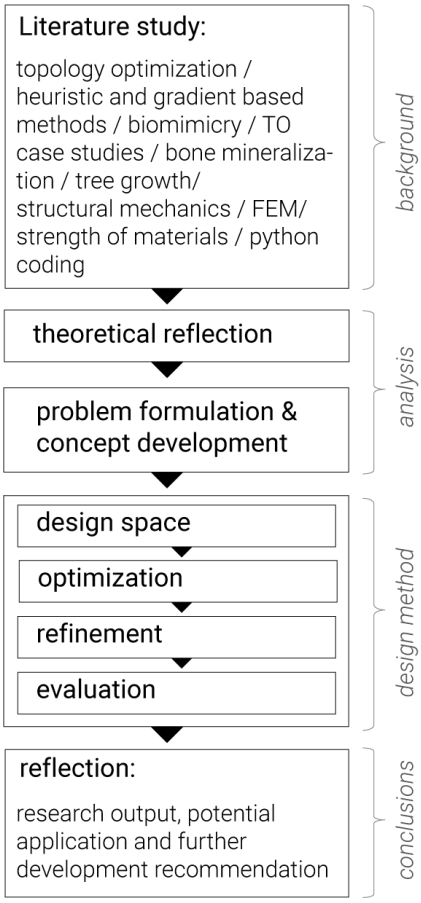

Figure 2. Research and design framework

1.9 Methodology

1.9.1 Research Design

The research design is based on four main steps taken towards a successful achievement of the designated research goals. A visual representation of the research can be observed in Figure 2.

Background:

This research is based on a literature study of mainly scientific background, but also on articles and publications from various commercial sources. Scientific databases such as Scopus, Google Scholar, Web of Science, Researchgate and the repository of TU Delft were searched for relevant information. The queries for doing so were formulated with key words derived from three major concepts (biomimicry, topology optimization, architecture) subdivided into research terms (synonyms for each concept). The search query that yielded the satisfactory number and quality of the results was: “biomimetic” OR “bio-inspired” AND “topology optimization” OR “optimization” AND “architecture” OR “design” OR “engineering”. The results were evaluated based on their relevance and reliability, considering the source, year of publication, information about the author, the audience and the purpose for which the information was written etc. Literature was organized using the reference management software Mendeley and subdivided according to topic and type of resource (books, research papers, reports…)

Analysis:

This study represents an exploratory research-by-design. As the topic of this thesis is the creation of an alternative, biomimetic approach to a common architectural design problem, it was first required to develop a set of theoretical underpinnings which will guide it. This is achieved mainly through literature study about how design occurs in nature, and how similar functional challenges of structural design have been solved by it, before continuing to devise a strategy about how to translate this knowledge into a valid design method.

As will be elaborated in detail in subsequent sections of this research report, one of the design rules which become apparent from all the sources is that succesful structural design in nature follows the axiom of uniform stress, as can be seen in examples of trees, bones, claws etc. This means that the stresses imposed on a certain element act uniformly over the surface, i.e. that the loads are fairly distributed (Mattheck, 1999). As a consequence, such designs are characterized by the lack of breaking points (locally excessive stresses) and material wastage (i.e. all parts of the design are loaded and utilized). This thesis thus advocates for a method which will result in uniform stress distribution within the final design.

In addition, among various approaches for achieving such designs, Topology Optimization (TO) has emerged as valid technique for the joint morphogenesis of form and structure. TO is concerned with finding an efficient structural layout and material distribution within a predetermined design space subject to loads and boundary conditions. Even though it has been mostly used in automotive and aerospace industry, recent years have seen the proliferation of these methods in the construction industry as well, albeit mostly for infrastructural design such as bridges. The literature review chapter of this report elaborates on the abundance of techniques for TO which testify about the popularity of this method. The aim of this research is to develop a novel, nature-inspired method and apply it to an architectural design problem.

The literature study additionally yielded the understanding of necessary mathematics and mechanics of topology optimization. The researched case studies showcase the successful implementation of these methods and hint towards ways in which Topology Optimization might be used on an architectural building scale, as well as the expected outcomes of the research.

Design method:

In order to apply a nature-inspired design to an architectural design problem, a direct formal copy of natural structures would seldom be suitable due to additional complex requirements imposed by an architectural design task. Therefore, the objective becomes creating a form-generating method, which would deliver designs of biological quality with respect to durability and resource efficiency. This research is concerned with creating one such method, inspired by the SKO and CAO methods proposed by prof. Claus Mattheck and which are elaborated in more detail in the following sub- section of the report. The method is implemented within the Rhino-Grasshopper working environment due to the familiarity and ubiquity of this software within the standard workflow of designers.

The initial phase concerns the formation of the design domain or design space within which the form-finding process will take place. At this stage the designer inputs all of the boundary conditions such as loads, supports, voids representing spaces and openings, as well as material properties. All of this data is assembled into a design space which is later passed to the optimization stage.

The optimization stage relies on the successful analysis via the Finite Element Method which delivers information about the occuring forces and stresses within the un-optimized design space. Based on this numerical data, the material of the design space is manipulated until only the necessary material remains while the underutilized material gets culled away.

Following the acquisition of a rough design, the proposal is further refined by removing notch stresses and smoothening the voxelized geometry. The result of this stage is a final design which can serve as a guidline to the designer about what the potential shape his design might take given the boundary conditions.

The final design is documented and measured against the results obtained by a commercially available software using a gradient-based SIMP approach. This

is done in order to estimate the performance and validity of the method as well its limitations, after which the study is concluded.

Conclusions:
The results of the proposed method are finally tested on the case study design of a multi story building. The case study is elaborated further to also address issues and limitations of the method, as well as places for future improvement.

1.9.2 Models and Tools

The biological model used to inspire the proposed method is the mineralization of bone tissue and shape optimzation found in trees, proposed by Mattheck (Mattheck, 1999), and is elaborated at length in the Literature part of this thesis.

The tools used in the process include computational design softwares Rhino and Grasshopper. Additional plugins Karamba 3D, Hoopsnake and Millipede are used for performing the FEM, looping the algorithm, and meshing respectfully. All necessary scripting is done in the GHPython and Cpython components using the Python programming language, with standard open-source SDK libraries rhinocommon.dll, grasshopper.dll, and rhinoscriptsintax.dll. For numerical manipulations numpy was used.

The SIMP method will be performed with a commercially available software Ansys as it simple to use and allows for models to be imported from Rhinoceros working environment. Additionally it is freely available for use by students of TUDelft.

Figure 3. Summary of the design method

1.9.3 Design method

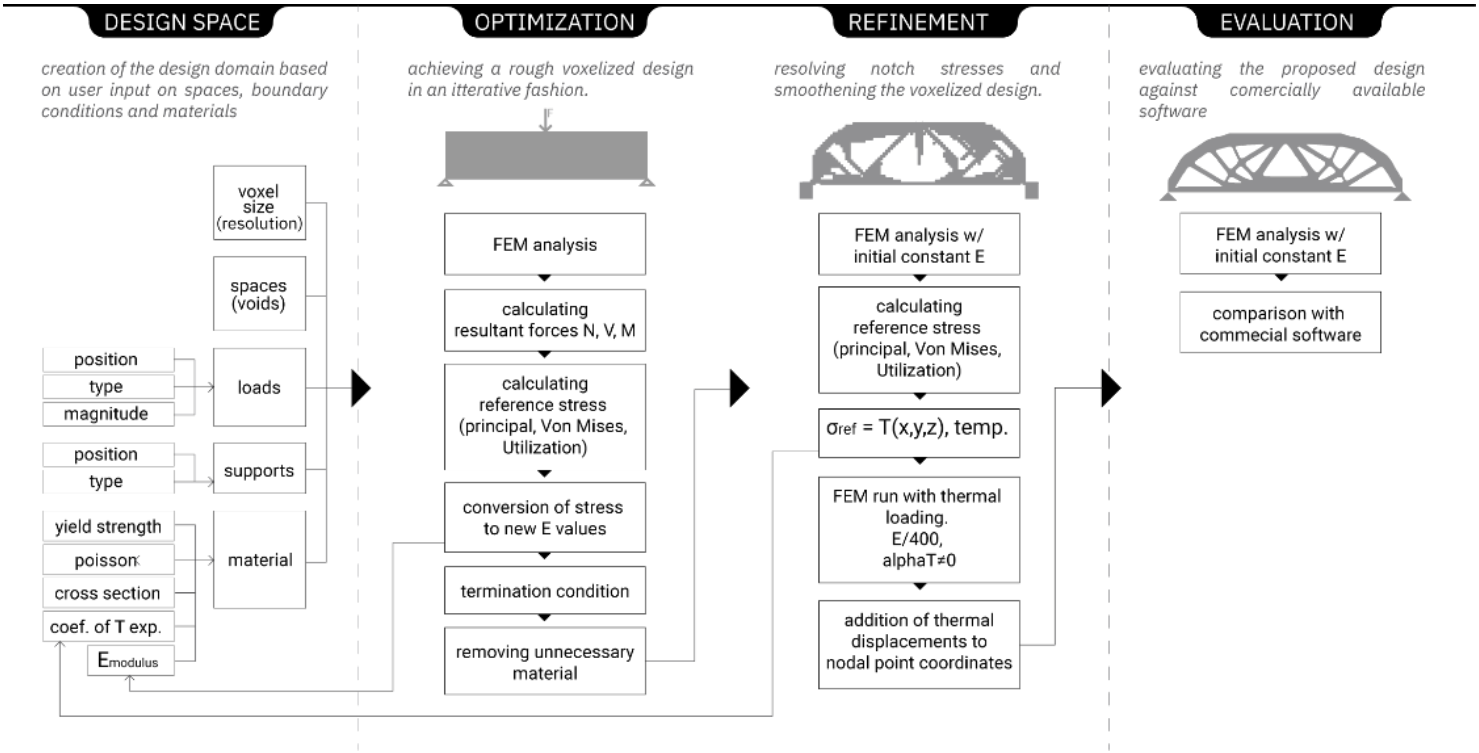

The envisioned method, summarized in Figure 3, is divided into four segments or stages: creation of the design space, the main optimization stage, design refinement, and evaluative stage. This structure for the method mimics the way in which the Grasshopper script was built up and allows the designer to easily manipulate through it.

The initial phase concerns the formation of the design domain or design space within which the form-finding process will take place, and is based on manual inputs from the designer. The user of the tool is prompted to create a volume larger than that of his expected final design since the unnecessary material will be removed at the end of the process in any case. Additionaly, the resolution of the design space is given in the form of the voxel size. Smaller voxel sizes lead to more detailed design drafts but significantly increase the necessary computation time. Preceding the voxelization of the design space is the introduction of voids in the form of breps which represent the functional spaces of the design, or openings. These volumes are immediately culled/carved out from the design space.

At this stage the designer specifies all of the boundary conditions necesarry for the constitution of the FEM model such as loads, supports, and the material properties. Similarly to the void areas, the load and support zones are input in a way which is intuitive for the designer, by manipulating 3D geometry (breps) and finding their intersection with the design space. In simple terms, the voxels which are found to be within the created support breps become the support points, while the voxels enclosed within load breps become the load points.

Lastly, the user specifies the material properties such as the Young's modulus (E), Yield strength (fy) poison ratio, and coefficient of thermal expansion(alphaT). All of this data is assembled into a design space which is later passed to the optimization stage.

Due to the fact that there are no freely available and open source volumetric FEM solvers for the Grasshopper environment, a Karamba3D solver was used. Since the Karamba3D solver only deals with linear(beam) and planar(plate) elements, the continuos design space had to be discretized into a series of interconnected beams, thus forming a spatial lattice that would mimic the continuous space. This was achieved by connecting adjacent voxel centerpoints with linear elements (beams) whose cross-section is equal to the dimensions of the voxel. Given a fine enough resolution (small enough voxel size) the results obrained from this approximation very closely resemble the results of a volumetric FEM solver of commerical software used in the evaluation stage of the method.

In the following stage, an elastic FEM calculation is performed on the beam lattice with the asigned working load expected in service of the design, and an equal Emodulus in all beams, which will produce a stress distribution withing the design space. In order to extract those stresses as numerical values per beam element, the outputs of the Karamba3D solver are taken, namely Normal forces **N**

[kN], shear forces **Vz** in the local Z direction [kN] and bending moments **My** around the local Y axis [kNm]. Based on the maximum values of these forces (tension or compression) it is possible to further calculate the reference stress per beam which will later be used to guide the changes of the material properties. In this research three such reference stresses were used: principal stresses, vonMises stresses, and utilization. The reasons for each of the reference stresses is elaborated in the literature review part of this report.

At this point the local E modulus of each beam is set equal to the reference stress calculated in the previous step. Three methods for doing so are proposed: the stress controlled method, the local stress-increment-controlled method, and global stress-increment-controlled method. They are different functions for converting the calculated stress into the new Young's modulus, and mainly differ by the step size. By converting the local stress into the new young's modulus, the more highly loaded areas become stiffer while the less loaded areas become softer. The beams which do more work become stronger, while the under-loaded zones become even more work-shy. Ultimately the former homogeneous design space becomes a non-homogeneous material characterized by the varying E-modulus at different zones.

This new non-homogeneous structure is again passed through an FEM calculation, after which the more loaded beams carry even more load, while the under-loaded beams carry even less load, leading to a gradual contouring of the structure into loadbearing and non-loadbearing zones. The process is repeated multiple times, and the stresses below a certain minimum get set to 0 so that those beams don't carry any more load. The looping is terminated either after a certain amount of iterations after which the user sees no more change in the design, or by setting a termination condition such as the maximum allowable stress in any beam which should not be exceeded.

At this stage, it is necessary to remove the materials (voxels) which are underutilized, for which purpose a stress per voxel is calculated. This value is obtained as an average of the stresses of the adjoining beams. The voxels with a stress below a certain threshold which is set by the user, get culled away. The outcome of this procedure is a rough design draft which contains material only in the load-bearing areas, and in which the E-modulus varies only slightly, before it is set to the initial material value (transition to a homogeneous material state).

The design which was just obtained should not be taken as final since it can still contain considerable notch stresses making it prone to failure. This design draft thus needs to be refined, which is done by the CAO method proposed by Mattheck, and which is elaborated in detail in the literature section of this report.

In the final stage of the method, a final FEM is run in order to get an understanding of the actual performance of the design. In order to double check the validity of the outcome, it is proposed to make a comparison with results obtained with a commercial software.

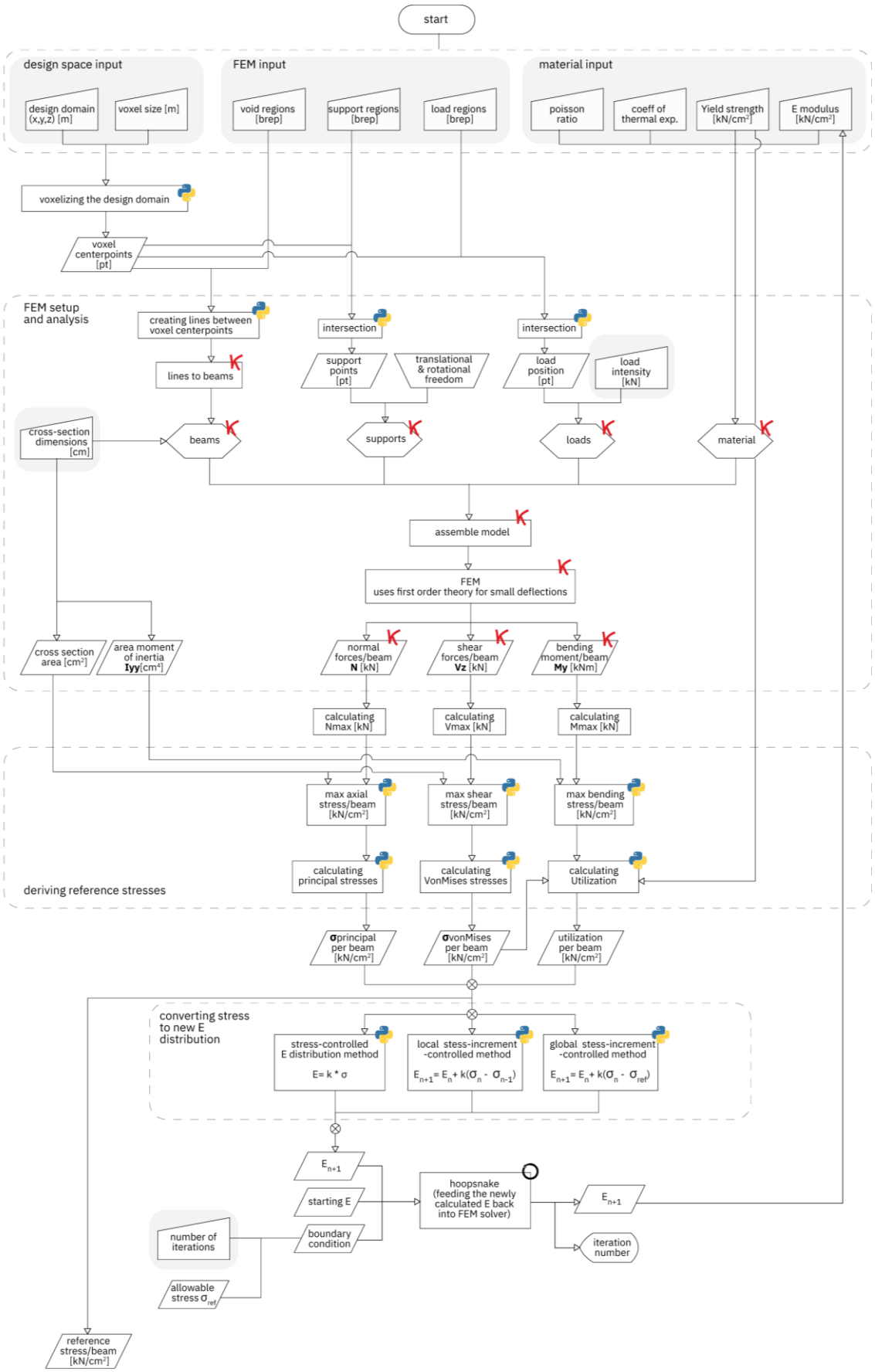
start
design space input
design domain (x,y,z) [m]
voxel size [m]
FEM input
void regions [brep]
support regions [brep]
load regions [brep]
material input
poisson ratio
coeff of thermal exp.
Yield strength [kN/cm²]
E modulus [kN/cm²]
voxelizing the design domain
voxel centerpoints [pt]
FEM setup and analysis
creating lines between voxel centerpoints
intersection
intersection
lines to beams
support points [pt]
translational & rotational freedom
load position [pt]
load intensity [kN]
cross-section dimensions [cm]
beams
supports
loads
material
assemble model
FEM
uses first order theory for small deflections
cross section area [cm²]
area moment of inertia Iyy[cm⁴]
normal forces/beam N [kN]
shear forces/beam Vz [kN]
bending moment/beam My [kNm]
calculating Nmax [kN]
calculating Vmax [kN]
calculating Mmax [kN]
max axial stress/beam [kN/cm²]
max shear stress/beam [kN/cm²]
max bending stress/beam [kN/cm²]
calculating principal stresses
calculating VonMises stresses
calculating Utilization
deriving reference stresses
σprincipal per beam [kN/cm²]
σvonMises per beam [kN/cm²]
utilization per beam [kN/cm²]
converting stress to new E distribution
stress-controlled E distribution method
E= k * σ
local stess-increment -controlled method
E_n+1 = E_n + k(σ_n - σ_n-1)
global stess-increment -controlled method
E_n+1 = E_n + k(σ_n - σ_ref)
E_n+1
starting E
boundary condition
hoopsnake (feeding the newly calculated E back into FEM solver)
E_n+1
iteration number
number of iterations
allowable stress σ_ref
reference stress/beam [kN/cm²]

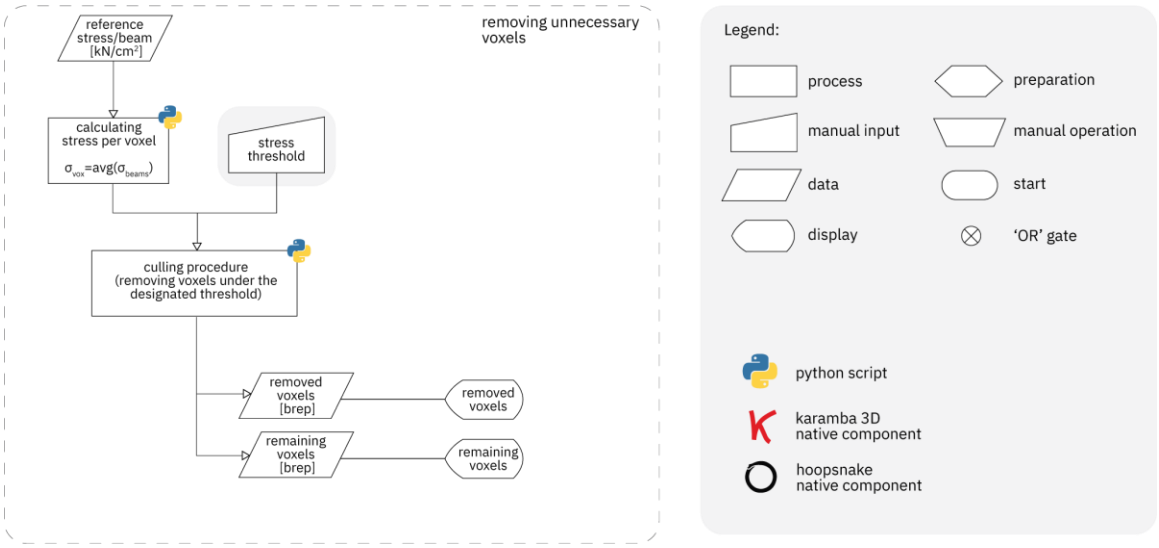

Figure 4. Main flowchart of the design method

1.10 Planning and Organization

The planning and organization (Figure 5) of the work conducted towards the realization of this research was divided into 5 phases, corresponding to the project presentation dates. The five phases align with the way the research design was planned, such that:

- The P1 phase entails literature study and acquisition of relevant resources to be used for the research after which the general research topic is established.

-The P2 phase is reserved for analysis, which entails the reflection on the literature, and gaining theoretical understanding of the most important concepts. At this point the research framework is established.

-The P3 phase was conceptualised around the computational part of the research methodology and is oriented towards learning python and shold result in a working design space and FEM model for both 2D and 3D cases.

-The P4 phase of this research corresponds to the simulation section of the research methodology which is focused on performing Structural Topology Optimisation simulations on various 2D and 3D TOY problems, before progressing to the application on an two storey building.

- The P5 phase is reserved for finalizing the script, its code, and proprietary material such as the report and a physical model.

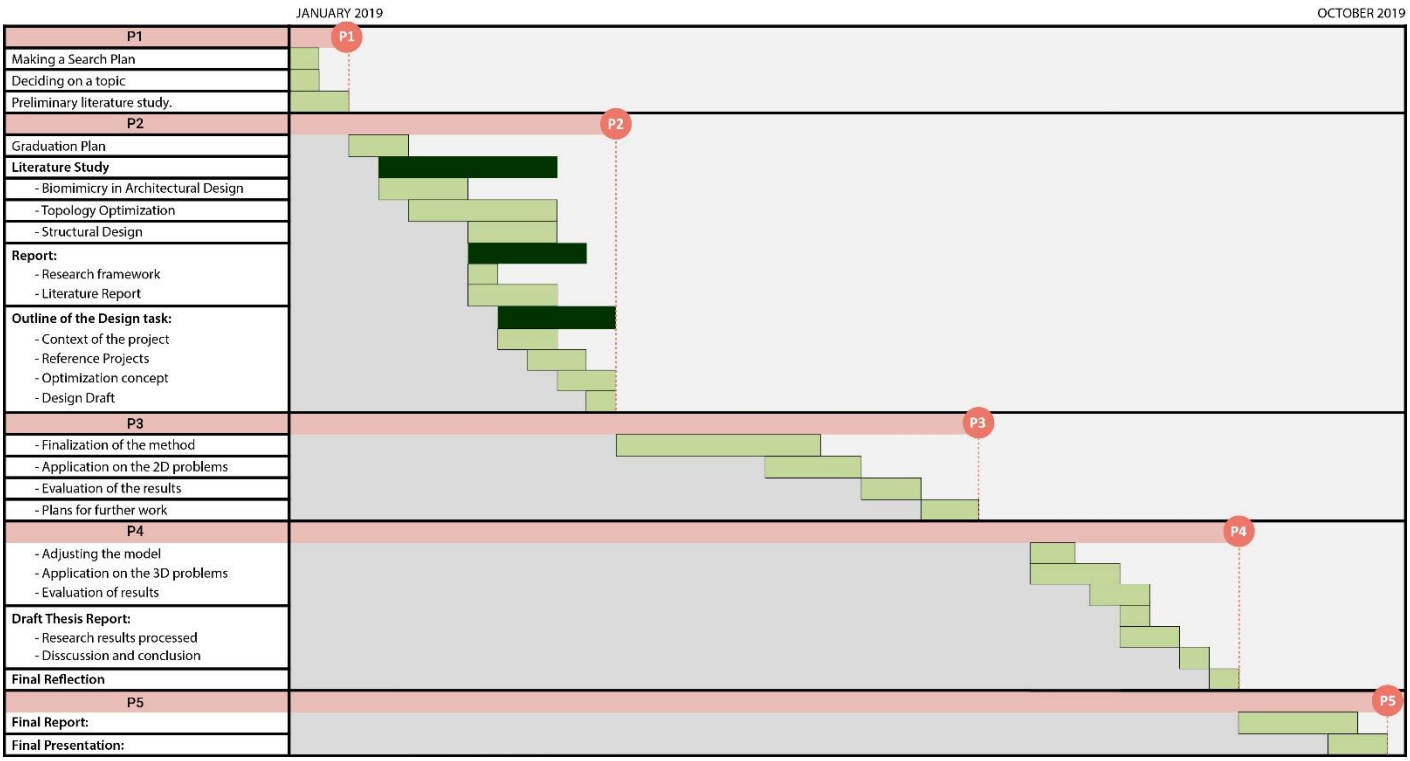

Figure 5. Planning and organisation of the research on a time scale.

02. LITERATURE STUDY

"We can probe a buttercup with the eye of a mite, ride the electron shuttle of photosynthesis, feel the shiver of a neuron in thought, or watch in color as a star is born. We can see, more clearly than ever before, how nature works her miracles.

When we stare this deeply into natures eyes [...] we realize that all our inventions have already appeared in nature in a more elegant form and at a lot less cost to the planet. Our most clever architectural struts and beams are already featured in lily pads and bamboo stems. Our central heating and air conditioning are bested by termite tower's steady 86 degrees F. And our new "smart materials" can't hold a candle to the dolphin's skin or the butterfly's proboscis. Even the wheel, which we always took to be a uniquely human creation, has been found in the tiny rotary motor that propels the flagellum of the world's most ancient bacteria. [...]

Perhaps in the end, it will not be a change in technology that will bring us into a biomimetic future, but a change of heart, a humbling that allows us to be attentative to nature's lessons." (Benyus, 2092, p.8)

2.1 Introduction

This section of the research will aim to elaborate on the field of practice called biomimicry. It will commence by trying to give an overview of the field, its definitions and purpose in the larger scope of sustainable development. Furher elaboration of the necessities of a transition towards a biomimetic future will be given before showcasing examples of how biomimicry and architecture work together to create built environments that are beneficial to their surrounding.

Figure 6. A go-to example to summarize biomimicry is the burdock burr and the invention inspired by it - velcro.

2.2 A Case for Biomimicry

2.2.1 What is Biomimicry

Seeing how there is no grand unified theory of biomimicry, similarly lacking is a definition of this field. Several notable researches in the field propose their own definitios. For Benyus (2009) it is a 'conscious emulation of life's genius', while Michael Pawlyn (2016) proposes that 'it is a design approach inspired by the way functional challenges have been solved in nature'. Similarly to Pawlyn, Julian Vincent (1997) in his numerous books about the topic, simply formulates biomimicry as the 'implementation of good design based on nature'. The Association of German Engineers uses the term Bionik to describe the process of 'decoding the inventions of animate nature and their innovative implementation in technology' (Gruber, 2011).

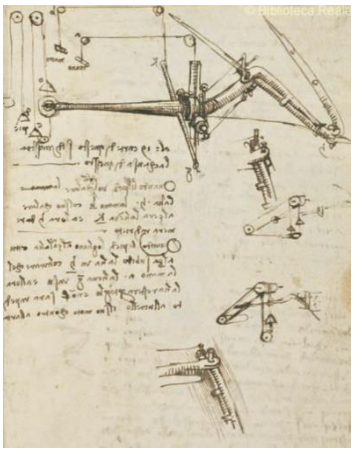

Figure 7. Diagramatic representation of the evolutionary process in nature (source: Nagy 2017).

It is worhwile making an effort to distinguish between various terms which can be found throughout literature about the relation between the natural and the manmade. The emergent field of emulating nature's creatins has brough upon a need for a systematic discipline, and thus separate groups of researches have coined different terms for describing such research. Most commonly found terms include 'bio-inspired design', 'bio-design', 'biomimicry', 'bionics'.

Regardless of the terminology used, it is essential to agree on a common ground, which is that this field of study is inherently transdisciplinary, evidence-based, focused on solving functional challenges rather than formal appeal, and is geared towards delivering a necessary transformative change.

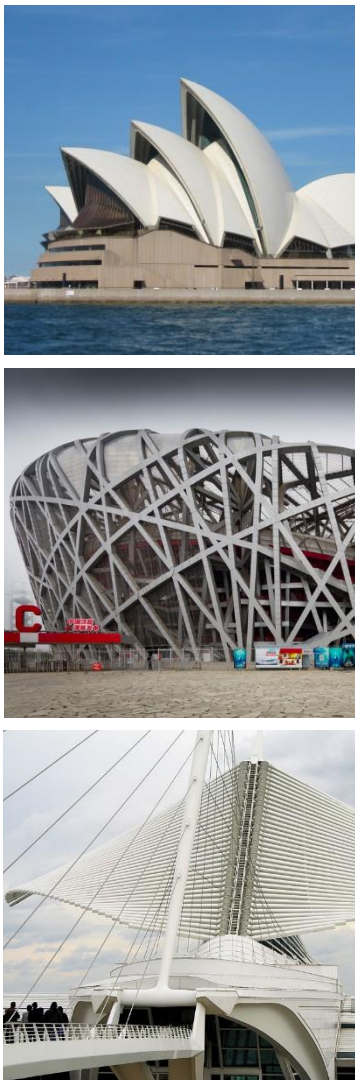

Figure 8. Examples of 'biomorphic' rather than 'biomimetic' architecture. Top to bottom: Jorn Utzon's Sydney Opera house, Sydney, Australia; Herzog and de Meuron's 2008 Olympic stadium in Beijing, China; Santiago Calatrava's Milwaukee Art Museum, Milwaukee, USA.

The mutuality which can be found across all of these authors is that biological organisms (but not only them, as will be discussed later) can be seen as having developed techniques and technologies that are quite similar to the ones invented by us humans. However, they have managed to solve the challenges we are trying to solve, with greater economy of means (Pawlyn 2016). We, as humans, have realized that there is an abundance of knowledge hiding withing organisms, ecosystems and natural occurances which can serve as guidance towards better design.

These researches have come to the realization that throughout millenia, the everlasting process of evolution and ruthless process of refinement it brings with it, has forced organisms to adapt to some amazingly resource-constructed environments such as areas with severe drought, excessive rainfall, extreme heats etc. These lessons become relevant when thinking about the anticipated constrictions humans will face in the near future within urban environments due to climate change.

It thus becomes of paramount importance to take a more humble look at sustainability and realize that aside from ever greater technological achievements, there is much more to learn from nature about how to not only build more efficiently, but also how to behave more in line with natural processes, and make sure we don't overstay our welcome on the planet.

I would advocate that it is a perfect time fully embrace biomimicry as a guiding principle in our design endeavors (and not only there) as we are now able to revisit nature's genius with an immensely expansive body of scientific knowledge, unprecidented digital design tools and standpoints about aesthetics which are unconfined by stylistic conventions of the previous centuries.

Throughout history, we have always been drawn to nature in search for inspiration. A pioneer in this field, da Vinci shows a comprehensive study of birs, their anatomy and flight patterns in his Codex on the Flight of Birds (Figure 7). In the realm of architecture, many architects have drawn inspiration from nature-made forms and tried to replicate them within their designs. Among the more well known modern examples are the Sidney Opera house by Jorn Utzon, Santiago Calatrava's Milwaukee Art Museum, and Herzog & De Meuron's 2008 Olympic stadium, to name a few.

However, this type of emulation of nature, strictly based on it's formal qulities should not be regarded as 'biomimicry' but rather as 'biomorphism', A distinction is necessary, since the former is a formal and aesthetic position, whereas the latter is a functional discipline. This is not to say that these two

approaches are mutualy exclusive and can not co-exist ina single project, since, according to Pawlyn (2016) biomorphism can add a deeper meening to a purely technical biomimetic solution, through it's use of associative symbolism.

Göran Pohl and Werner Nachtigall (2015) clearly elaborate that if we are to meet the goals of sustainable development, and reduce the impact of the building industry on the environment, a direct copying of nature will never lead us to that goal. Instead, architects and engineers need to grasp the fundamental ideas from nature and apply them to buildings only after the process of abstraction. A case in point would be the environmentaly friendly, thermoregulating systems of termite mounds which are based on solar effects. Rather than trying to copy the exact same structure of a mound in the hopes of achieving the same on a human scale, we should rather extract their underlaying principles and through the processes of abstraction and reverse engineering, lead to their technical implementation.

2.2.2 Example of biomimetic structural design

Since the body of biomimetic architecture is vast, and the topic of this research mainly pertains to the design of structures, an examples of biomimetic structural design will be showcased. The example was chosen not only based on the performance, but also because it showcases the importance of integrating cutting edge computational design and fabrication tools in bringing biomimetic solutions from paper to reality.

Some of the most thought provoking and elaborate research into biomimetic architecture is undertaken at University of Stuttgart and the Instite of Building Structures and Structural Design (ITKE) led by prof. Jan Knippers, and Institute of Computational Design and Construction (ICD) led by prof. Achim Menges. Many of their most successful projects emerge after taking a microscopic look at an organism of interest and materials they are constructed from.

Such was the case with the series of 'Elytra' pavilions in which the model organisms were beetles which posses a protective wing shell known as 'elytra' (Figure 9-b). The elytra was chosen due to it's high strength while using minimal material. The research concluded that the performance of the elytra relies on the propper arangement of chitin fibres embeded in a protein matrix, which allows for local differentiation in material properties of the wing. The team performed scanning electron microscopy (Figure 9-c) to create detailed 3D models of the fibre structure inside the elytra, after which it was concluded that the fibres are always tangent to the lines of principal stress and that their density depends on the

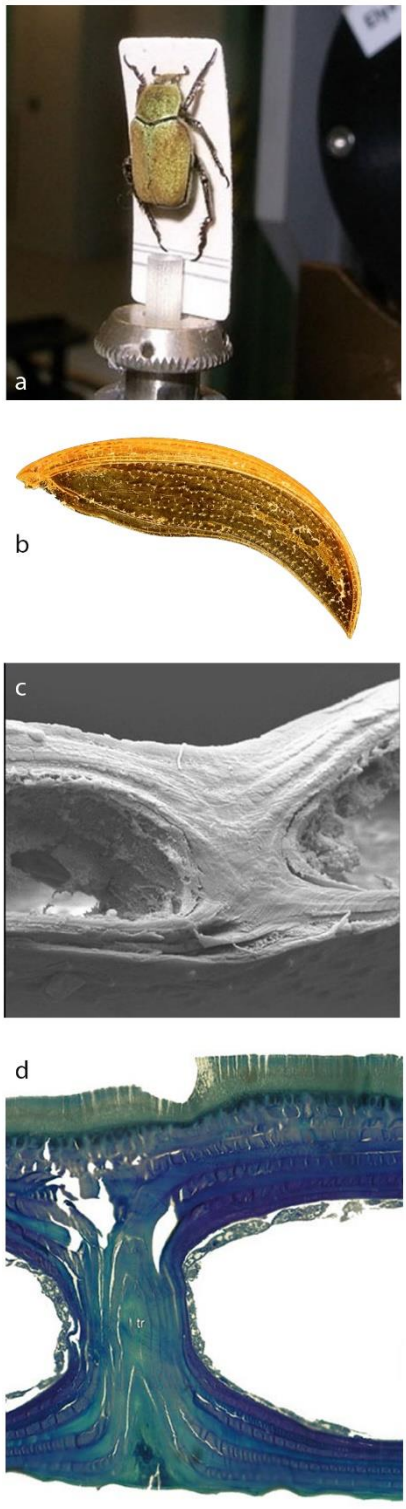

Figure 9. a)potato beetle; b)elytra tomography scan; c)SEM scan; d) correlation of fiber layout and structural morphology in trabeculae (source: icd.uni-stuttgart.de).

intenisty of the stress. What resulted from this research is the creation of a double layered modular construction sistem, which was implemented in several architectural prototypes. The individual elements are made from GFRP and CFRP robotically wound around carbon fibre frames (Figure 10). The biggest element has a diameter of 2.6m and weighs only 24kg which made it possible for the entire 50m^2 pavilion to be constructed by only manual labor.

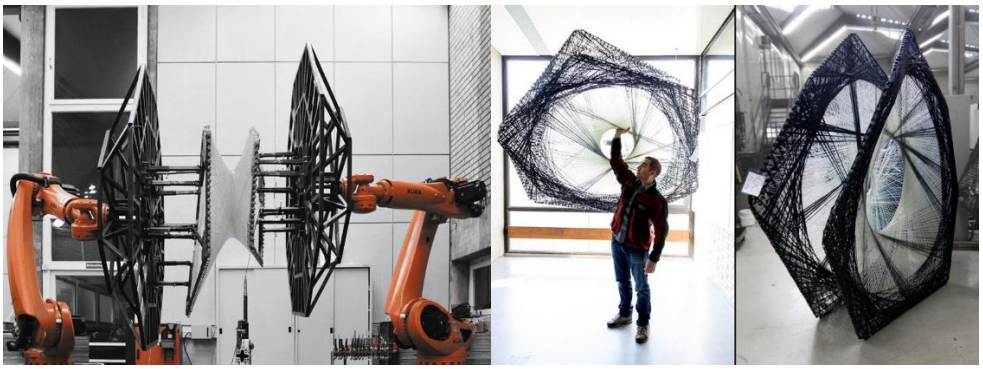

Figure 10. manufacturing of the Elytra pavilion modules (source: icd.uni-stuttgart.de).

Ultimately the Elytra research pavilions aim to showcase how the synthesis of computational design, biological structural principles, and new ways of manufacturing can lead to the generation of highly efficient and elegant architectural solutions, showcasing novel spatial solutions and tectonic possibilities.

Figure 11. ICD/ITKE research pavilion 2013/14 (source: icd.uni-stuttgart.de).

2.2.3 How does nature design structures?

In order to learn from nature about design, it is important to first consider how successful design occurs in nature. Consequently, we as humans can improve our methods and design processes by following nature's lessons. I will be focusing on the design of structures, even though nature offers plethora of solutions for architectural engineering and design in respect to materials, heating and ventilation systems, efficient energy use, resource management, lighting design etc. It should be stressed that this research does not advocate for biomimicry as an antithesis to our curent design practice - a 'silver bullet' which will solve all our design problems. It merely tries to suggest that biomimicry should be a synthesis of our ingenuity and ability for innovation coupled with the results of a 3.8bilion year long refinement process found in nature.

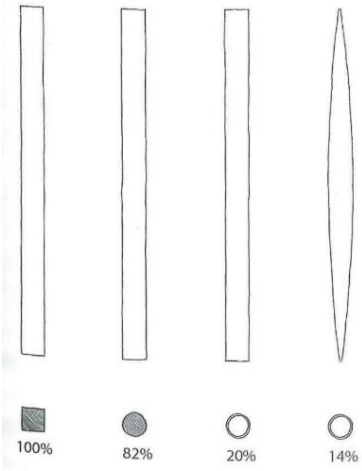

Figure 12. four equally stiff columns with various degrees of material efficiency (source: Pawlyn, 2016).

Almost everything in living nature is in tough competition for energy and living space, and only the best designs of high reliability and with minimum consumption of material and energy can survive. As a consequence, lightweight yet strong design is found in nearly every loadbearing natural construction (Baumgartner et al., 1992). To achieve a lightweight yet sound design, nature makes extremely smart use of materials often achieved trough ingenuity in form, which has led Julian Vincent (1997) to establish a maxim "in nature, materials are expensive but form is cheap". This observation provides a rich sourcebook of ideas for future manmade structures which can be radically more efficient than the ones we are building now. In Pawlyn's words the challenge thus becomes using "less material and more design" (Pawlyn, 2016).

The theoretical and mathematical elaboration of nature's design strategy was given by a Scottish mathematician and biologist D'Arcy Wentworth Thompson in his seminal work "On growth and form". Thompson identified a mechanical rule which guides the design of all biological structures, later coined into the 'axiom of uniform stress' by Claus Mattheck (Mattheck, 1999), and which states that biological constructs always try to grow in a state of constant stress throughout the structure on a time average.

In simple terms this means that in areas of stress concentrations, material is built up until there is enough to evenly distribute the forces, while in underloaded areas, material is removed to conserve material consequently leading to weight decrease. The result of such a process are components of optimal efficiency in

which there is no waste material and all the material which exists is carrying its fair share of load. By contrast, manmade structures are designed in such a way that the most onerous load conditions, which happen only in few locations and often incidentally, determine the size of the whole beam or column.

2.2.4 Bones as optimal structural designs

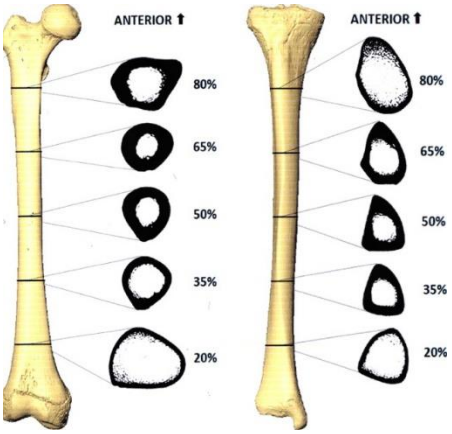

Figure 13. variance in cross sectional thickness along the length of femur and tibia (source: Gosman, 2013).

This abovementioned axiom of uniform stress will be examplified by looking at skeletal tissues and their mechanical behavior, as bones are well optimized biological load carriers which sustain abundant number of load cycles during their lifespan. Before speaking about the form of bones, it is worthwile saying a few words about their mechanical properties in relation to the strength they have to manifest in order to resist the forces impeded upon them. For this reason, parallels will be made with elementary manmade structures such as the column and the beam.

In all structures, provision has to be made, in some way or another, for strength of two kinds, strength to resist crushing i.e. compression, and strength to resist pulling apart i.e. tension. Often these forces act simultaneously, such in an eccentrically loaded column or a simply supported beam both of which become subject to bending.

In a manner simmilar to an unevenly loaded pillar, or a simple beam, the bone will tend to bend and thus endure compression on its concave part and tensile stress on the convex part. It follows that in some intermediate layer there is a neutral zone, where fibres are subjected to no stress at all. From an engineer's point of view, there is a redundancy of material in this zone, which allowed for the creation of **I** beams and columns, or tubular sectiones to resist bending in all directions with minimal material (Figure 12). We can notice that many objects in nature demonstrate this structural knowledge such as plant stems, feather quills and ultimately bones. If our beam is exposed to high bending stress it will tend to buckle or snap midway along its length, for which it would be prudent to make the walls thicker in that zone and thinner towards its ends. Looking at a longitudinal section of a femur, that is exactly what happens – the pressence of a 'danger point' has been avoided by careful redistribution of stresses by addition of material. The thickness of the bone becomes a diagram or a graph of the bending moments (Figure 13).

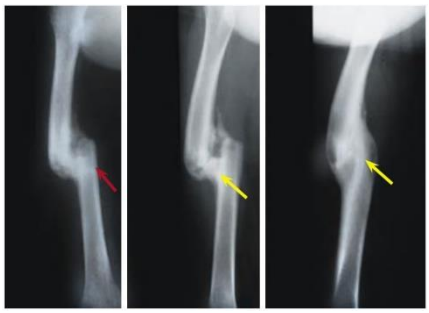

Figure 14. x ray images showing the process of remodelling of a broken femur, and the formation of new bone.

In all load-carrying bones there is a differentiation between zones experiencing higher stress and zones experiencing lower stress, manifested

through different material densities. Thus, the volume between the areas of maximum tension and compression is filled with a lattice work of interlaced trabeculae of bone, also called as the spongious bone. Wolff (1892), continuing the work of Hermann Meyer and Carl Culmann has managed to show that the trabecular bone tissue (Figure 15) spreads in intricate curving lines from the loaded area to the hollow shaft, and that these lines are crossed by other lines in an orthogonal fashion. He elaborates that the arrangement of tiny trabeculae is nothing less than a diagram of the lines of principal stress in the loaded structure, and that the thickness of the trabeculae corresponts to the experienced intensity of the stress. In short: nature strenghtened the bone precisely in the manner and direction in which strength was required. This notion becomes even more impressive if we consider the fact that bones are part of a mechanical system and have a multitude of dynamic rather than static load cases to resolve.

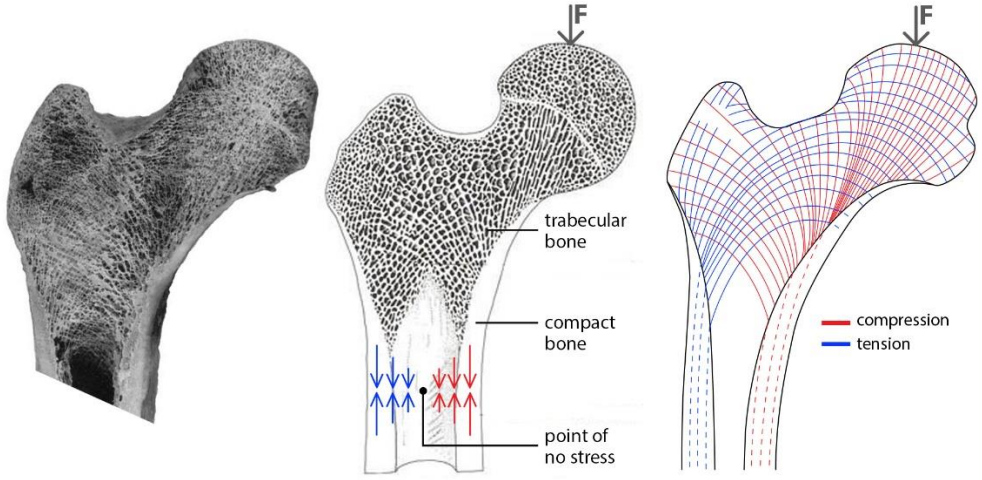

Figure 15. lines of stress through a femoral bone (adapted from: Wentworth, 1942).

Bones reveal ways in which asymmetrical forces are resolved. What becomes aparent is the precise match between the density of the bone fillaments and the concentration of stresses; where there is higher stress, there is a higher degree of mineralization than in places of lower stress, and elsewhere there is a void. In this way a distribution of Young's modulus develops which is fine tuned to the experienced load case. The same is observeable in any laod carrying bone, but the example of a human femoral bone was found to be the simples in giving a clear illustration of the point and analogous to a man-made structure like a beam.

We should keep in mind that bones are living structures, and that the little trabecuale are continiously demolished and formed anew. Their making and udoing is the result of direct action of forces they are exposed to. If a bone is broken and put together in a way that the two parts lie somewhat out of their original place, the tension and compression lines will change path and the

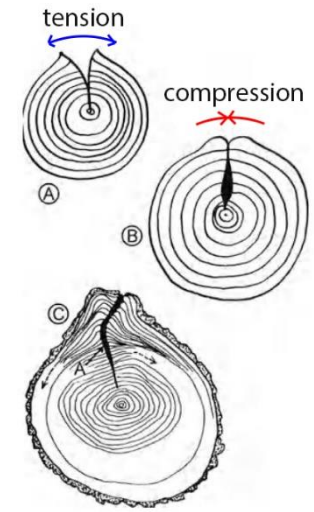

Figure 16. A) crack induced due to tensile stress in cold period on a tree's surface.
B)renewed contact in warm period imposing local compression. C) frost rib formation as a consequence of repeated crack formation and repair (Mattheck,

trabecular system will be found to have remodelled so as to fall in line with the new system of forces. This occurance has come to be known as Wolff's law. Partially associated with the same law is that strain, as a result of stress which is a direct stimulus to growth itself. If a broken bone is fastened with a cast, the constant pressure by the cast is a direct stimulus to growth and an active agent in the process of repair (Figure 14). Consequently if stress is removed from a bone alltogether, an occurance of bone demineralization, and reduction in density will occur, as has been observed in astronauts who spend much time in microgravity.

The same ocurances are observed in plants, as can be seen by the formation of frost ribs in trees (Figure 16). In trees, this local stress accumulation is solved in much the same way as in bones. Namely in plant tissue such as a tree, a strain caused by a constant or increased weight leads to the increase of strength of that branch partially by increasing the bulk of the tree in highly stressed places and partially by histological physical alteration of the tissue.

One can't help but notice a poetic dimension of his phenomena, where things get stronger only after experiencing stress, and that the key to sustenance is distributing/sharing a burden, without it being carried by a single part.

The major difference between trees and bones is in that in the trees, material cannot be removed, whereas in bone tissue it can. The explanation resides in the fact that skeletal tissue is subject to selective pressure for lightness in order to give the organisim the ability to move at speed to catch or avoid becoming, prey. Most of the volume of the tree is dead material used to support tits growth and it is only the outer layer which is alive. For the purposes of developing a topology optimization method, this research will take inspiration from bones, as it also aims at creating components with high degree of weightsaving i.e. material saving.

The extreme cases which showcase the ingenuity of design in bones as responses to selective pressures are avian skeletal systems, where a need to achieve high strengths with minimal weight yields impressive results. Figure 17 shows a metacarpal bone of a vulture which efficiently supports the 2.8m wingspan of this animal, and closely resembles a spatial Warren truss.

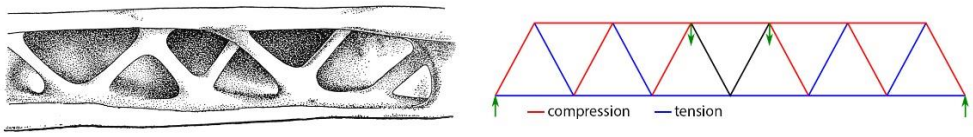

Figure 17. A vulture's metacarpal bone (lef), and a Warren truss (right) (adapted from: Pawlyn, 2016).

Avian skulls in particular are great materialisations of the “Material is expensive, form is cheap” postulate. The section of a magpie’s skull shown in Figure 18 displays how a radical lightness is achieved by an increase in the bone thickness. The observed structure is simillar to a spaceframe in which two layers are connected with struts and ties to efficiently transfer and distribute the load, while simultaneosly forming a dome shape with the associated load-transfer benefits.

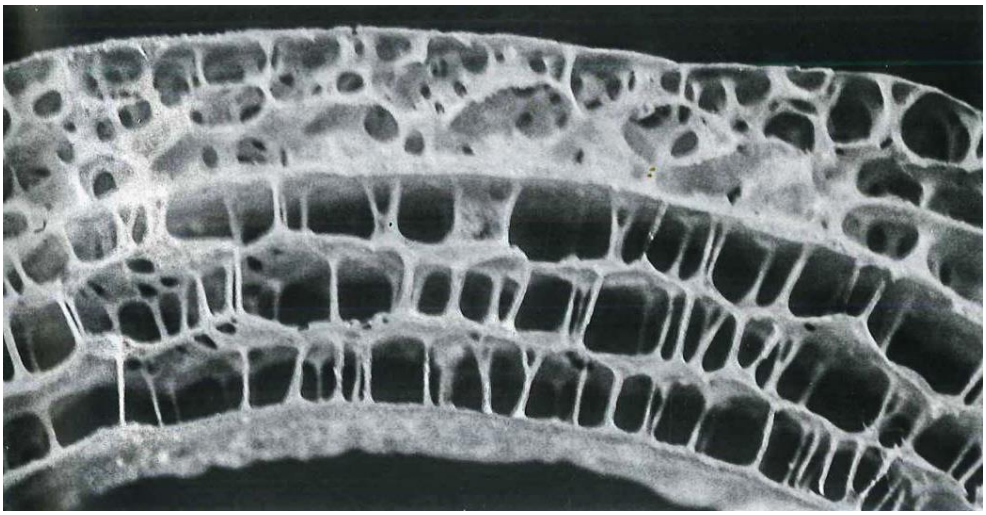

Figure 18. Section through a magpie’s skull showing thin domes of bone connected by struts and ties (source: Pawlyn, 2016).

We can now see how bones reflect the earlier mentioned axiom of uniform stress. They are adapted to the most important (e.g. most common) load cases, for which purpose bones grow into a state of constant stress throughout the component.The two mechanisms which were elaborated: proliferation of material based on the distribution and intensity of the stress, and active remodeling/mineralization based on local stress occurances become central for the creation of a computational model, and is what Mattheck coined as the SKO and CAO methods respectivelly.

As far as the material properties go, live bone displays only slight disproportions with respect to its strength in compression and strength in tension. However there is a large variation in values of compressive and tensile strength in different bones depending on the load they carry, but also due to factors like age of the bone which alter its mechanical properties. As bone performs slightly better in compression than in tension, if we are to create structures of similar formal geometric complexity and loadbearing capabilities, it could be achieved with reinforced concrete or mild steel (Thompson, 1942)

2.3 Design Optimization

Structures found in nature, and the ones created by human hand undoubtedly have many similarities, most prominent of which being that they abide the same law of physics, statics, elasticity and dynamics (Addis 2016). However, we can observe an increased resource and energy efficiency within nature made structures, often achieved through an evolved ingenuity in form (materials are expensive, and shape is cheap maxim). As in nature the form perfectly befits the function, the many manifestations of this phenomenon can serve as a blueprint of ideas for human scale structures which can be drastically more efficient.

The idea of optimization is conceptualized towards solving just that challenge. It seeks to integrate the evaluation of the design's performance in the early phase of its conceptualization and form finding. The mathematical construct of the optimization problem suggested by Nagy (2017), can give us a concrete approach to tackle it Figure 19.

Figure 19. General formulation of the optimization problem (source: Yang, 2010).

$$\underset{\boldsymbol{x}\in\Re^n}{\text{minimize}} \quad f_i(\boldsymbol{x}), \qquad (i=1,2,...,M), \tag{1.1}$$

$$\text{subject to} \quad h_j(\boldsymbol{x})=0, \quad (j=1,2,...,J), \tag{1.2}$$

$$g_k(\boldsymbol{x})\le 0, \quad (k=1,2,...,K), \tag{1.3}$$

$$\text{where } f_i(\boldsymbol{x}), h_j(\boldsymbol{x}) \text{ and } g_k(\boldsymbol{x}) \text{ are functions of the design vector}$$

$$\boldsymbol{x}=(x_1,x_2,...,x_n)^T. \tag{1.4}$$

As can be inferred from the above mathematical formulation, in order to solve an optimization problem, we need three components:
- design variable (x): A vector of input data or parameters that describes every possible design in a system;
-A set of objective functions (f) which delineate the goals of the optimization process. This can be either minimizing or maximizing the values of these functions. For every outcome, *f* returns a number indicating its goodness.
-A set of constraint functions (h, g) which establish the limits of the system;

The ultimate goal is the achievement of a globally "best performance" which meets all the objectives while staying within various constraints (Yang, 2010). Geyer and

Rueckert (2005) delineate the objectives and constraints of building structures, shown in Figure 20.

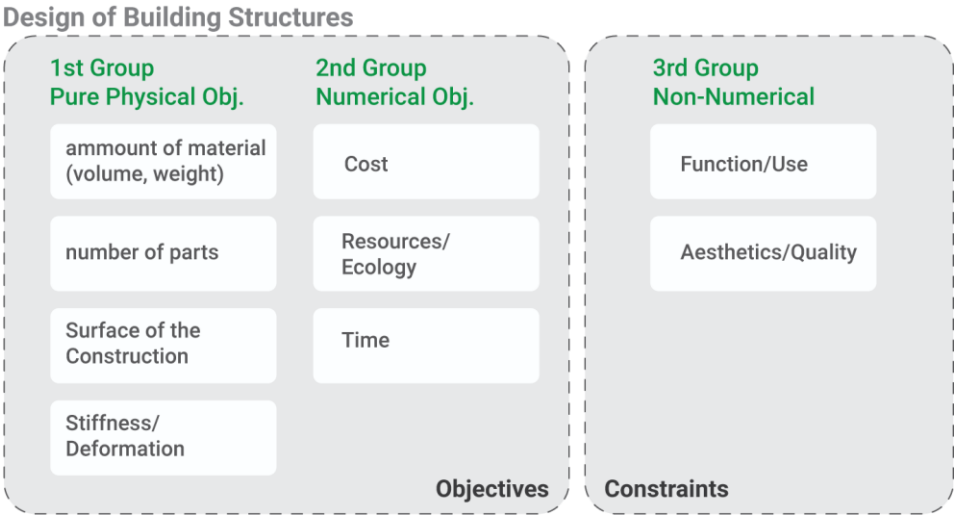

Figure 20. Objectives and Constraints of building design (source: Geyer and Rueckert, 2005, pp2).

In the context of building structures, the previously mentioned goal of "best performance" can be a multitude of things such as maximizing the structure's stiffness, or minimizing its mass (equivalent to minimizing the amount of material used). The constraints determine the boundaries of the optimization functions and can be formulated as maximum allowable stresses within the structure, allowable displacements etc. (Baalen, 2017). It is thus of critical importance to properly define the goals and constraints. A case in point would be the false outcome of the optimization if we were to set a goal of maximizing the stiffness and set a constraint of unlimited material, which would result in very suboptimal solutions.

2.3.1 Approaches to Design Optimization

Bendose (1995) distinguishes between three types of structural optimization: size, shape and topology optimization. Each of them address different aspects of a structural design problem, and their respective objectives have been illustrated in Figure 21.

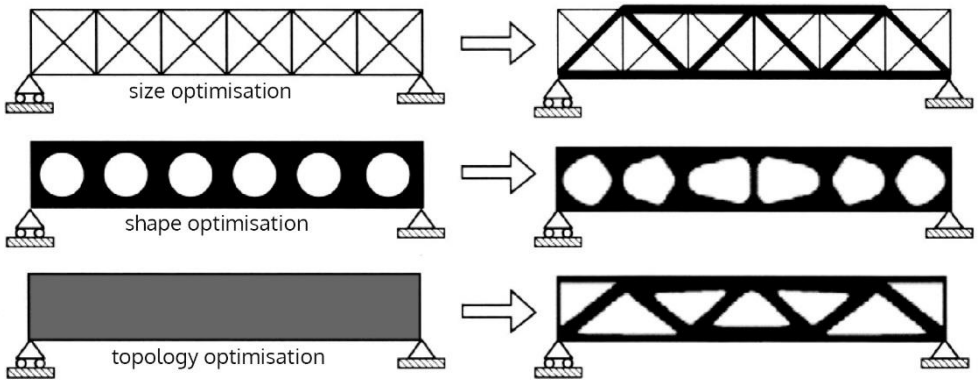

Figure 21. Objectives and Constraints of building design (source: Bendose and Sigmund, 2003).

Size optimization:

In a size optimization problem, the goal is to find a subgraph of loadbearing elements within an already existing design topology, and effectively increase their thickness while simultaneously decreasing the thickness of underutilized members. The goal is to find an optimal thickness distribution which minimizes or maximizes a certain objective such as peak stress, deflection etc. This method is usually applied on designs comprised of linear elements such as beams, columns, trusses and panels or slabs. The shape and topology remain unchanged during this process.

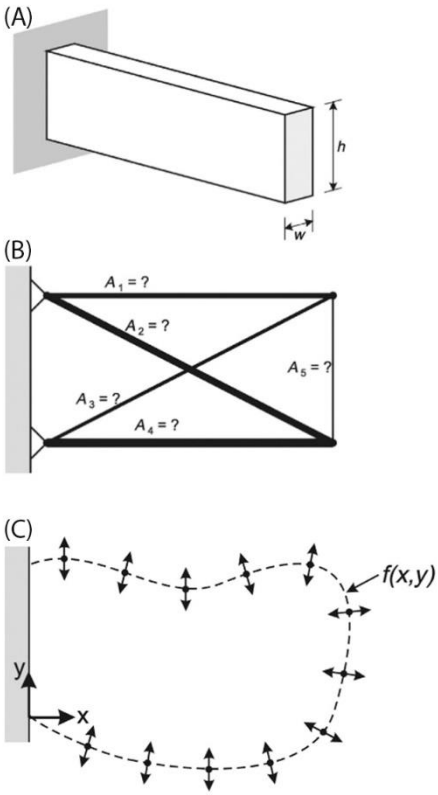

Figure 22. Examples of where optimization can be used: A) finding the cross-section of a beam; B)finding approapriate member thickness in a truss; C) finding an optimal design within a given domain (source: Querin et al., 2017).

Shape optimization:

In a shape optimization problem, the definitions of curves, surfaces, lines and nodes that construct the design domain become the design variables. The goal is to reduce the stresses at boundaries of these variables within the given topology that best satisfy the objectives. In the example given in Figure 21, the boundaries of the beam remain constant, but the shapes of the orifices are changed to obtain the best performing structure. Since the topology remains constant, shape optimization is often used as a post-processing method for Topology Optimization to reduce the high "notch" stresses at the boundaries.

2.3.2 Topology Optimization and its Methods

Topology is an area of mathematics concerned with properties that are preserved under continuous deformations of objects regardless of their geometry.

The idea behind topology optimization is the most general of the three previously mentioned optimization methods. It is essentially a material distribution

problem. The initial topology of a structure is defined as a design space within which the final design is to occur, and the goal becomes determining the ideal number of holes and changing the connectivity of the domain (Bendose, 1995).

In case of a discretized 2D domain, the cross-sections of the discrete beam elements become variables, allowing them to take a value of 0, thus removing them from the structure. In a three-dimensional case, the density of the elements becomes the variable, and can take the value between 0 and 1. As an output, a suggestion of a layout of structural elements is given with a specific material distribution for the given boundary conditions, objectives and constraints.

Numerous methods have been developed for performing Topology Optimization both on discrete and continuous geometries. According to Querin et al. (2017) they can be broadly separated into two categories: Optimality Criteria Methods, and Heuristic (intuitive) Methods. The former methods are more mathematically rigorous and very useful for finding efficient solutions for problems with a large number of design variables and few constraints. The latter, often derived by intuition and observation, don't guarantee a globally optimum solution, but are easier to implement and understand (Querin, et al, 2017). The following table lists the most well-known methods of both groups.

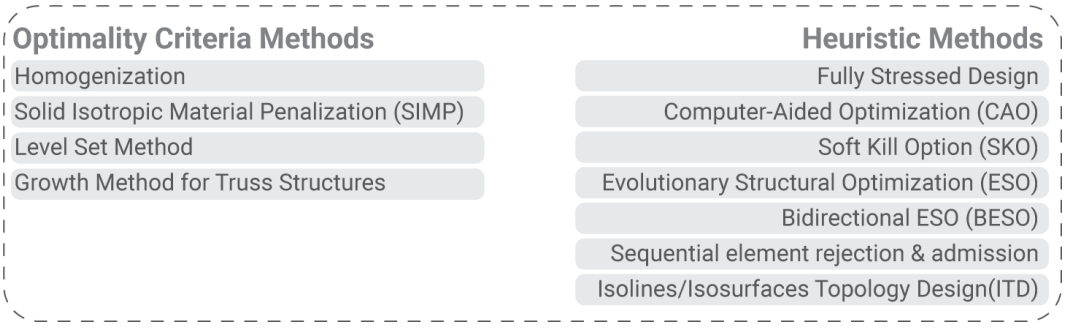

Figure 23. types of topology optimization methods according to (Querin et al., 2017).

This report will elaborate on one method from each category to give an understanding about the potential benefits and constraints of using any of the two types of algorithms. Firstly, the Solid Isotropic Material Penalization (SIMP) method will be elaborated, as one of the most popular methods today, before moving on to give detailed elaboration of the SKO and CAO methods, on which this research paper is grounded.

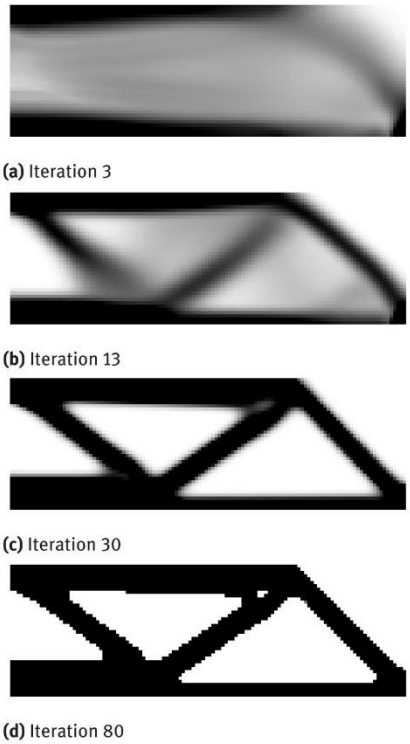

Figure 24. Results of a TO of a cantilever beam using the SIMP method. Evident intermediate densities and effect of penalization.

SIMP:

The Solid Isotropic Material Penalization (SIMP) method is currently the most used mathematical method for performing topology optimization (TO), and is implemented in the majority of commercially available software (Rozvany, 2009).

The SIMP method bypasses the traditional topology optimization techniques in which the design domain is discretized into a grid of finite elements which can have only a binary state: 1-presence of material (full density of element), or 0- absence of material (no density). This is achieved by allowing each element to have a relative density between a minimum value ρ_{min} and 1, which allows for intermediate densities, and a more accurate distribution of material, e.g. porous materials. The ρ_{min} is introduced so as to maintain the numerical functionality of the FEM solver since it cannot perform an analysis on an element that has no material (Ansys, 2019).

Simultaneously with the change of every element's density, the Young's modulus (E) changes, and is calculated based on the power law:

$$E(\rho_e) = \rho_e^p E_0$$

Here, E is the new modulus of elasticity of an element, E_0 the original material modulus, ρ_e is the density of the element *e*, and the exponent *p* is the so called penalization factor which steers the density of an element towards a more binary one, thus producing a geometry with distinctive contours (Figure 24). By tweaking the penalization factor, the user can define how much grey material there is. A penalization factor of 3 has been found to produce a binary i.e. black & white solution, with most success.

A common objective of a TO problem is the maximization of the structure's overall stiffness, which is equivalent to minimizing its compliance throughout the process of material (mass) removal. Compliance (C), a reciprocal of stiffness, is a measure of the overall softness of a structure, and is globally calculated by summing the strain energies of all individual elements (Bendose, 1995). The SIMP method seeks to find appropriate element densities (density is the only design variable) which will minimize the global compliance of the structure. The objective function thus becomes:

$$minimize\ C(\{\rho\}) = \Sigma_{e=1}^{N} (\rho_e)^p [u_e]^T [K_e][u_e]$$

where u_e is the vector of displacement of the element, K stands for its stiffness, and the vector { ρ } indicates the relative densities of the elements ρ_e. During all of the iterations, a constraint of the target mass has to be satisfied, along with functional constraints and the global equilibrium law.

$$Subject\ to\ \ \Sigma_{e=1}^{N} \{v_e\}^T \rho_e \leq M_{target}$$

where *v* stands for the volume of the element *e,* and the M is the target mass of the final design, previously set but the user.

$$And\ subject\ to\ \ [K\{\rho\}]\{u\} = \{F\}$$

An important part of the SIMP method is the sensitivity analysis, which serves the purpose of evaluating the impact the changing of density has on the objective function of stiffness maximization. During this process, the less dense elements get eliminated in further optimization steps (Ansys, 2019).

$$\frac{dC}{d\rho e} = -p(\rho_e)^{p-1}[u_e]^T[K_e][u_e]$$

The looping of the algorithm continues until the objective function variations become very small, and the criteria is met. The general flowchart of the method is given in Figure 25.

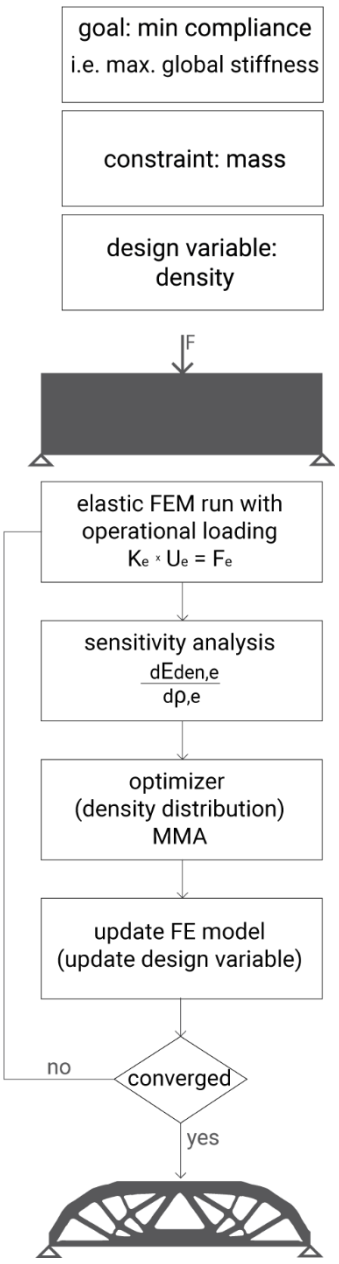

Figure 25. simplified flowchart of the SIMP method (source: author)

2.3.3 SKO and CAO method

The logic behind the Soft Kill Option (SKO) and Computer Aided Optimization (CAO) methods have briefly been hinted at in the Methodology section of this report. The methods have first been proposed by Claus Mattheck, and have been thoroughly elaborated in numerous publications. Several successful implementations of the method for mechanical engineering design testify to the validity and ease of their implementation.

Both SKO and CAO rely on the use of Finite Element Method analysis to provide the information about the current stress states and performance of the design.

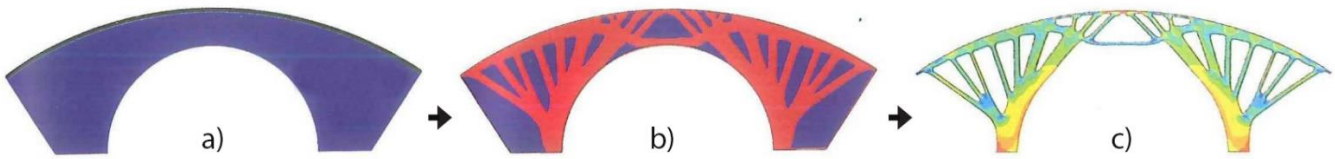

Figure 26. a) initial design space; b) rough lightweight design draft by SKO; c) lightweight and equally stressed design by CAO (source: Pawlyn, 2016)

SKO:

The Soft Kill Option method has been inspired by the earlier elaborated phenomena of adaptive bone mineralization, in which the bone tissue proliferates in zones of high stress, while simultaneously being removed from areas of low stress. This occurance over a time period leads to a differentiation in the Young's modulus throughout the bone component, i.e. the highly stressed parts have an increased Young's modulus and become stiffer, while the less loaded zones have their Young's modulus decreased, thus becoming softer (Baumgartner, 1992). The method, which relies on this phenomena, is illustrated through a flowchart in Figure 27. Mattheck (1999) provides a stepwise explanation of the method:

1. A design space is to be created by specifying the volume in which the final design is to occur. Additionally, all boundary conditions expected in the working component should be assigned at this stage, such as load positions and intensities, supports and material properties.

2. The first FEM analysis is carried out with an equal stiffness throughout the component, which will yield a stress distribution in the design space. Mattheck suggests using the Von Mises stress indicators or the Tresca stress indicator as a reference stress for further steps. The difference between the two reference stresses will be elaborated in further sections of the report.

3. At this point, the previously calculated stress at each finite element is set formally equal to it's young's modulus for the next iteration.

$$E_{n+1} = k\sigma_n$$

n-iteration number

This means that the more highly stressed zones become harder and less stressed zones become softer, analogous to a bone tissue. Hence, the previously homogeous component becomes non-homogeneous.

4.With the newly distributed Young's modulus, another FEM analysis is carried out, in which the strong load-carrying parts carry even more, and the work-shy elements carry even less. The previous two steps are repeated itteratively, and the

stresses which approach 0 are set to a constant minimum, thusby being “killed”. The iterations are halted when the designer stops noticing changes in the design.
5. The Young’s modulus is again set equal to the initial E modulus of the material throughout the entire design draft, before it is again analized with a FEM analysis to obtain final stresses in the component.

The algorithm described above has a great success rate at converging to lightweight designs. However, to do so, a large number of iterations are needed, due to which reason Mattheck proposes the local and global stress-increment controlled methods described in further text.

These methods pertain to the way in which the calculated reference stress is converted into the new E modulus. The local stress stress-increment-controlled method given by the following equation,

$$E_{n+1} = E_n + k(\sigma_n - \sigma_{n-1})$$

suggests that the Young’s modulus of the following iteration be incrementally changed based on the difference of the calcualted reference stress. The advantage of this method is noticeable as it only requires a few iterations to converge to a solution. The factor *k,* which needs to be bigger than 1, is a constant which determines how big the incremental jumps will be. Additionally, a maximum and a minimum value of the Young’s modulus need to be appointed, outside of which the E modulus is kept constant. The E_{min} is set in order to avoid the Emodulus becoming a negative value and assuring a proper functioning of the FEM solver. The E_{max} is given so as to diminish the influence of stress peaks in areas of point loads or other singularities such as cracks or notches (Baumgartner, 1992).

The downside of the previous two methods is the chance to overshoot the optimal design by increasingly dispersing the stresses within the component, leading to parts which are discontinuos and unmanufacturable. A resolution of this problem presents itself in the global stress-increment-controlled method, given below:

$$E_{n+1} = E_n + k(\sigma_n - \sigma_{ref})$$

Figure 27. flowchart of the SKO method (adapted from: Mattheck, 1999)

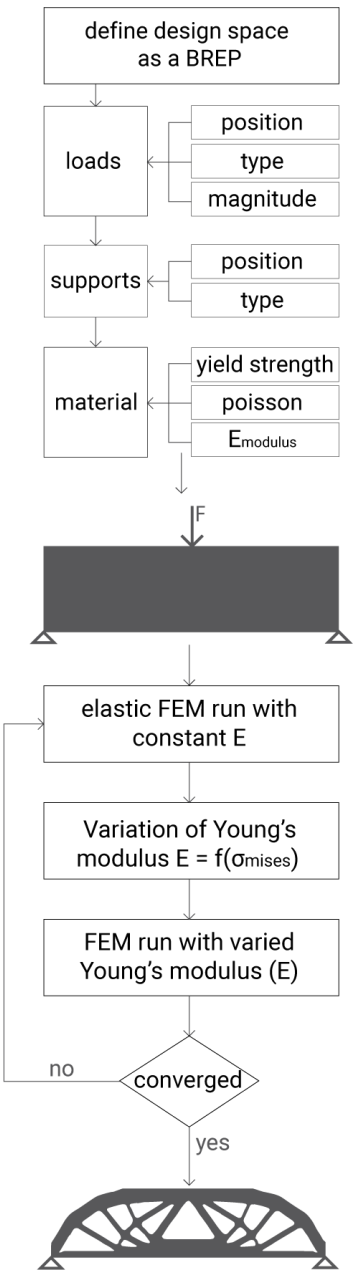

Where σ_{ref} stands for a global reference stress which is wanted as the maximum allowable stress within the working state of the component. It represents the uniform stress value after which the axiom of uniform stress is named, and to which all living structures tend to, according to Mattheck (1999). Few recommendations for implementing this formula are given by the author, first of which is to initially set σ_{ref} to a low value, and increase it up to a working stress value in each iteraiton. The second recommendation is to again define a bound of E modulus (a maximum and minimum) value as that leads to a better conversion. The value E_{max} should be set equal to the original stifness of the material.

Figure 28 gives a comparative view of the results emerging after the implementation of the previously discussed methods, on an example of a canteliver beam loaded at its end with a point load.

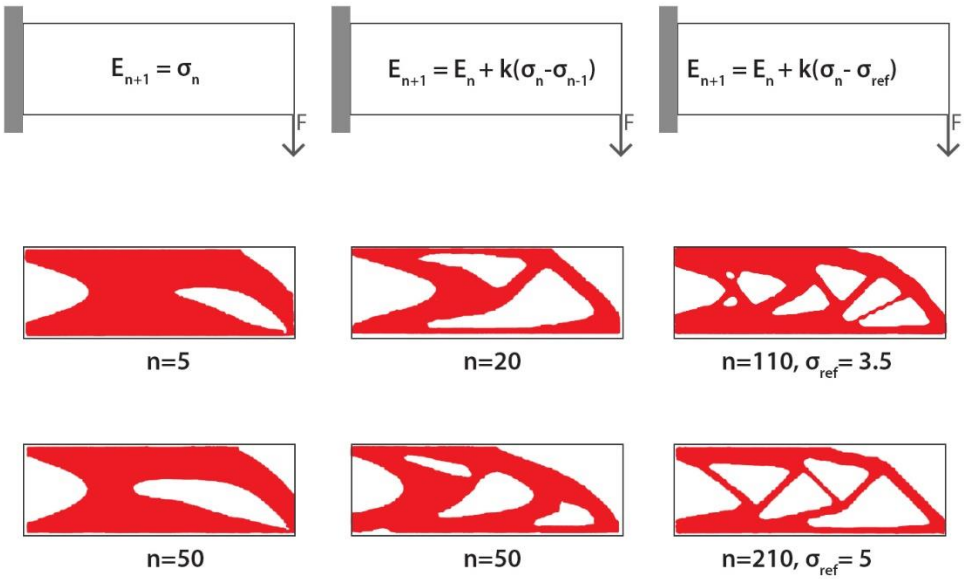

Figure 28. Results of various SKO mathods demonstrated on a cantilever beam. **Left:** stress method; **middle:** local increment method; **right:** global increment method (source: Mattheck, 1999)

All three SKO algorithms result in designs with material only in load-bearing places, but may still contain local stress concentrations, a.k.a 'notch stresses' which need to be resolved using the CAO method.

CAO:

A standalone method, but also a complementary method to SKO is the Computer Aided Optimization, first proposed by Claus Mattheck and developed at the

Karlsruhe Research Centre (Mattheck, 1999). The method is based on an earlier explained phenomenon present in trees and bones, in which growth occurs at zones of exceptional load, and shrinkage occurs at zones lacking load of any kind. The CAO procedure is summarized by the provided flowchart Figure 29, and is explained in a stepwise manner in the following section:

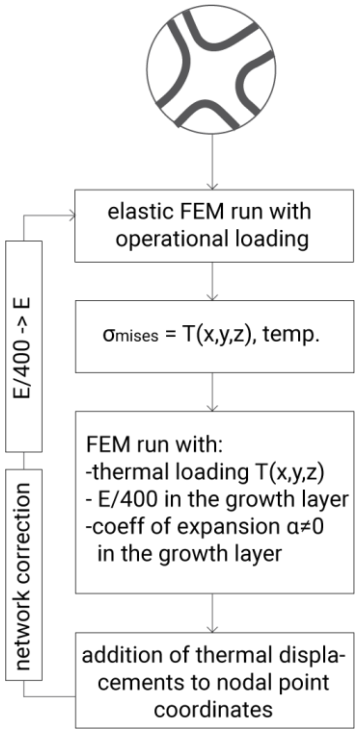

Figure 29. Flowchart of the CAO method (source: Mattheck, 1999)

1.The draft structure previously obtained by SKO is set up for a Finite Element Analysis. If possible , the the FE mesh should be finer in the zones where notch stresses occur, which is expected at the boundaries of the mesh, since those are the areas where later "growth" is expected to occur.

2. The Finite Element Analysis will yield information about nodal displacements for every elements of the mesh, along with stresses, of which we are interested in the VonMises stresses, which are used as a reference stress in the following step.

$$\sigma_{mises} = \frac{1}{\sqrt{2}}\sqrt{(\sigma_1 - \sigma_2)^2 + (\sigma_2 - \sigma_3)^2 + (\sigma_3 - \sigma_1)^2}$$

3. At this stage, the computed VonMises stresses are set formally equal to the temperature distribution within the component. The parts experiencing the highest stress will have the maximum temperature. This temperature distribution does not relate to any actual measures (even though Mattheck suggests that the material does get warmer at point of locally high stress), but is proposed as a workaround to simulate the later 'growth' process. Moreover, the Young's modulus of the Finite Elements on the surface is set to 1/400th of the original value, and the coefficients of thermal expansion (α) is set to be larger than 0. In this manner a 'soft' surface layer where stresses occur was produced, and a 'stiff' inner layer where no growth is expected.

$$T_{ref} = \sigma_{ref}, \quad E = \frac{E_0}{400}, \quad \alpha > 0$$

4. Now, another FEM analysis is performed, but the mechanical load is set to 0, as we want to only take into consideration the thermal load. During this phase, the soft upper layer will get displaced based on the temperature distribution, and is what Mattheck (1999) reffers to as 'growth'. The zones on which the largest thermal load was mapped with get displaced most intensely, i.e. they will grow the most. The displacement is calculated incrementally, similarly to SKO:

$$\Delta l = l_0 \cdot \alpha \cdot (T - T_{ref})$$

Where T_{ref} = σ_{ref} i.e. the desired maximum experienced operational stress within the component.

5. After a small ammount of iterations the material is homogenized by setting the E modulus to be equal throughout the entire component. A final FEM analysis is performed to see how effective the growth was and notice the more homogeneous stress distribution throughout the design.

6. If an existance of notch stresses is still observed, the steps from 3-5 are to be executed again until there is an even stress distribution throughout the component.

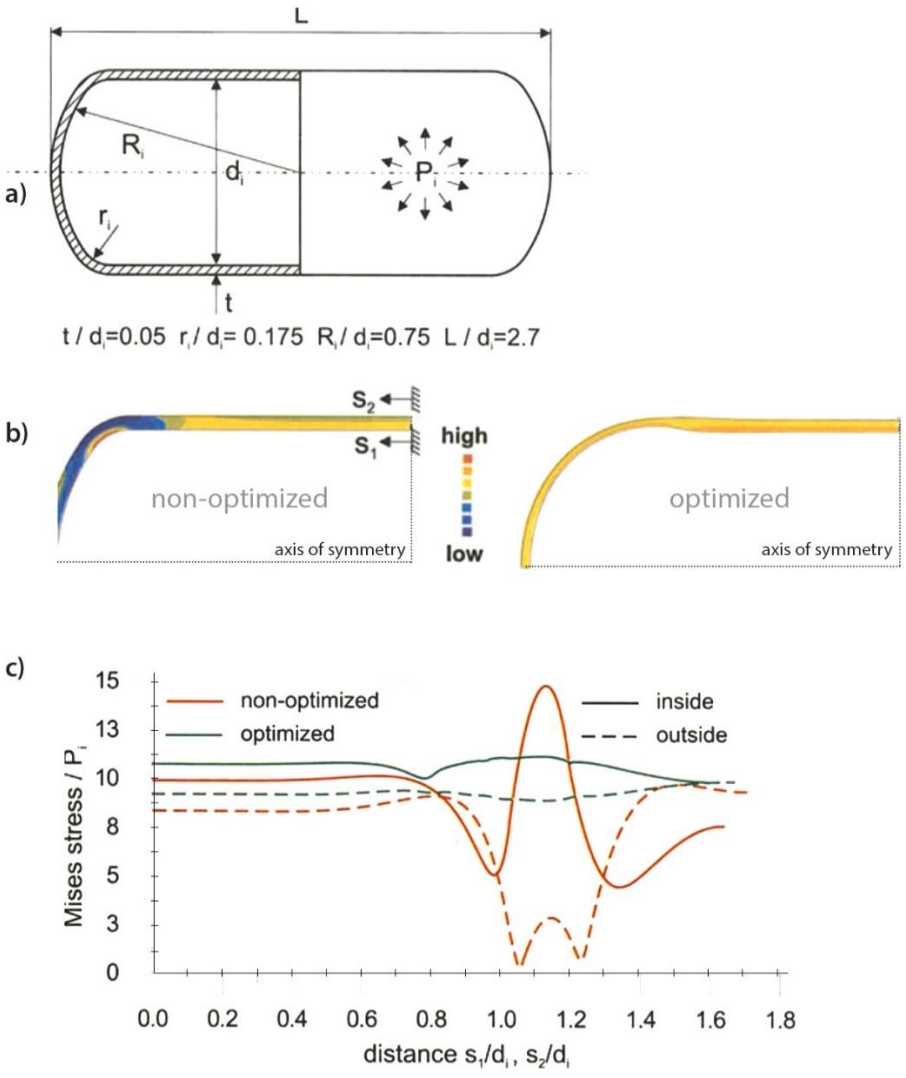

Figure 30 Application of the CAO method for the optimization of the walls of a cylindrical pressure vessel shown in a); b)von mises stress distribution; c)misses stresses along the internal and external contour (source: Mattheck, 1999)

Conclusion:

After exploring various methods for topology optimization of structures, it was decided to pursue the implementation of SKO and CAO methods due to several reasons which will be elaborated in this section:

One of the key ideas of integration Topology Optimization into architectural design, was the integration of this tool within the standard workflow of architects, which includes 3D modelling software such as Rhino. The simplicity of Heuristic algorithms makes them more understandable and intuitive to designers. In addition, most Optimality Criteria methods require specialized 3rd party software to conduct the required FEM analysis, whereas methods such as SKO and CAO rely on standard FEM packages to perform the analysis. In addition to this, the simplicity of these methods makes them very easy to implement and code independantly, even without using code, but rather visual scripting such as Grasshopper.

It was observed that the success of both types of methods relies heavily on the propper formulation and setup of the optimization problem. Optimality criteria methods have a higher degree of complexity due to a possibility of having numerous design variables among which a global minimum is harder to find. Heuristic methods, which usually deal only with one variable are more likely to converge to a global optimum for a described problem, but this however does not guarantee an overal more optimal design.

Furthermore, the final outcomes of most Optimality Criteria methods, which utilize gradients and thus sensitivity analysis, require post-processing to achieve a vectorized result. For example, if we consider the density SIMP approach, the way to achieve a discrete output is to tweek the the sensitivity threshold after the final convergence, albeit this idea only works for problems with a single constraint (Ole Sigmund, 2011). In contrat, Heurstic methods, mostly working in binary states (presence/absence of material) produce a vectorized output at every step of the process, and in every iteration.

In his reserch on the comparison between the two types of algorithms Sigmund(2011) elaborates on several applications where standard TO gradient methods fail, such as problems with a multitude of local minima, disjoint design spaces or discontinuous problems which are difficult to smoothen.

2.3.4 Topology Optimization Software

At a certain point during this research a short investigation of the various topology optimization software was conducted. This was done so as to gain insight into the funcionalities one such tool would need to posses as well as choose a software for verifying the results obtained by the methods proposed by this research.

Millipede:

Millipede is a Grasshopper plugin developed by Sawapan focused on optimization of structures. At its core is a library of fast structural analysis algorithms for linear elastic systems. The topology optimization feature uses the homogenization method, and due to its speed can be used in conjunction with Galapagos for solving various form finding problems. Alongside shells and 2D structures, its functionality also extends to 3D problems. The interface is intuitive, although it takes a bit of time to set up the model and all the parameters before the optimization can be executed.

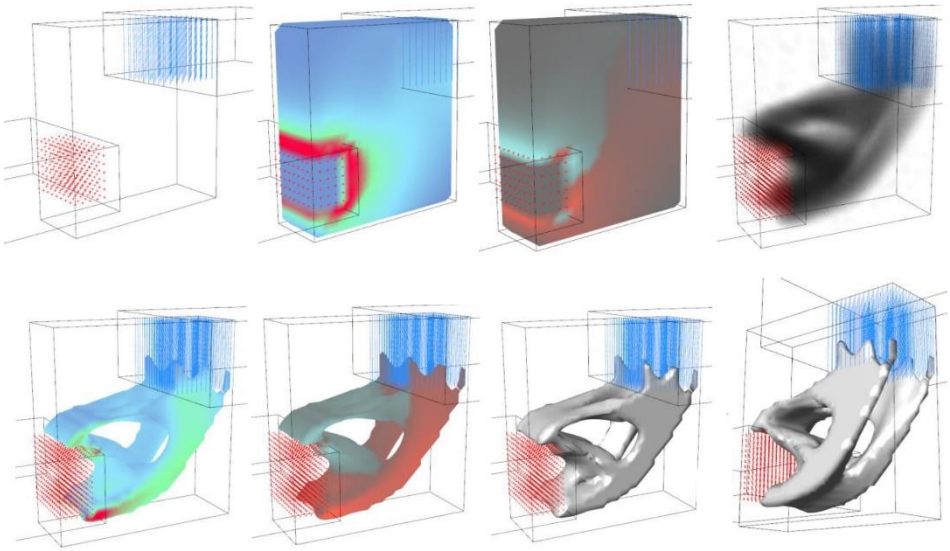

Figure 31. Three dimensional topology optimization in Millipede (source: sawapan.eu)

Topostruct:

Topostruct is a standalone software developed by Sawapan and is tailored towards architects and designers, allowing them to get more familiar with topology optimization. It is very easy and intuitive to use as the user only needs to specify the dimensions of the design space, the attributes of the loads and supports, and the volume fraction constraint. It has a variety of options for visualizing results,

helping the user gain a better understanding of the outcomes of the optimization procedure and get acquainted with the method.

TopOpt:

TopOpt is a standalone app as well as a grasshopper plugin for 2D topology optimization of continuum structures based on the SIMP method. Its development is a join effort of Technical University of Denmark, Israel Institute of Technology, and Aarhus school of Architecture. The solver is based on the 99-line Matlab code for basic mechanical topology optimization proposed by professor Ole Sigmund from DTU (O. Sigmund, 2001). The application, although working only in 2D offers the user the ability to change many parameters mid-optimization and view the consequences such changes have on the final outcome.

Ansys:

Ansys is a commercial software package for structural and mechanicial multiphysics simulations. This standalone software is capable of performing topology optimization using the SIMP method along with shape and size optimization. It is available through a student licence altough with limited functionality. It is currently the most widely used FEM analysis environment and is ISO 9001 certified. The program allows for importing geometries from other software as well as in-place modelling.

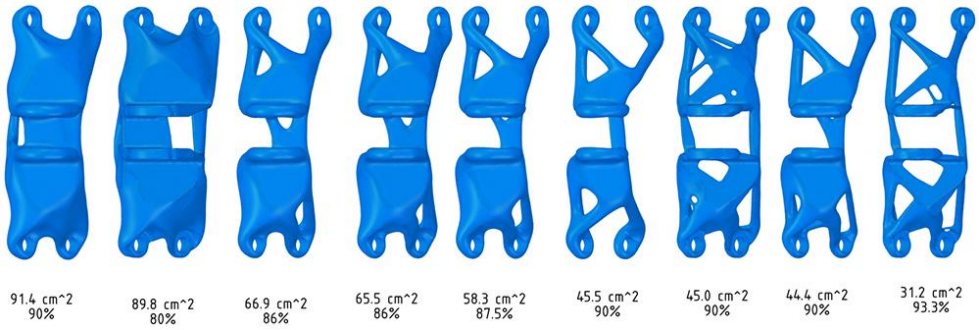

Figure 32. Topology optimization of a bracket within Ansys. A case where target mass is varied and other constraints are fixed. (source: ansys.com/blog/real-time-generative-design-drives-innovation)

Karamba3D:

The Karamba3D plugin for Grasshopper has embedded components for topology optimization of 2D beam, truss geometries, and shells based on the BESO method. In order to analyze continuous geometries, they are discretized into beams through the creation of a triangular mesh grid from which the edges are extracted. The output of the component is an optimized structure with a desired volume fraction, in which only the utilized beams are left active, while the remaining beams are

culled. The component does require a bit of time to be set up in a way which yields reasonable results.

Altair Optistruct:

This commercial topology optimizer is part of the Altair HyperWorks engineering software package. It it is capable of performing size, shape, and topology optimization along with multiphysics FEM analysis, making it a very popular software with numerous real life applications and successful implementations. The topolgy optimization is based on the SIMP method. The complexity of use of the program is justified by the ability to fully control and adjust every aspect of the optimization procedure.

BESO by RMIT:

The Python scripts developed by Zuo & Xie (2015) take advantage of FEA capabilities of Abaqus software to provide a topology optimization method which can be implemented in a variety of CAD software. The code, based on BESO, performs stiffness optimization, and is freely available for academics. The sccessful use of the optimization method requires manual input of parameters within the code, but is susceptible for integration within the parametric design workflow.

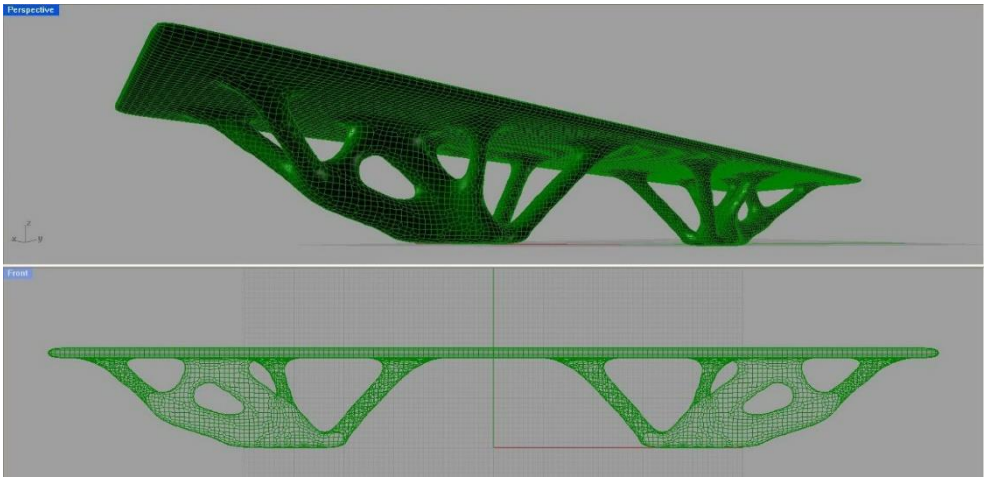

Figure 33. Implementation of BESO3D within Rhino for a conceptual design of a bridge (source: http://www.360doc.com/content/16/0509/09/30514273_557475935.shtml)

Ameba:

Ameba presents an implementation of the previously mentioned BESO Python code within the Grasshopper environemnt. It was developed by XIE Technologies, led by proffessor Yi-Min Xie. It was developed in a way to be intuitive and easy to

use. The optimization process takes advantage of cloud computing and requires a licence to be run.

software	environment	method	availability	2D/3D
Millipede	grasshopper	homogenization	free	2D&3D
Topostruct	standalone	homogenization	licenced	2D&3D
TopOpt	grasshopper	SIMP	free	2D
Ansys	standalone	SIMP	licenced	2D&3D
Karamba BESO	grasshopper	BESO	free	2D
Altair Optistruct	standalone	SIMP	licenced	3D
BESO 3D- RMIT	Python	BESO	free	2D&3D
Ameba	grasshopper	BESO	licenced	2D&3D

Figure 34. Comparison of existing software for topology optimization (source: author)

Conclusion:

After getting first hand experience with the above mentioned topology optimization software several conclusions can be made. Firstly it becomes apparent that the SIMP and BESO methods are the most present within both commercial and non commerial software. The SIMP being and optimality criteria method is more prevelant in commercial software, while BESO being a heuristic method is more pevelant in applications geared more towards learning rather than actual industrial application. The programs differ largely from a user experience point of view making some of them more intuitive for use, while others require a lot of time setting up the analysis, which has its benefits if doing more meticulous problem solving with immediate real life application.

For the purposes of this research, a commercial software Ansys will be used in order to compare the results obrained by the methods proposed by this thesis.

2.3.5 Topology Optimization in AEC

The following text showcases several projects brought to fruition using Topology Optimization on large scale applications. The common thread between all of the project is the notion that the structural behavior and architectural design are combined to manifest objects of higher performance.

Illa de Blanes, Blanes, Catalonia, 2002:

One of the first attempts at using Topology Optimization on a larger scale is examplified by a never-realized project by Isozaki & Associates, designed with the help of Matsuro Sasaki Structural Engineering. The 75000m^2 multifunctional

complex for leisure, recreation and culture, called Illa de Blanes, is located on the coastal area of Girona (Costa Brava). The structure consists of a tree-canopy-like load bearing columns supporting the large elevated plateau, which is covered by double curved shell (Figure 35). The columns were designed using the 3D ESO method and were to be the most iconic piece of the resort, albeit never realized due to budget constraints. Isozaki designed the roof shell using the Extended ESO method (Januszkiewicz & Banachowicz, 2017)

Figure 35. Arata Isozaki and Matsuro Sasaki, 'Illa de Blanes', Blanes, Catalonia (source: Januszkiewicz & Banachowicz, 2017)

Qatar National Convention Centre, Doha, Qatar, 2011:

The QNCC (Figure 36) marks the first realized attempts of Arata Isozaki to implement his ideas of topologically optimized architecture. The main feature of the building are the structural columns simoblising the Qatari renowned sidra tree, which support the 250 meter long overhead canopy. Isozaki again used the Extended 3D ESO method for deriving the form of the columns, starting from a single block of metal.

Figure 36. QNCC exterior part of the topologically optimized columns (source: http://archdaily.com)

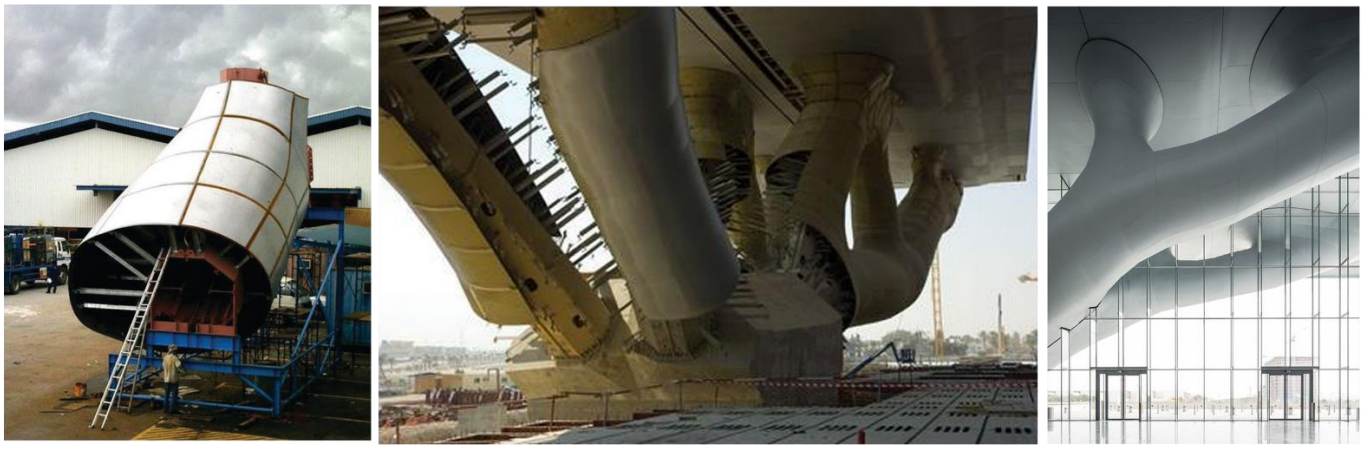

Figure 37. Assembly of the QNCC tree from steel structural elements. (source: building.co.uk)

Alongisde Buro Happold, the inital concrete columns were redesigned as a branching steel structure comprised of octagonal tubes which are covered with steel cladding (Figure 37). The initial design derived by Topology optimization did not take into accoutnt the manufacturability of the design, which resulted in a very expensive project with respect to engineering.

Akutagawa River Side Office Building, Takatsuki, Japan, 2004:

The office building, designed by Ohmori et. al depicted in Figure 38, came into being after an extensive research into the possibilities of using the extended ESO method on a large scale (Ohmori et al., 2004). The 10mx6m office building has topologically optimized load bearing facade walls on which the four floor slabs are supported.

The EESO procedure was applied on the south and west facades facing the street. Starting from a full concrete wall, the procedure removed material from non load-bearing zones and added material in zones of high stress. The FEM analysis included multiple load-cases such as live loads, dead weight, and loads due to earthquakes. The result is an expressive facade with minimized usage of concrete, allowing for more glazing area.

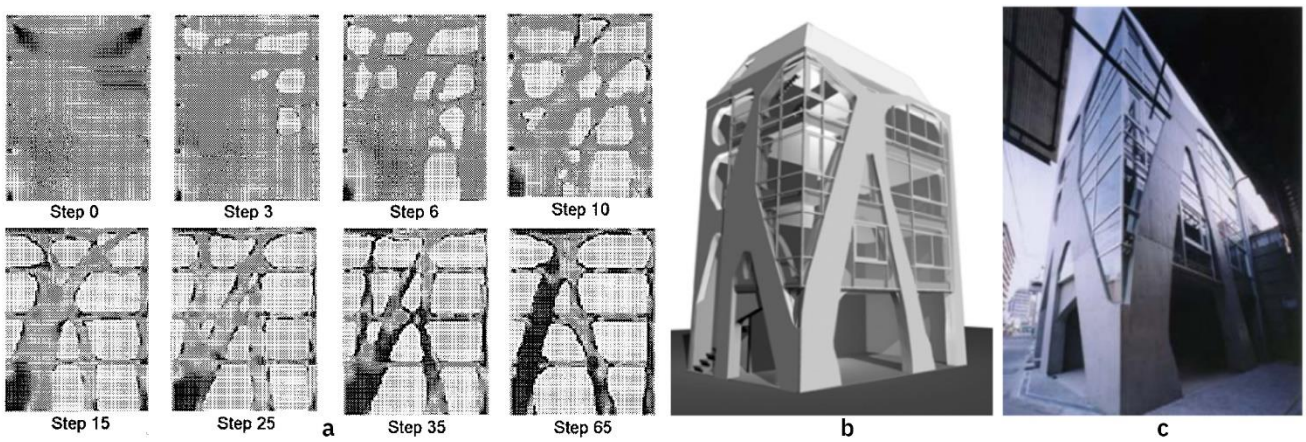

Figure 38. a) EESO method; b)3D model of the final building; c) realized state. (source: Ohmori et al, 2004)

Pedestrian bridge, Melbourne, Australia:

Topology optimization is becoming a standard tool used by bridge designers. An australian office, BKK architects in accordance with RMIT university in Australia, were comission to design and construct several pedestrian bridges crossing the highway. The design brief called for 65m spanning pedestrian bridges, which would also have a sculptural quality with which to enrich the context (Xie et al., 2011). The team initially used the BESO topology optimization method to research the way in which different support conditions might influence the design of the bridges (Figure 39). The results of this research became the inspiration and the starting point for the architectural design of tubular pedestrian bridges. The proposed tubular forms which were further optimized using the same TO method to achieve reduction of material use and reduction in mass. This was important as the production of the bridges is envisioned through 3D printing of interconnected segments with embedded reinforement, for which the Felicetti Consulting Engineering are currently making tests (Figure 40).

Figure 39. influence of support conditions on TO results by BESO a) both supports pinned; c) one pin and one roller support. (source: Xie et al., 2011)

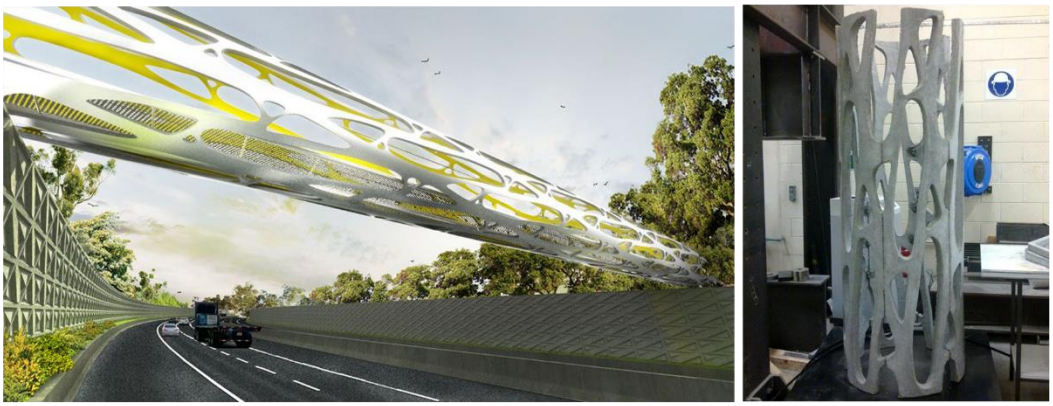

Figure 40. visualization of the bridge and the 3D printed concrete prototype of a bridge segment. (source: Xie et al., 2011)

Unikabeton Project, Aarhus, Denmark, 2007:

As part of their research into the use of Topology Optimization in architecture, Aarhus School of Architecture realized the Unikabeton project (Figure 41). The aim of the research was to design and construct a project showcasing a successful integration of generative design and robotic fabrication. The result is a 12x6x3m double curved canopy structure derived by the use of a SIMP method for topology optimization. The obtained geometry was manufactured by using reinforced concrete casting in EPS moulds and would not have been possible in traditional manufacturing methods. The canopy, which rests on three slender colums has a 60% reduction of material in comparison with the same structure designed and constructed in traditional manner. It served to start a discussion about the possible CO2 emission reductions in the construction industry by using topology optimized structures, as well as about the viability of new construction methods which would support such new tectonic forms (Naboni & Paoletti, 2018).

Figure 41. the concrete canopy prototype of the Unikabeton project (source: insider.altairhyperworks.com)

Conclusion:

The previously exemplified projects are but a few samples of how topology optimization is used in the domain of architectural engineering and construction. They aim to show the possibilities and limits of using TO methods on a large scale.

A primary conclusion which stands out from researching these project is the importance of considering the manufacturing and construction of the design during the optimization process. Even though the final geometry may lead to cost reduction from a material usage standpoint, a project may still end up being expensive due to engineering costs and costs of construction. Since Topology Optimization inherently yields novel and organic tectonic forms which are not suitable for traditional construction techniques, it necessitate innovative techniques such as customizable molds or 3D printing.

In addition, all project recognize the fact that optimal design forms can not be obtained solely through structural optimization, and require a successful integration of other design criteria and other disciplines including, but not limited to, thermal comfort, acoustics, lighting, social aspects, manufacturability etc.

Majority of project start out by taking inspiration from nature and recognizing the extreme resource efficiency with which it constructs. This realization by the project architects has geared them towards pursuing the idea of sustainable architecture through resource efficient construction, which leads to ecological and economic success.

03. DESIGN

[speaking about her experience on the Galapagos islands] "...I watched a quiet engineer named Paul stand motionless before a mangrove as if in deep conversation. He finally called me over and pointed: 'This mangrove needs fresh water to grow but its roots are in saltwater, which means it somehow desalinates using only the sun's energy. No fossil fuels, no pumps. Do you know how we do it? We force water through a membrane at 900psi, trapping salt on one side. When it clogs, we apply more pressure and more energy.

Then Paul asked the question I've been working to solve ever since: 'How is it that I, as a desalination engineer with a five-year degree and twenty-year experience, never once learned how nature strips salt from water?' ". (Benyus, 2009, pp.200)

3.1 Introduction

The following section of the report is aimed at presenting the results of the proposed SKO approach to topology optimization. Firstly, the design workflow will be elaborated. This part is aimed at showing how the user creates the design space within which the final design will occur, and to what extend he can influence the optimization process. This is done in order to illustrate the usability of the proposed tool.

Secondly, the results of several 2D toy problems will be presented, namely that of a cantilever beam, simply supported beam and continuous beam. Each toy problem has been tested with 6 different methods: 2 different reference stresses x 3 methods of caluclating the new young's moduli for the next iteration. The best results of each method have been compared to a comercially available software Ansys to draw conclusions about the validity of the proposed method. These toy problems served the purpose of finding the best overall method which yields the most satisfactory results before moving onto the 3D problems.

The 3D problems presented in this report start from simple and move towards more complex ones. Firstly a ground floor house with just one room is ran, after which a single story house with a single door and a window was tested. Lastly a house with an added staircase and balcony was optimized using the proposed method.

3.2 Design workflow

It was very significant that the developed tool ends up being easy to understand and to use. For that purpose the number of user inputs has been kept at a minimum, and only the inputs which greatly influence the final output have been left to the user to specify.

Figure 42 gives a detailed overview of the grasshopper script and outlines the inputs which are required by the user. A detailed explanation of the Python code embedded within the GH_Python and C_Python components of the script has been provided as an appendix to this report.

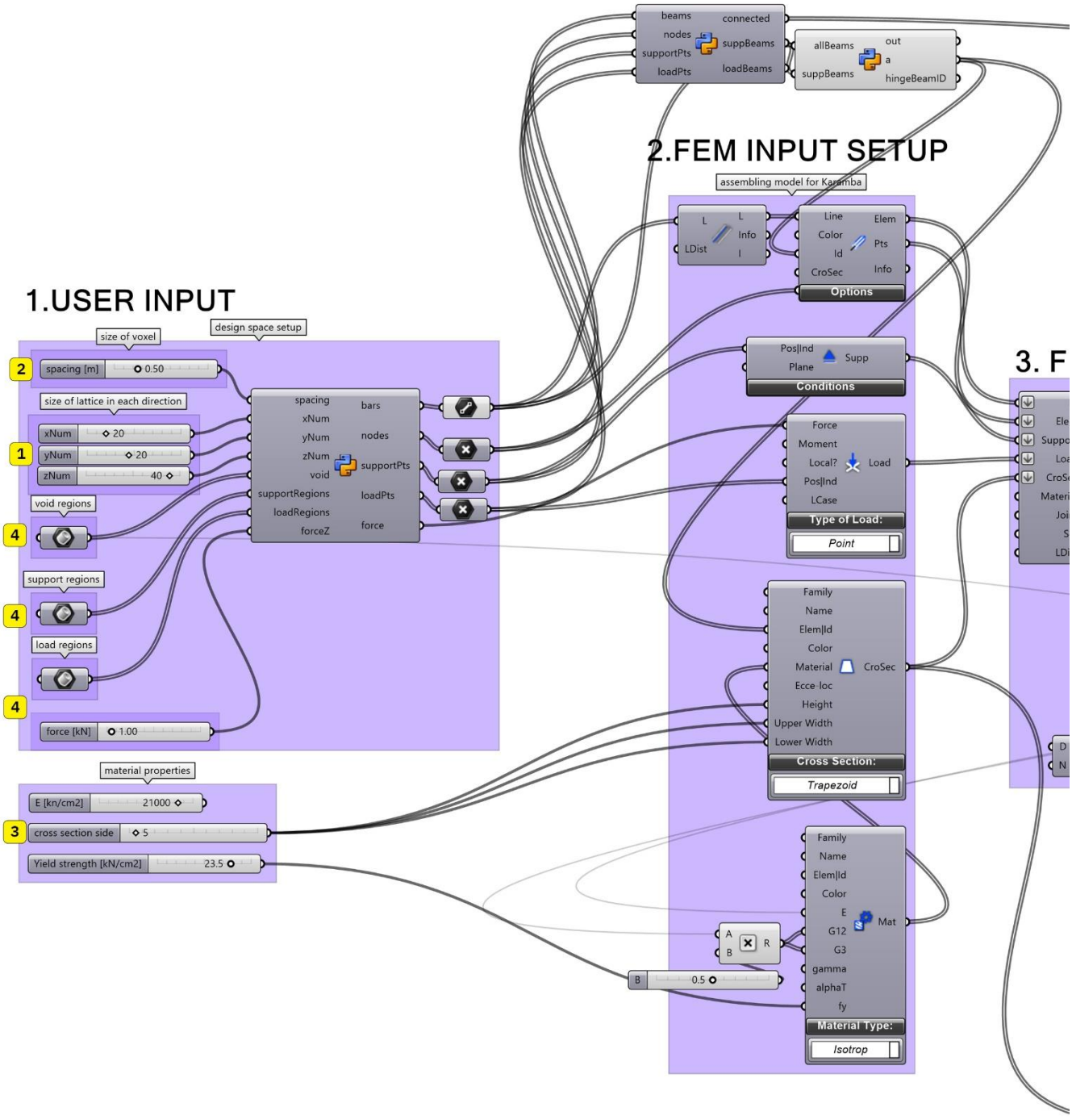

Figure 42a. Screenshot of the Grasshopper script with marked components that require user input (part I)

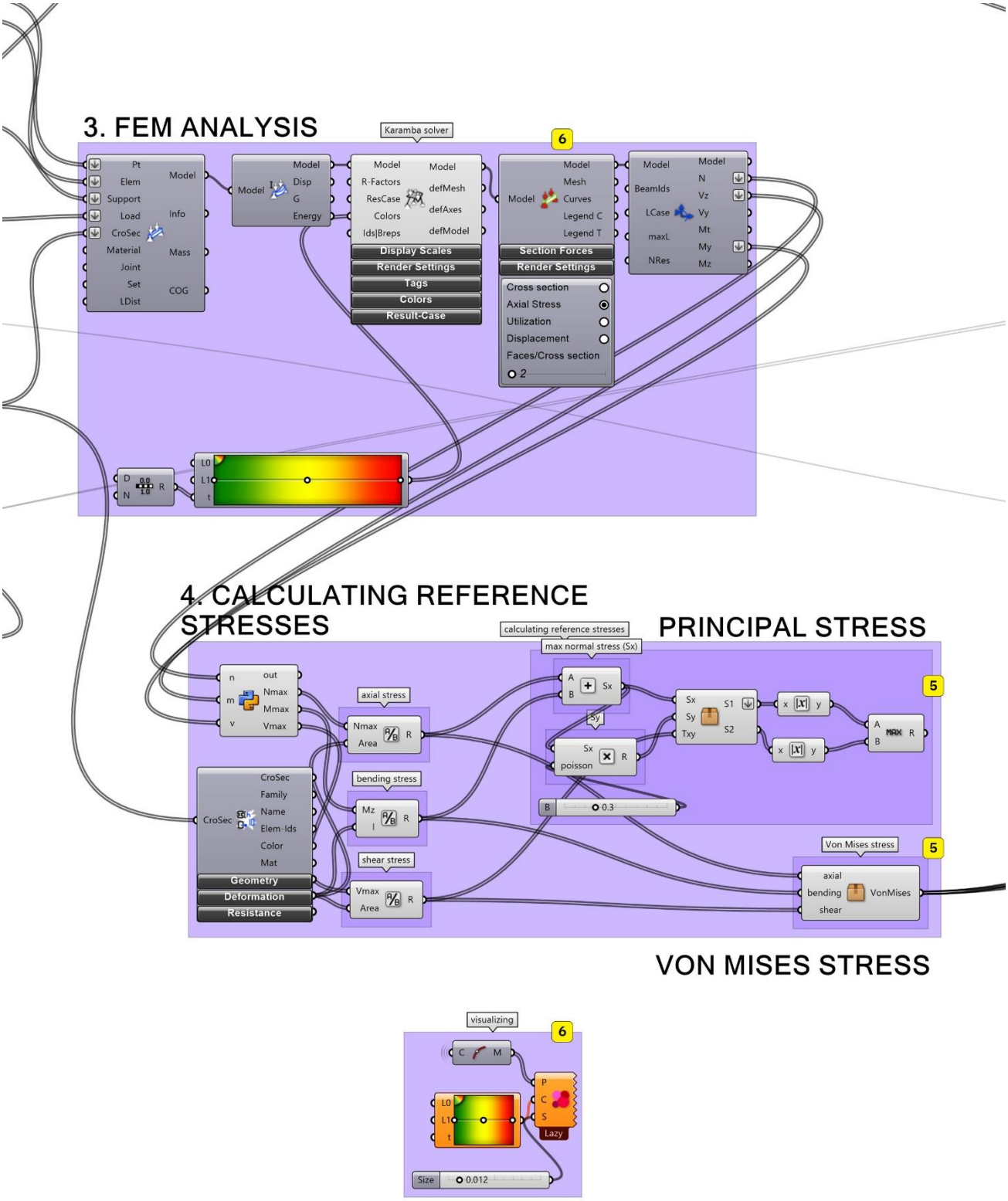

Figure 42b. Screenshot of the Grasshopper script with marked components that require user input

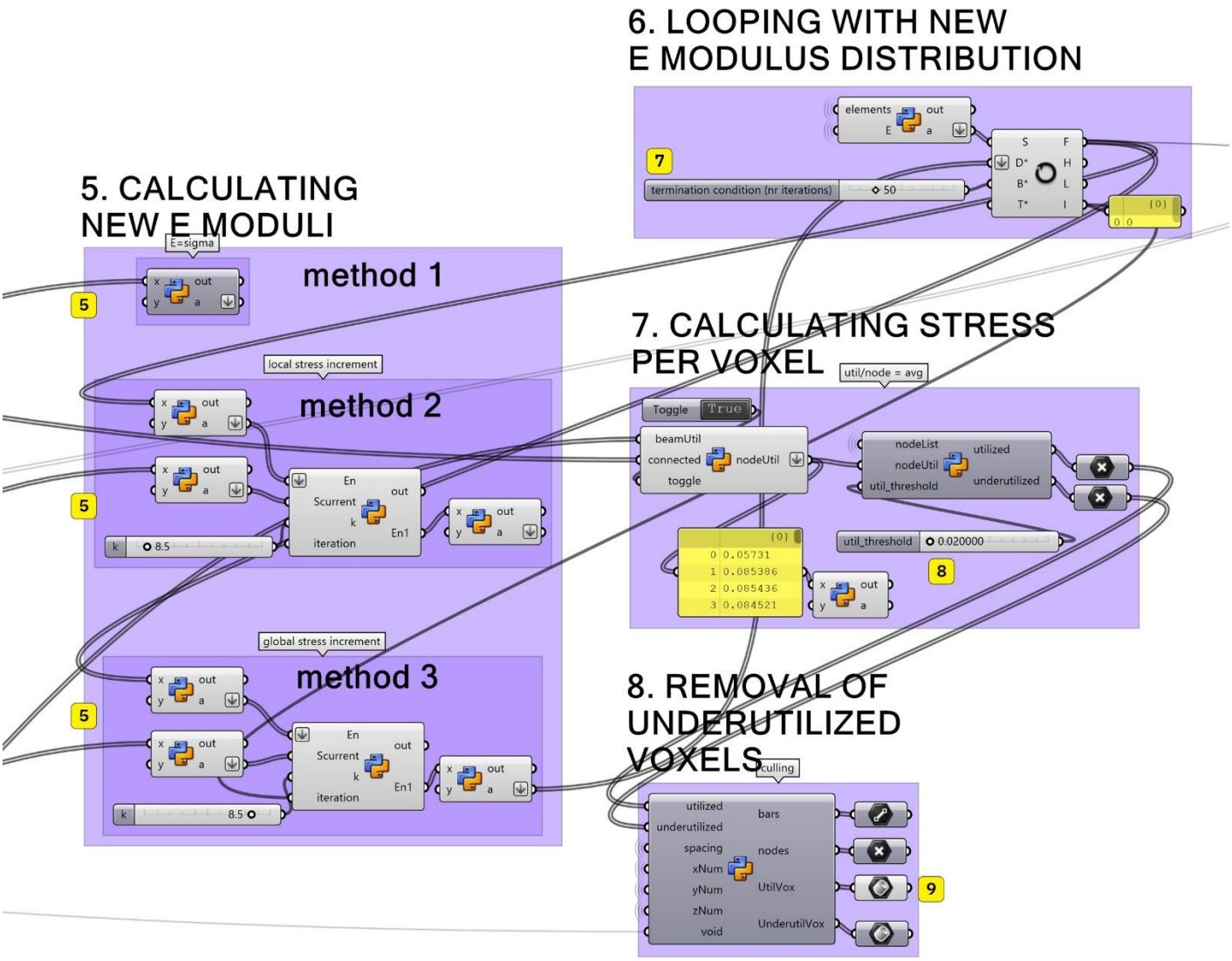

Figure 42c. Screenshot of the Grasshopper script with marked components that require user input (part III)

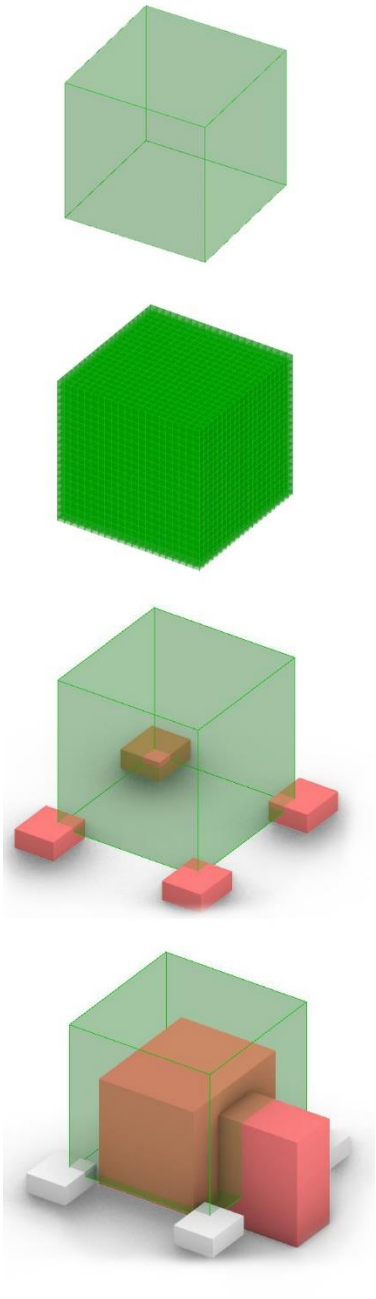

Figure 43. top to bottom: sizing of the design space; voxelization; support zones; void zones; load zones; visualizing stresses; final result of the procedure.

1. The user starts off by specifying the dimensions of the space within which the final design is to occur. The designer is prompted to input the X, Y and Z coordinates of this design space. If the Y coordinate is left at 0, the domain becomes 2D and the solver will run a twodimensional topology optimization. The general rule is that the design space should always be bigger than the expected design but never smaller. This is because the underutilized voxels will be culled away in any case.

2. Next, the user is expected to input the resolution of his design with which the design space will be discretized. Lower resolutions produce coarser results but converge faster, while higher resolutions produce smoother results and are better representation of a continuous space. However increasing the resolution exponentially increases the computation time. The chosen resolution depends on the type of problem being solved.

3. The design space is thus subdivided into voxels (volumetric pixels). In order to ensure that such a voxelized volume behaves as a solid block of material, the voxels are interconnected into a lattice of beams. Thus the latter FEM is performed on the beams of the lattice and not on the voxels themselves since there are no freely available volumetric FEM solvers. At this point the user is required to input the material properties of those beams

4.The last step of the design space assembly is the input of support regions, load regions and void regions. The user specifies these constraints by creating brep geometry and inserting it in the desired location within the design space. Additionally, before the FEM analysis is performed, the user specifies the desired degrees of freedom for the support regions and the load intensity for the loaded regions.

5. At this point the FEM analysis is already automatically run and the Von Mises and Principal reference stresses are calculated. In order to start the iterative process of refinement described by the SKO method, the user should chose one of the two reference stresses, as well as one of the three methods for convertion the stress distribution into the E modulus distribution of the next run.

6. Visualizing the displacements, and stresses of the non-optimzied design can be visualized using Karamba3D native components. Additionally, the calculated reference stresses can also be visualized using standard grasshopper components.

7. Choosing the number of optimization iterations also requires input from the designer. The suitable number of iterations varies for different methods, but through testing it was observed that for method 1 ($E_{n+1}= \sigma_n$) around 200 iterations is enough. For method 2 (local stress increment method) between 50 and 100 iterations is sufficient, while for method 3 (global stress increment method) good convergence is achieved even after 25 iterations.

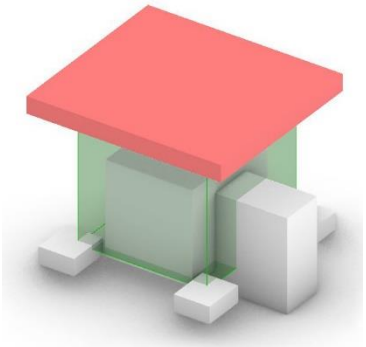

8.The resulting stress per voxel is calculated as an average of the adjoining beams. Before visualizing the results, the user of the script needs to specify a stress threshold below which voxels will be culled away, and only the voxels having a stress value above the threshold remain.

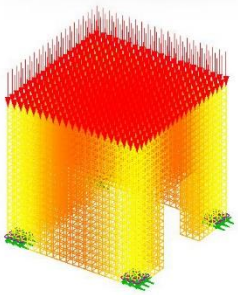

9. The final output can be visualized both as a beam lattice or as an aglomeration of voxels. The beam lattice can be assed through an FEM solver to validate the structural performance of the obtained results. The voxelized geometry can be baked into rhino for further manipulation.

The final visual outputs given to the user of the tool by the Grasshopper tool within the Rhino working environment are shown in Figure 43, exemplified by the TOY problem of a single room house with a side entrance.

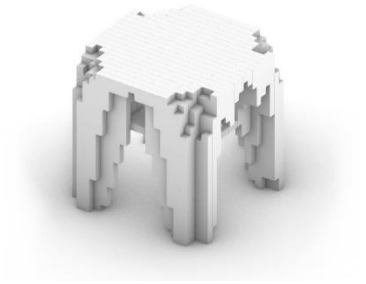

3.3 TOY problems

This section will elaborate on the results obtained from applying the proposed SKO method on twodimensional problems: a cantilever beam, a simply supported beam, and a continuous beam. The main aim of the 2D tests is to determine which method and parameter setting yield the best results and should be taken towards solving 3D problems. For the sake of checking the validity of the results a qualitative and quantitative comparison will be made with results obrained by a commercial software ANSYS which uses the SIMP method.

3.3.1 2D beam setups

The three two-dimensional toy problems share several commonalities in their setup. Namely, all three design spaces were discretized into a lattice of beams with the length of 5cm and cross-sectional dimensions of 4x4 cm. The voxel size i.e. resolution in all three cases was 5x5x5cm. Similarly, the material properties used in all three problems were that of structural steel S235 with a young's modulus (E) of 21000kN/cm^2 and a Yield strength (fy) of 23.5kN/cm^2. The applied load in cases of a cantilever and simple beam was 15 kN, while in the case of a continuous beam it was 100kN/m. The support conditions differ for each case. The cantilever beam is held by a fixed support running along its left edge, the simple beam has a single pin support and one roller support, while the continuous beam has a single pin support in the left corner while the other two supports are rollers.An overview of the design space setup for each toy problem can be observed in Table 1 while the placement of the applied loads and supports can be seen in Figure 44.

Table 1. overview of the inputs used for the toy problems

	Dimensions [m]	Load	supports	voxel size [cm]	Material properties		
					E [kN/cm^2]	Cross section	Yield strength
Cantilever beam	4.5 x 1.2	15kN	fixed	5x5x5	21000	4x4cm	23.5 kN/cm^2
Simple beam	4.5 x 1.2	15kN	pin + roller	5x5x5	21000	4x4cm	23.5 kN/cm^2
Continuous beam	6 x 1.5	100kN/m	pin + 2 rollers	5x5x5	21000	4x4cm	23.5 kN/cm^2

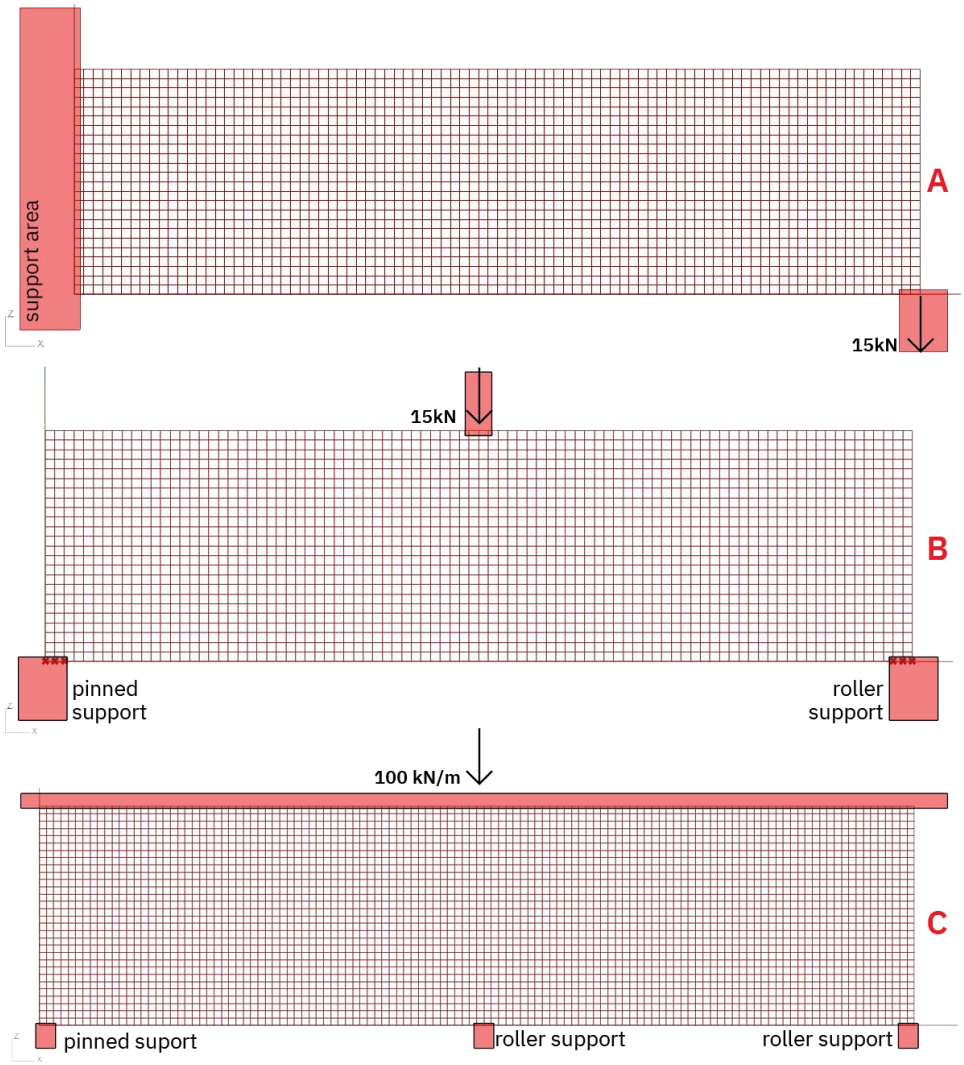

Figure 44. setup of the toy problems within the Rhino environemnt. A)cantilever beam; B) simply supported beam; C) continuous beam

All of the toy problems have been analyzed using Karamba 3D native components for assemblig the FEM model, and the FEM solver which was used employs the first order theory for small deflections.

The required Von Mises and Principal reference stresses have been calculated in all three cases in the same manner. In order to derive those reference stressese, the axial, bending, and shear stresses were calculated in the following manner:

$$\sigma_{axial} = \frac{F_{axial}}{Area}; \quad \sigma_{bending} = \frac{M_z}{I}; \quad \tau_{shear} = \frac{V_z}{Area}$$

where F_{axial} are the maximum axial forces of all beam elements, M_z is the moment around the local Y axis of each beam, I is the moment of inertia around the local Y axis, and Vz are the maximum shear forces in the local Z direction of all beams.
The resulting Von Mises stress criterion has been calculated by the following equation:

$$\sigma_{vm} = \sqrt{(\sigma_{axial} + \sigma_{bending})^2 + 3\tau_{sh}^2}$$

Additionally, the resulting principal stresses were obtained via the following equation:

$$\sigma_{pr} = \frac{\sigma_x + \sigma_y}{2} \pm \sqrt{\frac{(\sigma_x - \sigma_y)^2}{2} + \tau_{xy}^2}$$

Where σ_x and σ_y are the maximal normal stresses for each beam in the local x and y direction. The σ_x is obtained through concatenation of the maximum axial and bendind stresses ($\sigma_{axial} + \sigma_{bending}$) while the σ_y was approximated by multiplying the maximal normal stress σ_x by the poisson ratio of the material, which in this case was 0.3.

In all simulations the total number of iterations has been set to 200. The results of each previous iteration were recorded and later compared in order to see at what point the design converges to a stable configuration.

3.3.2 2D beam results

Each of the TOY problems has been tested with 2 different reference stresses, and three different methods for converting the reference stresses to the new E modulus distribution. This makes 6 different simulation setups for each toy problem, and 18 simulations in total. The following pages give an overview of the best results obtained from each of these 18 simulations. After this overview, the results will be elaborated on and compared, ultimately leading to the choice of a method to be used for 3D application. Several observations about the simulation setup settings and their impact on the results will be made before proceeding to the verification of the method against a comercially available software – Ansys.

TOY1 – CANTILEVER BEAM

TOY1.1 - reference stress= VonMises, method: $E_{n+1} = k * \sigma_n$

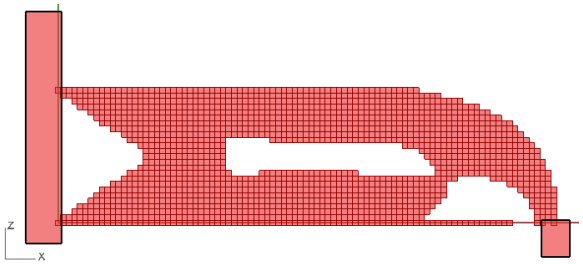

Culling after **iteration 200**: min σ_{vm} /node=2.4e-7; max σ_{vm} /node=1.556; avg σ_{vm} /node= 0.117; Threshold= 0.0754

TOY1.2 - reference stress= VonMises, method: $E_{n+1} = E_n + k(\sigma_n - \sigma_{n-1})$

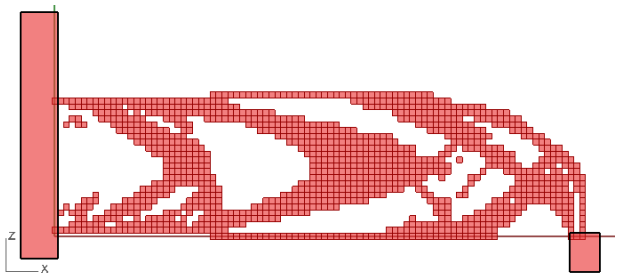

Culling after **iteration 200**: min σ_{vm} /node=1.7e-8; max σ_{vm} /node=1.18; avg σ_{vm} /node= 0.117; Threshold= 0.85

TOY1.3 - reference stress= VonMises, method: $E_{n+1} = E_n + k(\sigma_n - \sigma_{ref})$

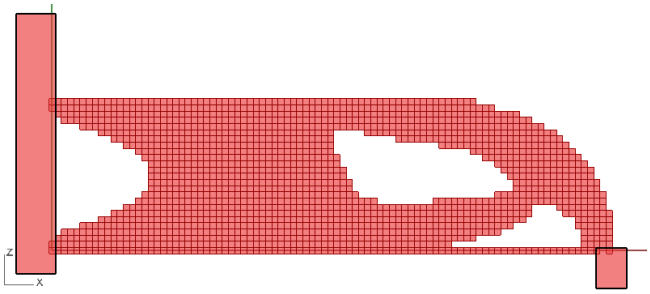

Culling after **iteration 200**: min σ_{vm} /node=2.4e-11; max σ_{vm} /node=1.155; avg σ_{vm} /node= 0.1152; Threshold= 0.75

TOY1.4 - reference stress= Principal stress, method: $E_{n+1} = k * \sigma_n$

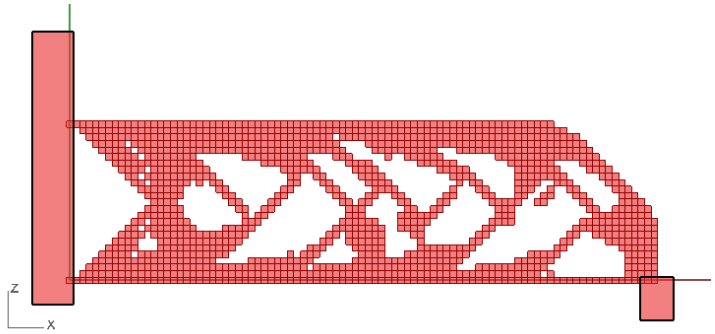

Culling after **iteration 200**: min σ_{pr} /node=0 kN/cm^2; max σ_{pr} /node=1.49 kN/cm^2; avg σ_{pr} /node= 0.083 kN/cm^2; Threshold= 0.031 kN/cm^2

TOY1.5 - reference stress= Principal stress, method: $E_{n+1} = E_n + k(\sigma_n - \sigma_{n-1})$

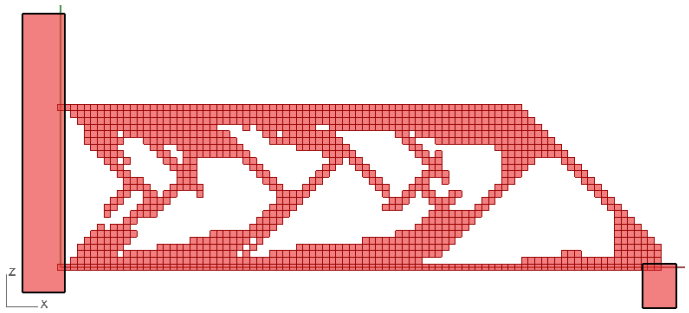

Culling after **iteration 200**: min σ_{pr} /node=7.15e-9 kN/cm^2; max σ_{pr} /node=1.49 kN/cm^2; avg σ_{pr} /node= 0.084 kN/cm^2; Threshold= 0.032 kN/cm^2

TOY1.6 - reference stress= Principal stress, method: $E_{n+1} = E_n + k(\sigma_n - \sigma_{ref})$

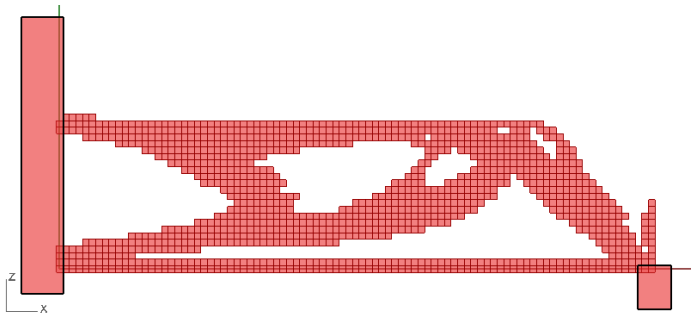

Culling after **iteration 200**: min σ_{pr} /node=1.54e-10 kN/cm^2; max σ_{pr} /node=0.974 kN/cm^2; avg σ_{pr} /node= 0.087 kN/cm^2; Threshold= 0.05 kN/cm^2

TOY 2 – SIMPLE BEAM

TOY2.1 - reference stress= VonMises, method: $E_{n+1} = k * \sigma_n$

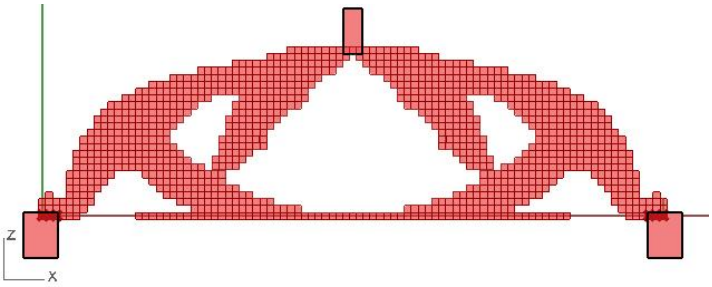

Culling after **iteration 200**: min σ_{vm} /node=0; max σ_{vm} /node=0.57; avg σ_{vm} /node= 0.037; Threshold= 0.00005

TOY2.2 - reference stress= VonMises, method: $E_{n+1} = E_n + k(\sigma_n - \sigma_{n-1})$

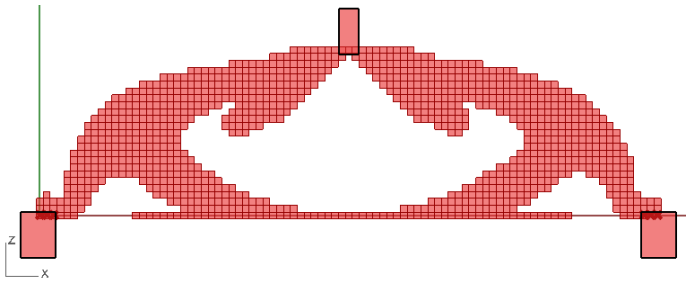

Culling after **iteration 200**: min σ_{vm} /node=1.78e-9; max σ_{vm} /node=0.57; avg σ_{vm} /node= 0.037; Threshold= 0.000015

TOY2.3 - reference stress= VonMises, method: $E_{n+1} = E_n + k(\sigma_n - \sigma_{ref})$

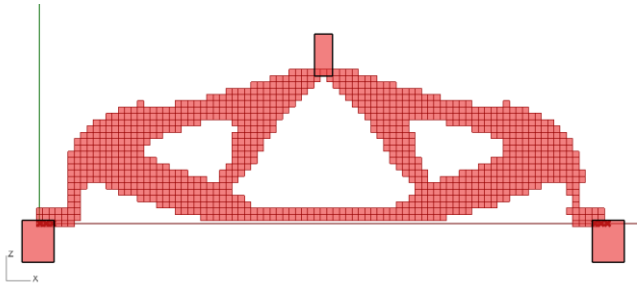

Culling after **iteration 200**: min σ_{vm} /node=2.92e-11; max σ_{vm} /node=0.598; avg σ_{vm} /node= 0.043; Threshold= 0.038

TOY2.4 - reference stress= Principal stress, method: $E_{n+1} = k * \sigma_n$

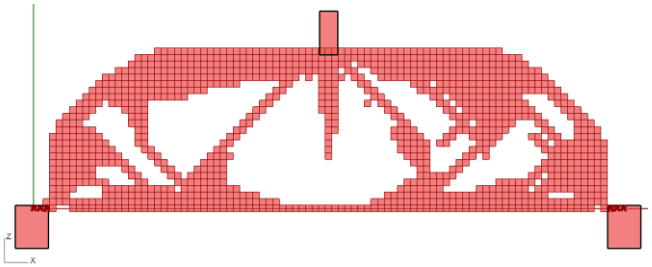

Culling after **iteration 200**: min σ_{pr} /node=1.46e-11 kN/cm^2; max σ_{pr} /node=1.27 kN/cm^2; avg σ_{pr} /node= 0.079 kN/cm^2; Threshold= 0.044 kN/cm^2

TOY2.5 - reference stress= Principal stress, method: $E_{n+1} = E_n + k(\sigma_n - \sigma_{n-1})$

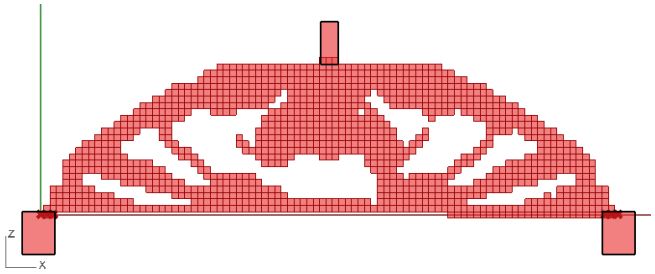

Culling after **iteration 50**: min σ_{pr} /node=1.46e-11 kN/cm^2; max σ_{pr} /node=1.27 kN/cm^2; avg σ_{pr} /node= 0.079 kN/cm^2; Threshold= 0.044 kN/cm^2

TOY2.6 - reference stress= Principal stress, method: $E_{n+1} = E_n + k(\sigma_n - \sigma_{ref})$

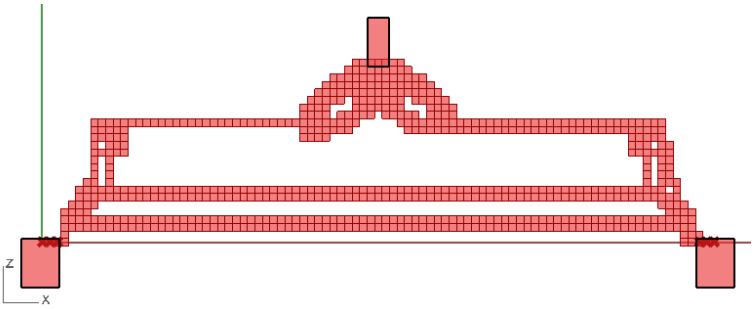

Culling after **iteration 200**: min σ_{pr} /node=1.79e-11 kN/cm^2; max σ_{pr} /node=1.14 kN/cm^2; avg σ_{pr} /node= 0.046 kN/cm^2; Threshold= 0.003 kN/cm^2

TOY 3 – BRIDGE

TOY3.1 - reference stress= VonMises, method: $E_{n+1} = k * \sigma_n$

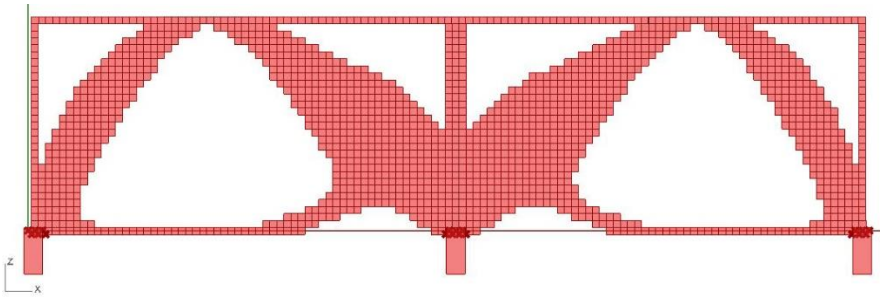

Culling after **iteration 80** (solver crashes at this point)**:** min σ_{vm} /node=0.002; max σ_{pr} /node=7.71; avg σ_{pr} /node= 0.35; Threshold= 0.28

TOY3.2 - reference stress= VonMises, method: $E_{n+1} = E_n + k(\sigma_n - \sigma_{n-1})$

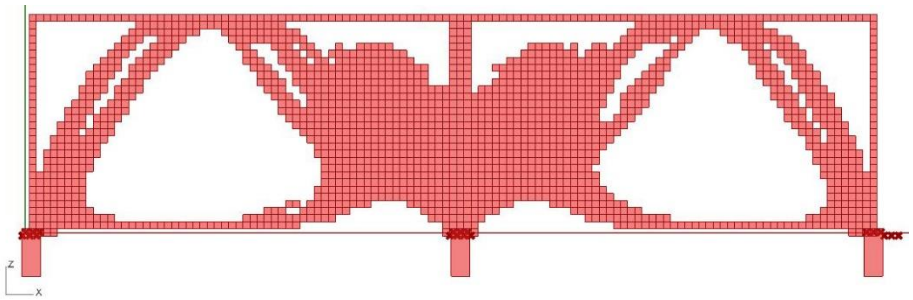

Culling after **iteration 100**: min σ_{vm} /node=6.18e-6; max σ_{vm} /node=7.96; avg σ_{vm} /node= 0.34; Threshold= 0.22

TOY3.3 - reference stress= VonMises, method: $E_{n+1} = E_n + k(\sigma_n - \sigma_{ref})$

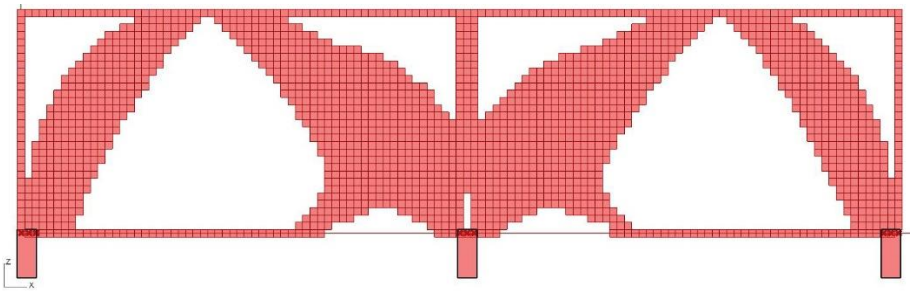

Culling after **iteration 200**: min σ_{vm} /node=2.8e-10; max σ_{vm} /node=6.75; avg σ_{vm} /node= 0.35; Threshold= 0.27

TOY3.4 - reference stress= Principal stress, method: $E_{n+1} = k * \sigma_n$

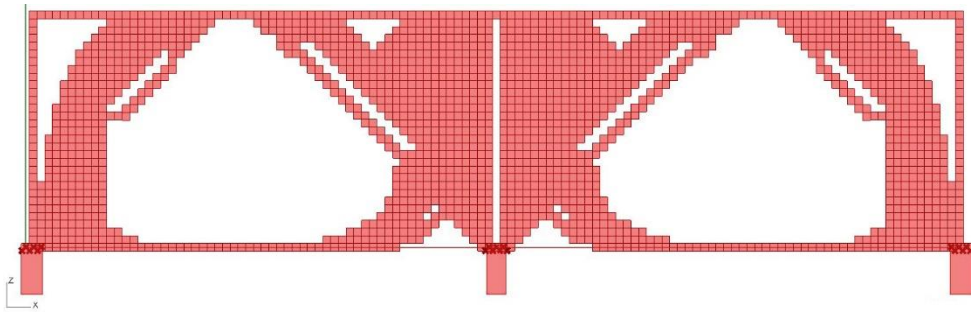

Culling after **iteration 200:** min σ_{pr} /node=1.33e-6 kN/cm^2; max σ_{pr} /node=7.17 kN/cm^2; avg σ_{pr} /node= 0.35 kN/cm^2; Threshold= 0.2 kN/cm^2

TOY3.5 - reference stress= Principal stress, method: $E_{n+1} = E_n + k(\sigma_n - \sigma_{n-1})$

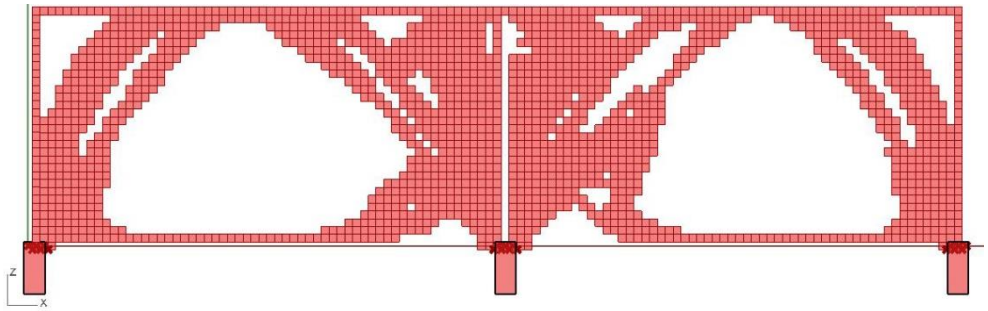

Culling after **iteration 200:** min σ_{pr} /node=4.5e-7 kN/cm^2; max σ_{pr} /node=4.66 kN/cm^2; avg σ_{pr} /node= 0.34 kN/cm^2; Threshold= 0.22 kN/cm^2

TOY3.6 - reference stress= Principal stress, method: $E_{n+1} = E_n + k(\sigma_n - \sigma_{ref})$

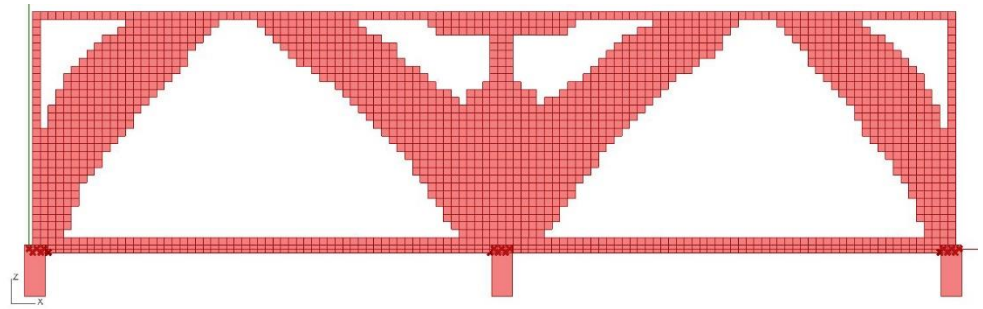

Culling after **iteration 200:** min σ_{pr} /node=4.5e-1 kN/cm^{2}0; max σ_{pr} /node=3.35 kN/cm^2; avg σ_{pr} /node= 0.22 kN/cm^2; Threshold= 0.21 kN/cm^2

At this point it is worthwile elaborating on several aspects of the method which should be considered by the user of the grasshopper tool.

Firstly, it becomes apparent that both choice of reference stress and method influence the final outcome of the optimization procedure (Figure 45). From a purely formal point of view, it can be observed that using the Von Mises reference stress yields more coherent and homogenous results, while the use of principal stresses produces designs with visible checkerboard patterns.

A checkerboard pattern is a term used in topology optimization research to illustrate an undesirable distribution of material. Designs exibiting this phenomenon are characterized by zones of discontiuous material arrangement which are not realistic, are not contributing to the improved performance of the design and are nearly impossible to produce (Gumruk, 2019).

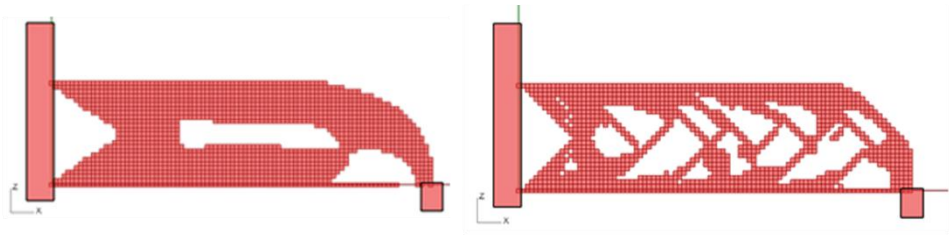

Figure 45. left- using Von Mises reference stress with method 1; right: using principal reference stress with method 1. The right image illustrates the checkerboard pattern.

Secondly, it was observed that the number of iterations which the simulations run for plays a crucial role in the final output. The choice of reference stress does not influence the necessary number of iterations for a succesful conversion, but the choice of the method does. As can be seen in Figure 46, in the case of the first method a larger number of iterations leads to a more refined result. It has been observed that after 200 iterations the stress values within the component start changing only slightly. The second and third method yield faster conversions as proposed by Mattheck, and have been succesful at reaching functioning designs around 100 and 50 iterations respectively.

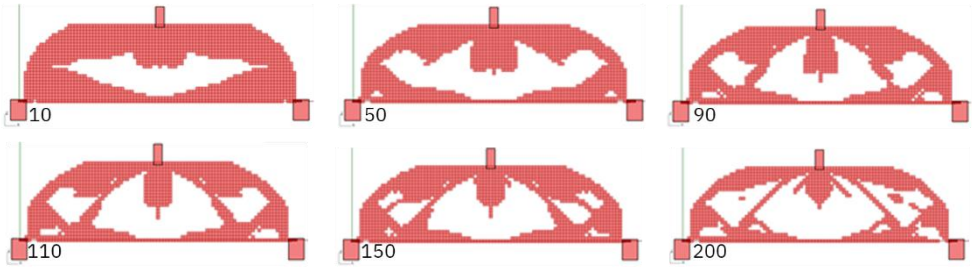

Figure 46. simply supported beam, principal reference stress. Influence of iteration number on the final geometry with an unchanging culling threshold.

Furthermore, the multiplication factor *k* present in each of the three methods for converting the reference stress values into the new E modulus distribution greatly influences the final outcome of the optimization procedure (Figure 47). Although larger k coefficients reduce the required number of iterations needed to achieve a certain design, it inevetably produces discontinuous results with visible checkerboard pattern effect. This can be explained by the fact that there is a much more drastic change in the values of the newly calculated E modulus distribution. Baumgartner et al., (1992) suggest that a safe option is to use a k value equal to 100/σref. In this case, that yielded the value of 8.5.

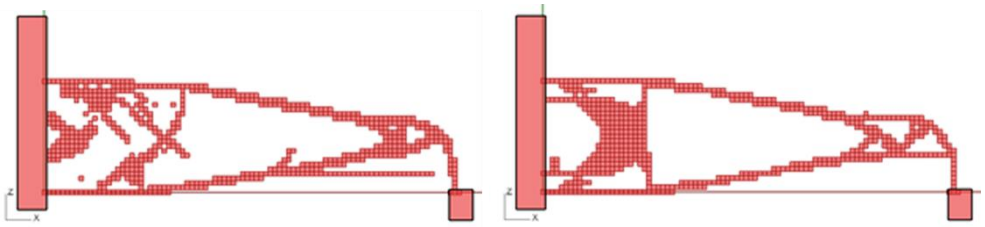

Figure 47. influence of the k coefficients on the optimization results after 20 iterations. left k=10, right k=8.5.

The previously mentioned σref, is a variable only present in the third method (global stress increment method) and was found to be of influence to the final optimization results. Namely choosing a σref which is equal to the desired working stress in the final component i.e. $\sigma_{allowable}$ produced very arbitrary and incoherent designs. The reference stress was calculated using the following equation:

$$\sigma_{ref} = \frac{\sigma_y}{sf}$$

Where σ_y is the yield strength of the material (23.5 kN/cm^2 in this case) and the *sf* is the safety factor. A common safety factor of 2 was taken for the purposes of this research, but should otherwise be taken from Eurocode 1 and other relevant eurocodes.

As proposed by Mattheck it was more beneficial to incrementally increase the the value of the reference stress, starting from a small one and increasing it up to the desired workign stress in the component. Based on that observation, within the developed Grasshopper script, the σ_{ref} is a function of the current iteration number:

$$\sigma_{ref} = \frac{\sigma_{allowable}}{i} * i_n$$

In the previous formula the *i* stands for the total number of iterations set forth by the user and the i_n represents the current iteration number. In this way the reference stress starts out at a minimal value and is gradually increased to the desired working stress.

After all of the iterations of the topology optimization procedure have been executed, a resultant reference stress per voxel is determined based on the stresses from the adjacent beams in the Von Neumann neighborhood of range 1. The removal of underutilized voxels further takes place based on the culling threshold set forth by the user. This threshold is a decisive factor which influences how the final geometry is displayed (Figure 48). Through testing, it has been found good practice to set the threshold to a value which will yield a reduction of material between 30 % and 50%. In some cases, setting the threshold to such value yielded discontinuous geometry, so the threshold has been set to a number which produces a continuous geometry with less visible checkerboard pattern.

Lastly, it is worthwhile mentioning that in cases of the simply supported beam and continuous beam the results are not always symmetrical. This can mostly be attributed to support conditions, where one side is resting on a pin support and the other is resting on a roller in order to produce a statically determinate structure.

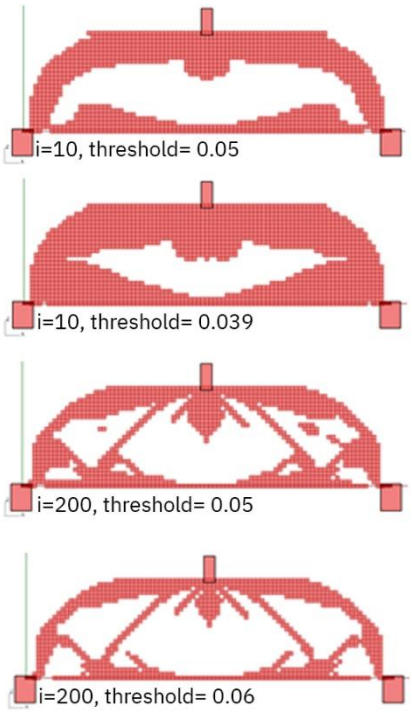

Figure 48. influence of the the culling threshold on the optimization results. Example of a simply supported beam, principal reference stress, method 1.

3.3.3 Conclusions

In this part of the report, an overview of the 2D toy problem results will be provided and a decision for the final method to be taken towards the 3D problems will be elaborated. The previously displayed best results from each method have been analyzed with the FEM method to obtain information about their structural performance.

Even though the results of the SKO method have not been further shape optimized using the proposed CAO method, which would reduce the occurring notch stresses and thus by alter the final geometry, the outcomes of the SKO can still provide information about the viability of the method.

The decision on the method to be used for the 3D problems was not solely based on quantitative data but was also opted for based on visual qualities such as continuity of geometry, and aesthetic appeal.

	Reference stress	method	original displacement [cm]	Displacement fter SKO [cm]	% mass remaining	% above allowable stress	number of iterations	score
Cantilever beam	Von mises	$E=\sigma$	0.031	0.13	70 %	0%	200	24
		$E_{n+1}= E_n + k(\sigma_{principal\ n} - \sigma_{principal\ n-1})$		0.16	51%	0%	200	23.9
		$E_{n+1}= E_n + k(\sigma_{principal\ n} - \sigma_{ref})$		0.126	71%	0%	200	24
	principal	$E=\sigma$		0.151	55.3%	0%	200	24.6
		$E_{n+1}= E_n + k(\sigma_{principal\ n} - \sigma_{principal\ n-1})$		0.18	47%	0%	200	29.6
		$E_{n+1}= E_n + k(\sigma_{principal\ n} - \sigma_{ref})$		0.186	50%	0%	200	24.8
Simple beam	Von mises	$E=\sigma$	0.004	0.042	45%	0%	200	34.2
		$E_{n+1}= E_n + k(\sigma_{principal\ n} - \sigma_{principal\ n-1})$		0.05	45%	0%	200	32.2
		$E_{n+1}= E_n + k(\sigma_{principal\ n} - \sigma_{ref})$		0.03	42%	0%	200	33.7
	principal	$E=\sigma$		0.04	46%	0%	200	31.3
		$E_{n+1}= E_n + k(\sigma_{principal\ n} - \sigma_{principal\ n-1})$		0.04	48.5%	0%	50	32.5
		$E_{n+1}= E_n + k(\sigma_{principal\ n} - \sigma_{ref})$		0.34	30%	0%	200	20.7
Continuous beam	Von mises	$E=\sigma$	0.02	0.45	44%	0.8%	80	19.2
		$E_{n+1}= E_n + k(\sigma_{principal\ n} - \sigma_{principal\ n-1})$		0.4	47%	0.6%	100	18.8
		$E_{n+1}= E_n + k(\sigma_{principal\ n} - \sigma_{ref})$		0.38	50%	0.6%	100	21.2
	principal	$E=\sigma$		0.1	49%	0%	200	26
		$E_{n+1}= E_n + k(\sigma_{principal\ n} - \sigma_{principal\ n-1})$		0.1	47%	0%	100	25.8
		$E_{n+1}= E_n + k(\sigma_{principal\ n} - \sigma_{ref})$		0.11	43%	0.02%	100	24

Table 2: overview of the best obtained results for the TOY problems with all setups

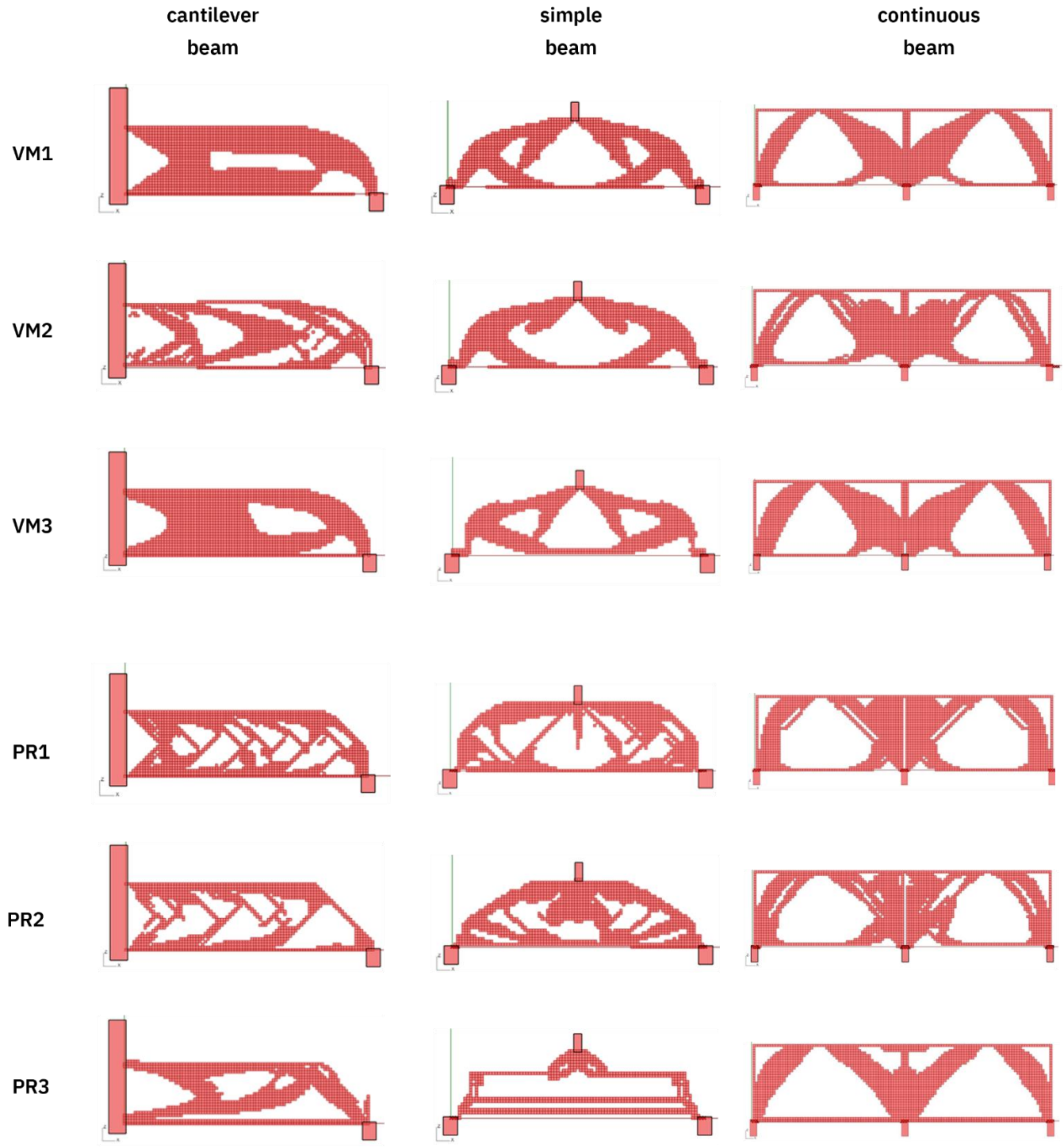

Figure 49. Best results for the TOY problems, for every simulation setup

A tabular overview of the numerircal results obtained through all the methods for all three toy problems is given in Table 2, while the a graphical overview is given by Figure 49. The same image gives an overview of the results obtained by the Ansys software and will further be elaborated on.

The original displacement before the optimization, and the displacements of the final designs were calculated using the Karamba3D finite element solver. In all cases the displacement has increased in value, which is expected as there is less material. Nevertheless, all of of the results are within the allowable deflections which has been calculated using a rule of thumb as L/500. Even though the continuous beam TOY problem exceedes the allowable stresses, it can be assumed that reducing the culling threshold, leading to an increased ammount of retained material would solve this issue.

The remaining mass at the end of all iterations was calculated as:

$$remaining\ mass = \frac{vox_n}{vox_0} * 100$$

Where vox_n is the number of remaining voxels after iteration n for a given threshold, while vox_0 is the original number of voxels within the design space. It was attempted to evaluate all results at around 50% mass reduction, however in some cases that was not possible due to the resulting discontinuous geometry. In those cases the culling threshold was reduced until a continuous mass of material was obtained.

The result of each method has been given a score value which indicates how well stress is distributed within the final obtained design. This was done by looking at the percentage of beams within the finally obtained lattice whose principal stress is close to the overall average principal stress of the entire component. The code for this calculation has been provided as an appendix to this report.

The three TOY problems have been topologically optimized using the Ansys software which utilized the SIMP method. In total three two-dimensional simulations were ran. The setups of the problems with respect to dimensions, load positions and intensities, support positions and coditions, as well as material properties were equivalent to those within the Grasshopper environment.
The Ansys numerical results are provided in Table 3, and the final geometries are given below.

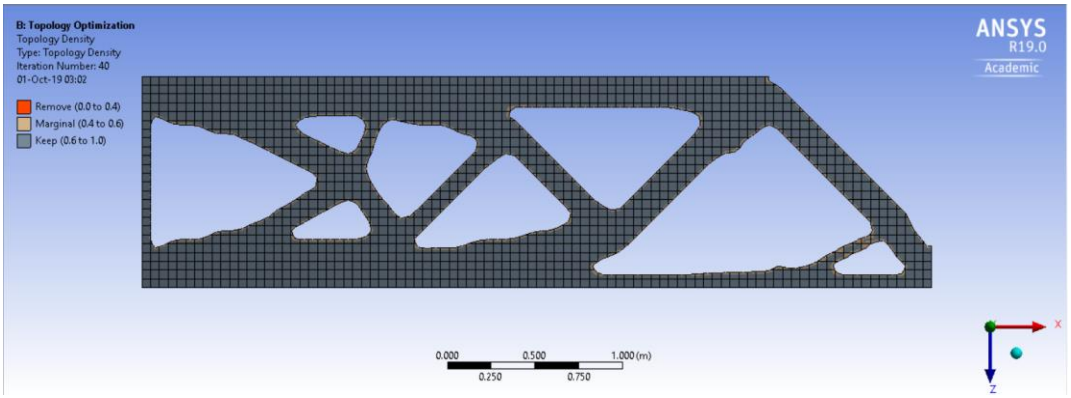

Results after **iteration 40**: min σ_{vm} =9.32e-7; max σ_{vm} =3.37; avg σ_{vm} = 1.7; remaining ammount of material: 52.5%

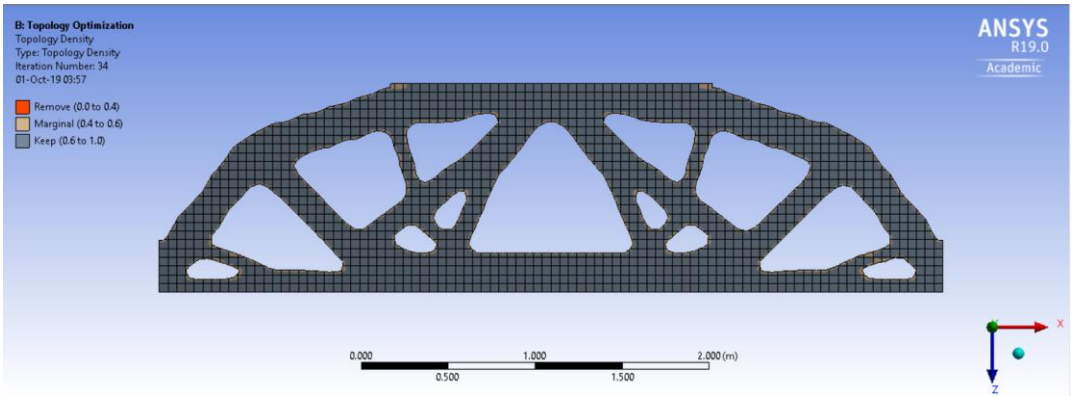

Results after **iteration 34**: min σvm=0.0016; max σvm=1.59; avg σvm= 0.7; remaining ammount of material: 52.6%

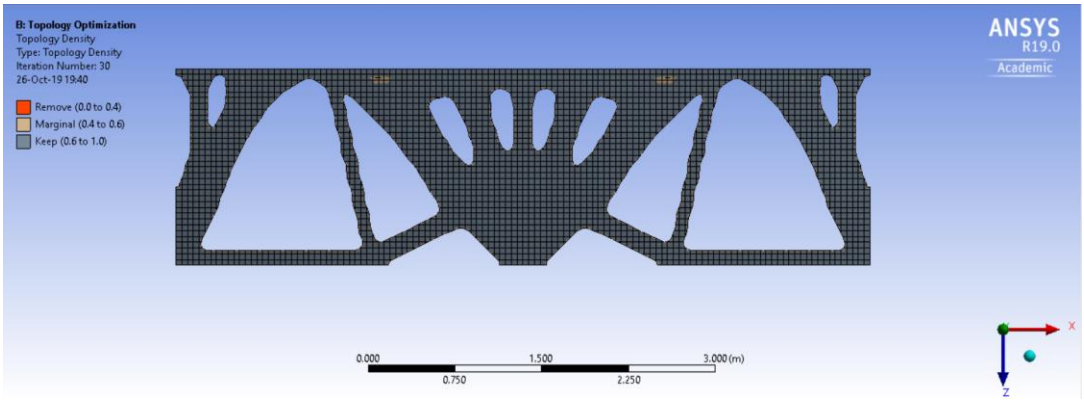

Results after **iteration 30**: min σvm=0.012; max σvm=28.2; avg σvm= 15.7; remaining ammount of material: 54%

	goal	constraint	original displacement [cm]	Displacement after SKO [cm]	% mass remaining	% above allowable stress	number of iterations	Elapsed time
Cantilever beam	compliance minimization	50% mass	0.02	0.04	52.5%	0%	40	1m37s
Simple beam	Compliance minimization	50% mass	0.0036	0.0037	52.6%	0%	34	1m14s
Continuous beam	Compliance minimization	50% mass	0.02	0.03	54%	0%	30	2m

Table 3: overview of results obtained by Ansys, using the SIMP method for topology optimization

The Ansys simulations, as expected, showed a faster rate of convergence towards achieving the designated goal of maximizing the structure's stiffness while reducing the ammount of material. In all three cases the number of iterations and elapsed time were lower than that used by the methods proposed by this research. Using the SIMP method by Ansys proves to be better at keeping displacements closer to the original displacements of the initial geometry with 100% of material. The results obtained by this software also show a more continuous and smooth geometry without a checkerboard pattern which can be observed in the results obtained by methods proposed by this thesis. Additionally, the resulting principal and Von Mises stresses occuring in the components optimized by the SIMP method are lower in value than those obtained by the SKO method proposed here. Detailed numerical results of the Ansys topology optimization are provided within the appendix of this report.

Considering the results present in Table 2 and Table 3 and the results of the Ansys simulations, the method taken to the next phase of this research is PR2. It employs the principal reference stress and the local stress increment method.

From a formal point of view, this method yielded results closest to the ones obtained by Ansys (Figure 50). When compared to the VM3 method which would be a second option, the PR2 does exhibit discontinuous geometry. This could be overcome by post processing in which the gaps in the geometry could be manually filled in by the designer. Even though the PR2 method does require more iterations

which leads to more calculation time, it does show a better stress distribution in the final design.

In case of the cantilever beam, even though the total displacements were slightly higher in when using the PR2 method, it used 25% less material to do so. In case of the simply supported beam both methods resulted in designs of near equal performance, while in the case of the continuous beam the PR2 method outperforms the results of the VM3 method in all aspects.

Figure 50. comparison of the TOY problem results obtained by the SKO method with the Ansys results obtained with the SIMP method.

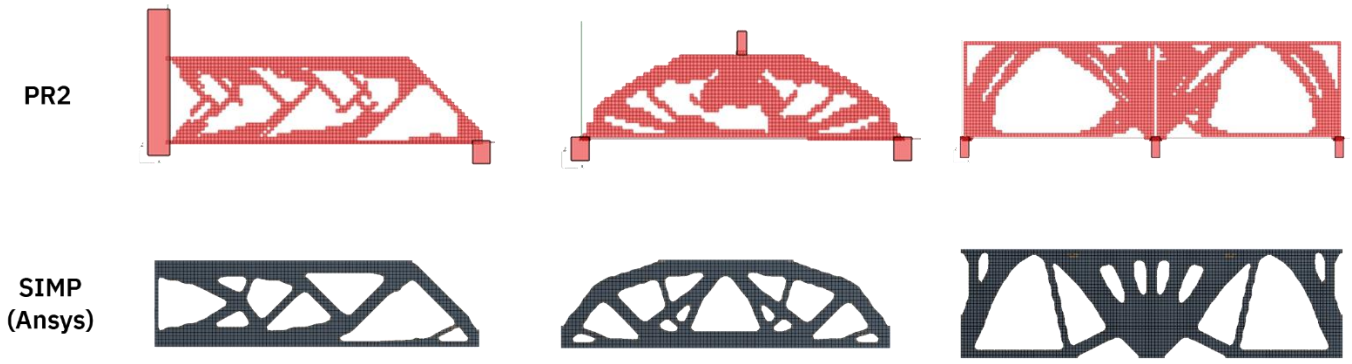

Another aspect which was considered when opting for this method was the fact that it can be adjusted to prioritize compression-only or tension-only structures. This can be achieved by choosing only the positive or negative principle stress values as reference stresses for further calculation. This would make this method applicable to a wider range of problems and materials. In contrast, the Von Mises reference stress is mainly suitable for materials which exhibit equal behavior in both tension and compression, making it suitable for only a handful of currently available materials.

3.4 3D Cases

In this part of the report, results from exploring the possibilities of using the designated method in 3D applications will be discussed. The cases considered include a simple ground floor house, a single story house and a complex house. The examples are aranged based on the complexity of the problem and the number of architectural elements needed to be considered by the topology optimization. The results of these three cases are qualitatively evaluated and compared with the geometries derived by again using the comercial software Ansys.

It should be noted that the obtained geometries in no way present all the possible applications of the method but are just current explorations into it's possible uses.

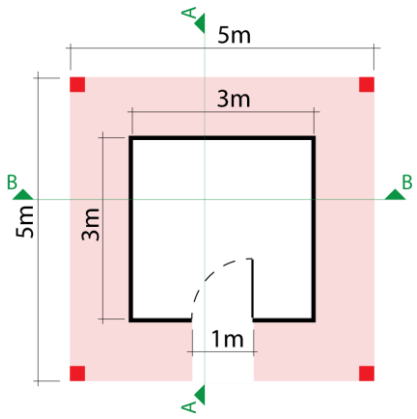

Figure 51. Floorplan of the ground floor house. Red squares are the supports, pink area is the design space

3.4.1 Ground floor house

The ground floor house has been envisioned as a single space object with a single entrance. A simplified floorplan of the house is given by Figure 51. This is the simplest 3D problem as it only has one void (space), one load area, and is symmetrical. The design space within which the topology optimization takes place is a 5x5x5m volume discretized into a lattice of 25cm beams. The room was designed as a 3x3m space with a height of 2.2m. This height was taken as the clear height of the space and is expected to increase once the topology optimization procedure is complete. The entrance was modeled as a 1m wide box of the same height as the room. An overview of the setup data is given in Table 4, while the graphical representation of the Grasshopper output is given in Figure 51.

	Dimensions [m]	Load [kN/m^2]	supports	voxel size [cm]	Material properties		
					E [kN/cm^2]	Cross section	Yield strength
Ground floor house	5x5x5	20	fixed	25x25x 25	21000	10x10cm	23.5 kN/cm^2

Table 4: overview of inputs used for the ground floor house problem

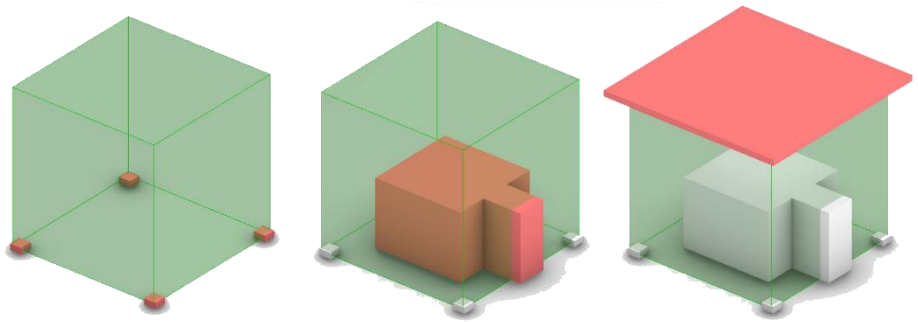

Figure 51. Input of the support areas, void regions and load region provided to the script

Figure 52 shows the results obtained after 50 iterations with a culling threshold of 0.028, which retained 47% of the original material within the design space. From a formal point of view, the results seem logical. The structure has been reduced to four columns, resting in the support zones and increasing in girth from the ground up. The voxels in the top corners of the space got culled leading to a chamfered result resembling a formation of a dome shape. Additionally, openings formed in the walls, although of coarse resolution, start resembling pointed archways. The final geometry did posses a slight ammount of checkerboard pattern which was removed during post processing.

Figure 52. Results of topology optimization for the case of a ground floor house

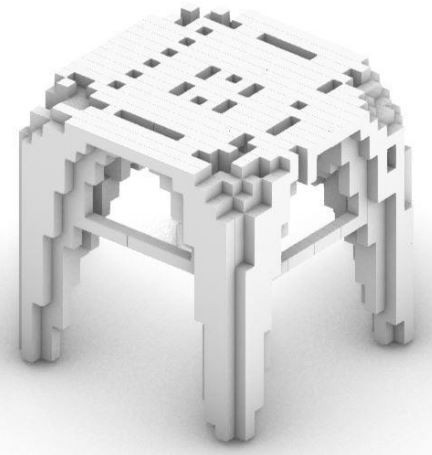

Culling after **iteration 50:** min σ_{pr} /node=5.29e-9 kN/cm^2; max σ_{pr} /node=1.42 kN/cm^2; avg σ_{pr} /node= 0.34 kN/cm^2; Threshold= 0.028 kN/cm^2 (47% of material remaining)

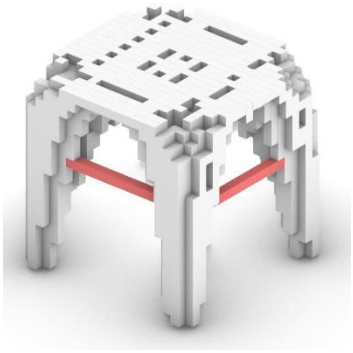

Figure 53. 'tension ties' highlighted in red

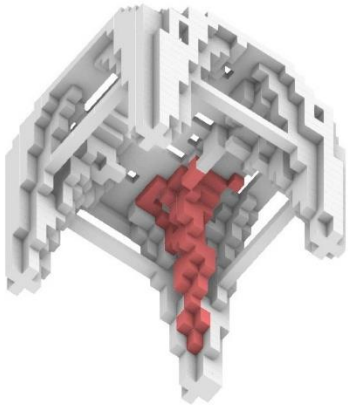

Figure 54. up-bottom view of the house highlighting one of the ribs or fans; down- illustration of a gothic fan vault (source:http://blog.stephens.edu/arh101glossary/?glossary=vault)

The final geometry posseses several interesting features which should be pointed out. Namely, at a height of about 3.5 meters a presence of horizontal elements connecting the columns is observed. There are a total of four such elements, one on each side of the house. These beams, loaded in tension, most likely serve as tension ties and prevent the columns from buckling (Figure 53).

In addition, the ceiling of the inner space has geometric resemblences to a rib vault or even a fan vault. From the bases of the four columns, voxels start portruding inwards towards the center of the room, and spreading radially (Figure 54). Even though the roof slab spans only 5 meters, and structural steel is used as a material, this occurance can be explained by the greatly increased load of 20kN/m^2 in contrast with a usual live load for buildings of 2kN/m^2 as prescribed by eurocode.

Lastly, it can be seen that the roof itself has material removed from it in the form of small perforations. During the optimization phase the Young's modulus of the loaded areas has purposefully not been set constant as doing so resulted in strangely shaped geometries.

Relationship between the initial design space and the final result can be observed in Figure 55.

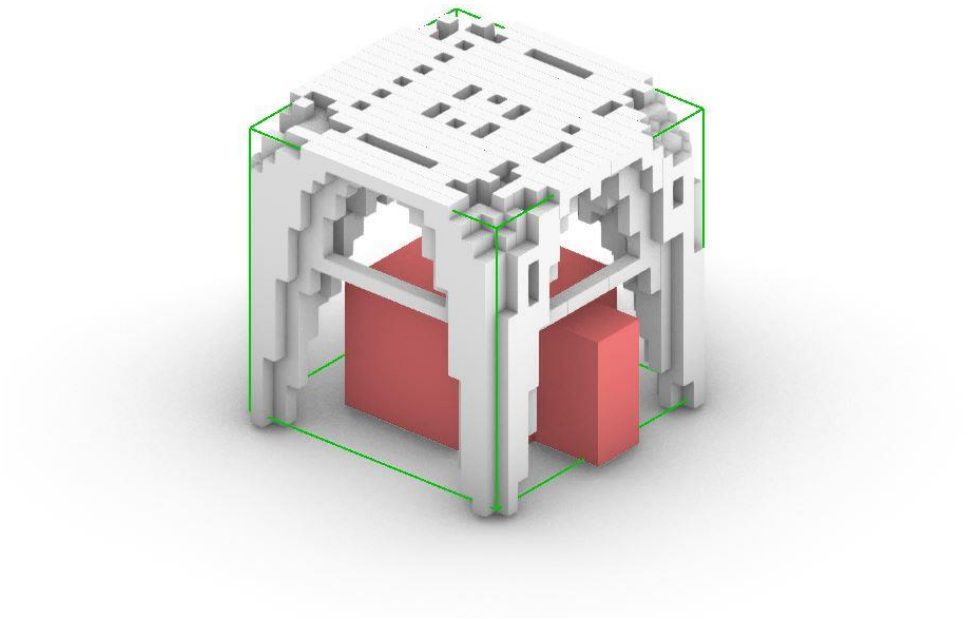

Figure 55: relationship between initial and final geometry; green- initial boundary of the design space, red- assigned voids

The following vertical and horizontal sections, and elevations provide a better overview of the resulting geometry. The horizontal sections have been taken at 1.5 meter intervals. The positioning of the vertical sections is illustrated in Figure 51.

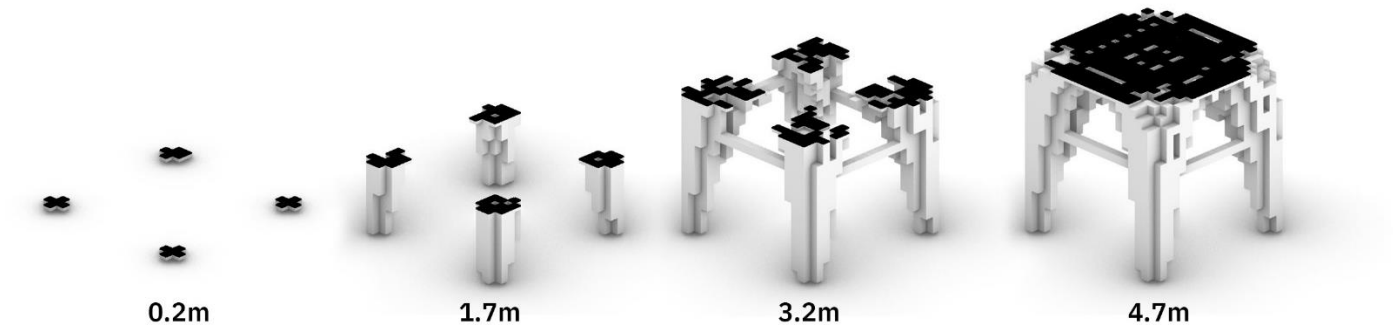

Figure 56: horizontal sections through the topology optimization results for the case of a simple house.

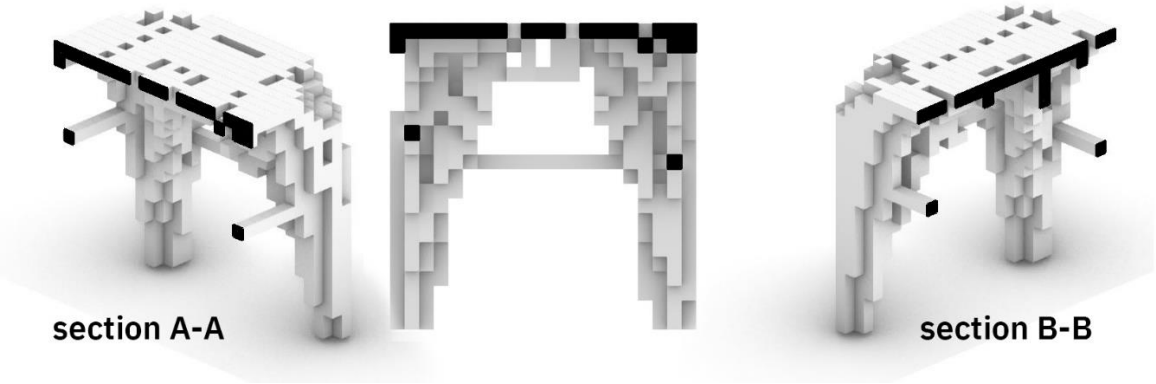

Figure 57: vertical sections

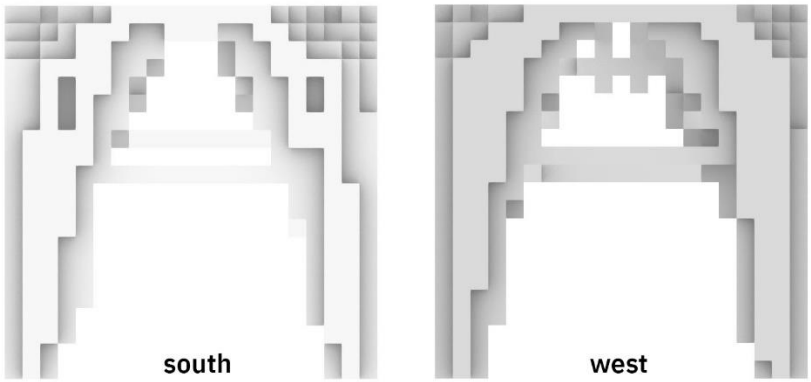

Figure 58: south and west elevation

A comparison with the optimization results made with Ansys will only be given qualitatively as the results of the FEM check of the optimized form were not possible due to a large mesh complexity. Similarly to the 2D TOY problem setups, the Ansys setup involved a compliance minimization problem with mass fraction constraint of 50%.

In general, the same formation of four columns is visible. The openings in the walls attain similar archway geometries. However, the upper half of the building seems have more material removed around the perimiter which was not the case with the SKO method. Additionaly, the loaded zone has remained unchanged.

Figure 59. Ansys results for the case of a ground floor house

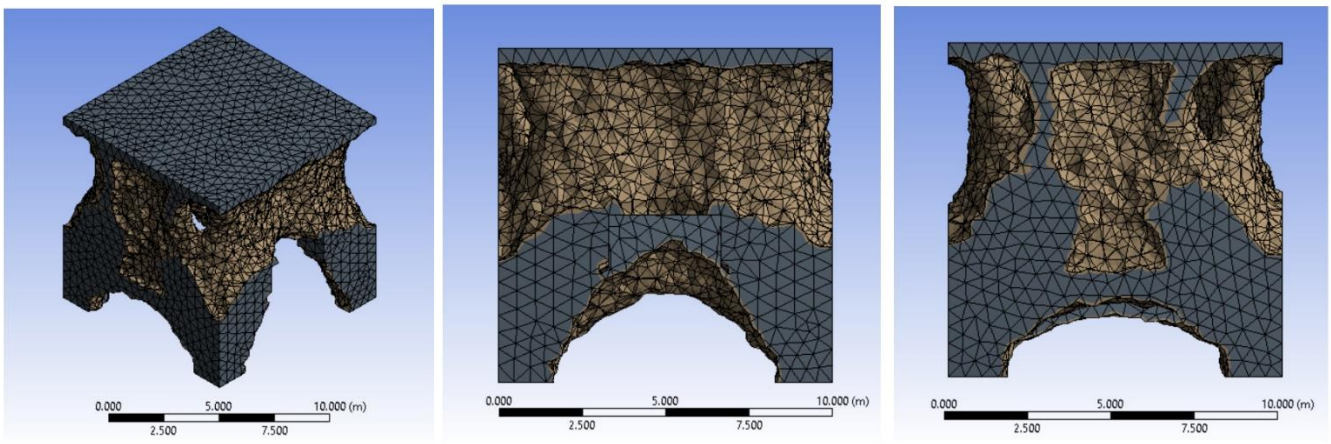

3.4.2 Single story house

The single story house is a slighly more complex variant of the previous problem. Here, another space with the same dimensions has been added on top, and instead of a door there is a opening for a window. Both rooms have a height of 2.1m and a space above them filled with material. A simplified foorplan is given in Figure 60. Aside from having two void areas, there are now also two load zones- one being the roof, and one being the slab of the upper floor. The setup of the design space was identical to the previous problem, with just the loads being corrected and set to 4kN/m^2. An overview of the setup data is given in Table 5, while the graphical representation of the Grasshopper output is given in Figure 61.

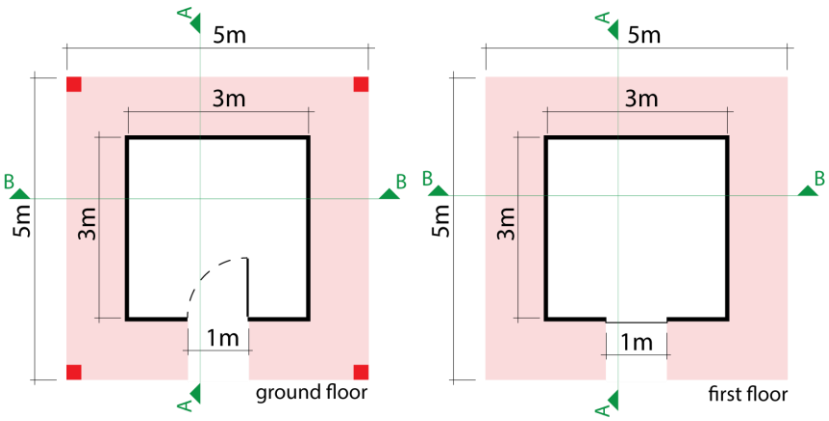

Figure 60. Floorplans of the single story house. Red squares are the supports, pink area is the design space

	Dimensions [m]	Load [kN/m^2]	supports	voxel size [cm]	Material properties		
					E [kN/cm^2]	Cross section	Yield strength
Single story house	5x5x10	4	fixed	25x25x25	21000	10x10cm	23.5 kN/cm^2

Table 5: overview of inputs used for the single story house

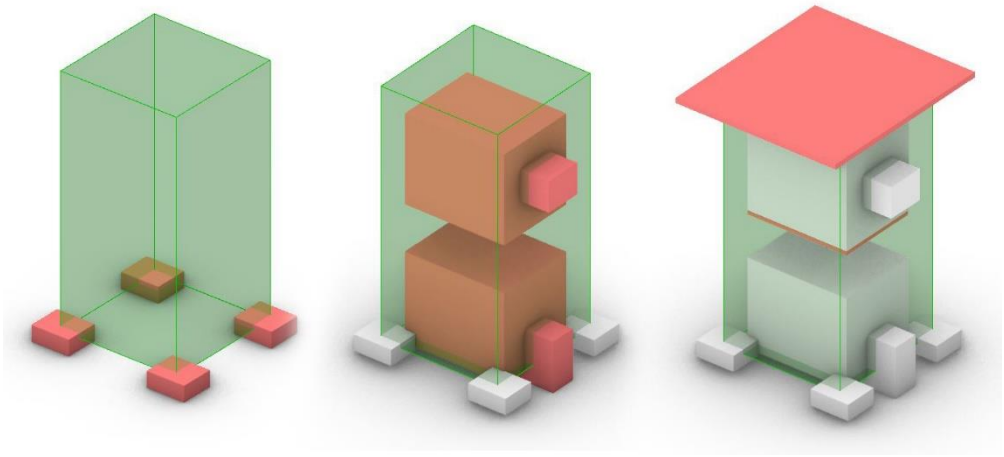

Figure 61. Input of the support areas, void regions and load region provided to the script

Figure 62 showcases the results obtained after 50 iterations with a culling threshold of 0.02, which retained 50% of the original material within the design space. The optimization again yields a structure similar to the previous one, in which there are four columns spanning the entire height of the design space and resting in the designated support areas. In this case there has been a more pronounced removal of voxels in the edges of the design space, leading to a chamfered building which

narrows towards the top. The openings in the walls span both floors and are again shaped as pointed archways, giving a somewhat gothic aesthetic to the obtained results.

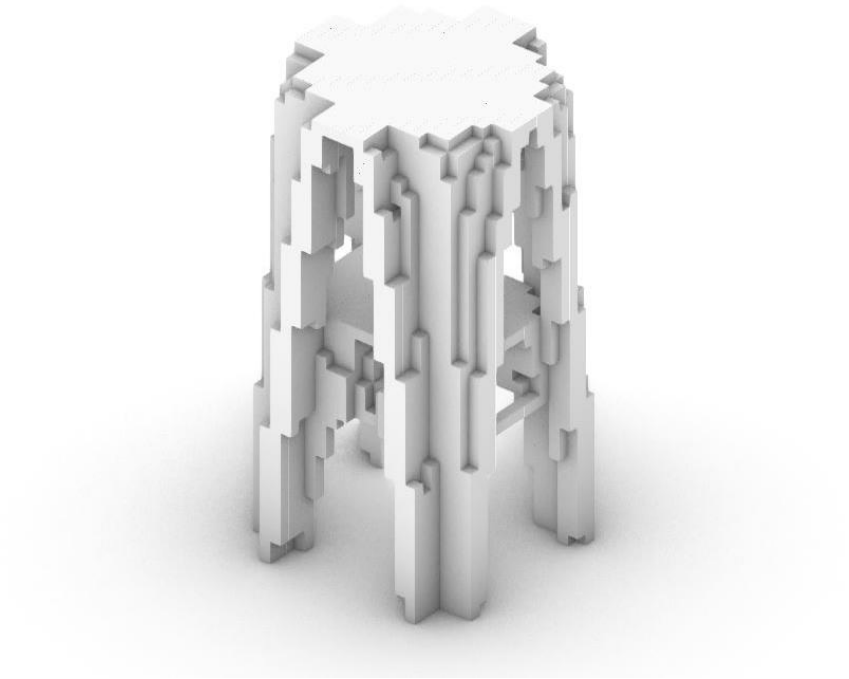

Figure 62: culling after **iteration 50:** min σ_{pr} /node=3.53e-9kN/cm^2; max σ_{pr} /node=1.74kN/cm^2; avg σ_{pr} /node= 0.047kN/cm^2; Threshold= 0.02 kN/cm^2 (50% of material remaining)

Similarly to the ground floor house, the presence of horizontal members between the columns can be observed.They probably serve the same function as in the case of a ground floor house which is keeping the columns from buckling.

As can partially be seen in the vertical section drawings, the ceilings of both spaces start resembling vault like formations. As the results are quite crude, It would be beneficial to try increasing the resolution by decreasing the voxel size and observing what kind of geometry is formed. The roof surface and the surface of the first floor slab where the loads are applied, in this case do not have any material removed from them.

The columns themselves seem to have profiled themselves into an L shape, which may have contributed to an increased stiffness and resistance to buckling.

A visual comparison between the initial design space and the final result can be observed in Figure 63.

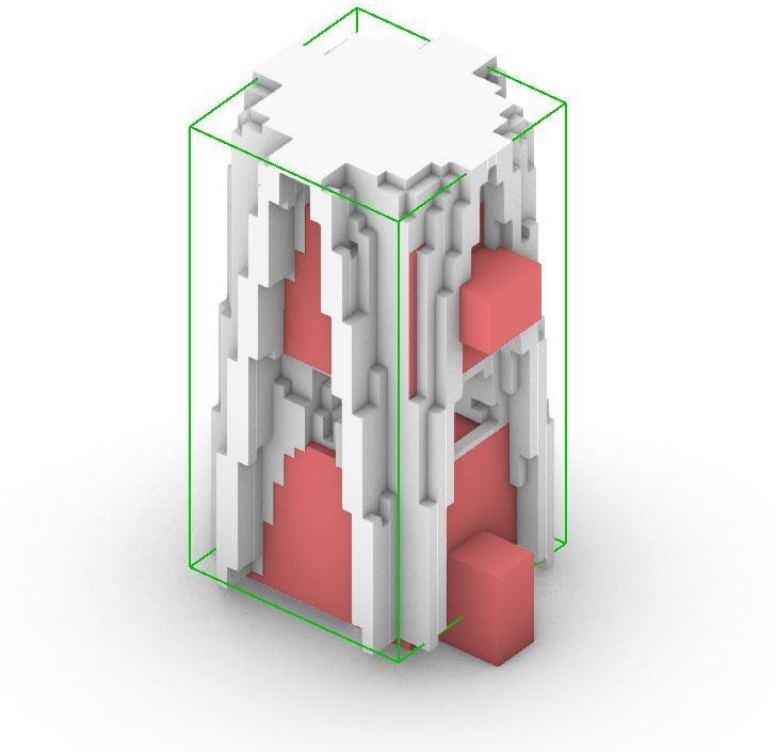

Figure 63. Relationship between the initial and final geometry; green-initial boundary of the design space; red-assigned voids

The following vertical and horizontal sections, and elevations provide a better overview of the resulting geometry. The horizontal sections have been taken at 1.5 meter intervals. The positioning of the vertical sections is illustrated in the floorplans (Figure 60).

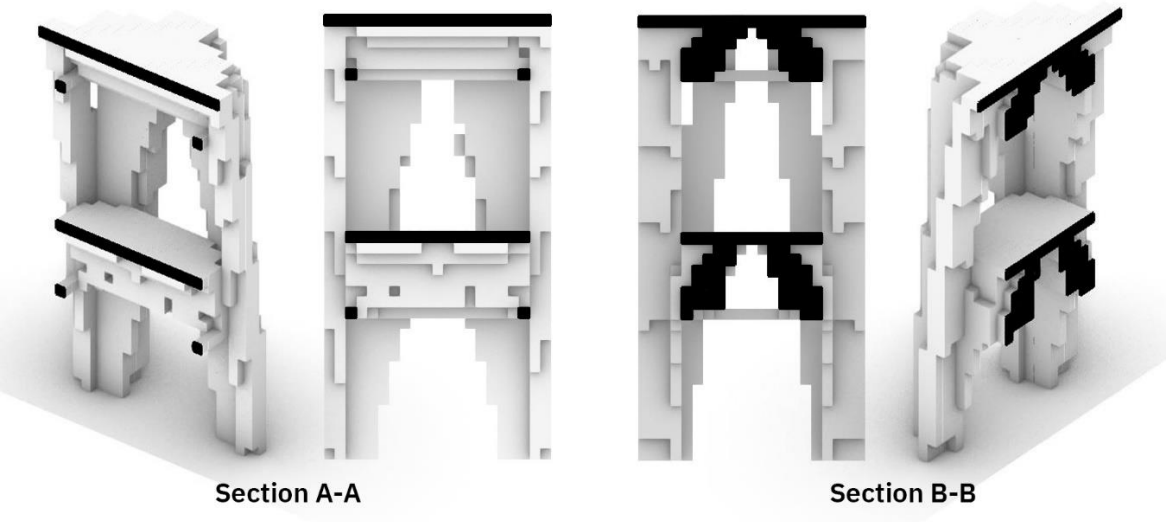

Figure 64: vertical sections

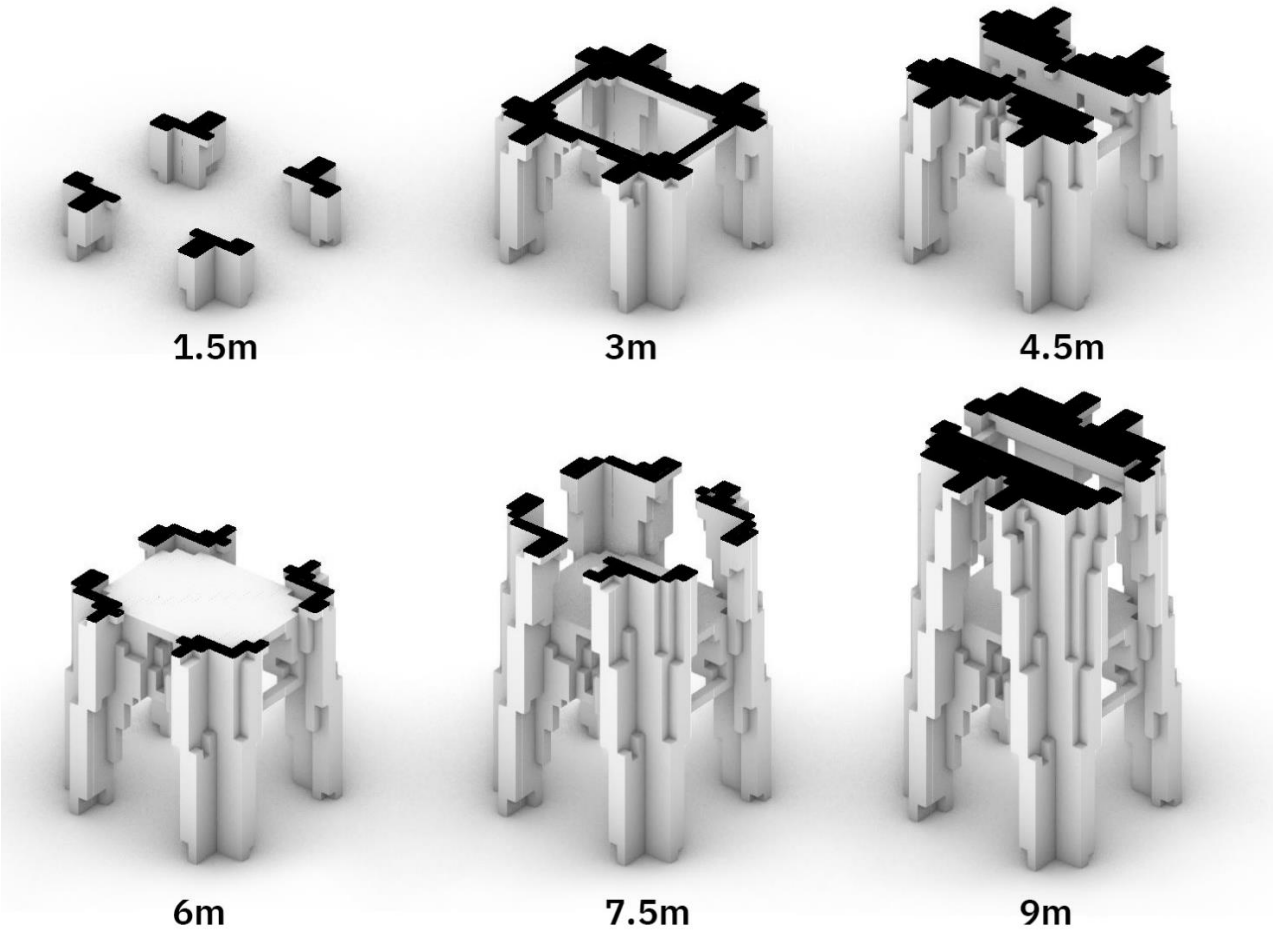

Figure 65. Horizontal sections through the topology optimization results for a single story house

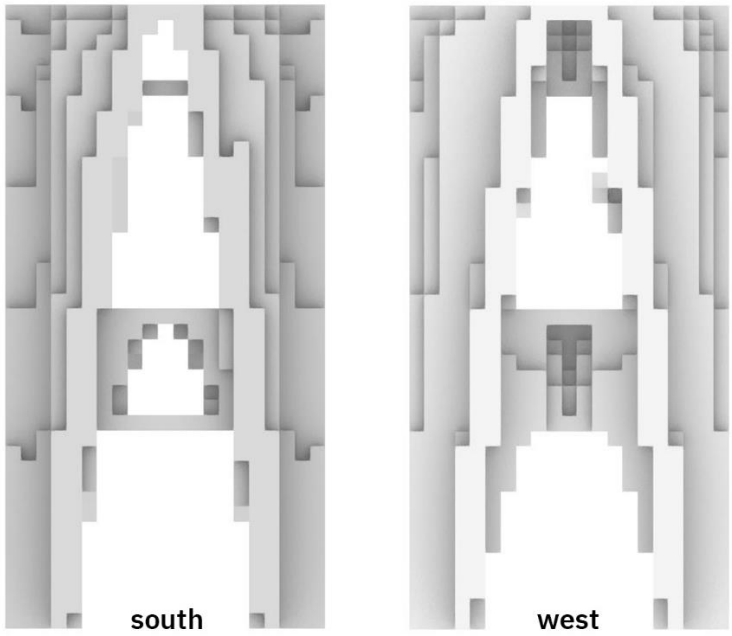

Figure 66. south and vest elevation of the single story house

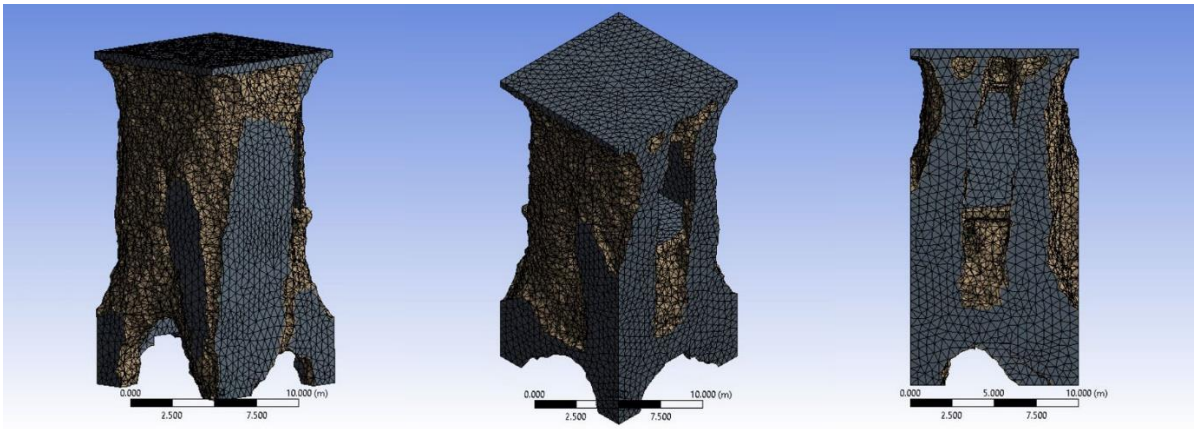

Figure 67. Ansys results for the case of a single story house. Left to right: north-east corner, south-west corner, south facade elevation

The results obtained by Ansys in which the setup again entailed a compliance minimization goal with a mass fraction constraint are formally different from the SKO results. A lack of symmetry in the results is observed and no two faces of the building are identical. The formation of columns is only evident in the lower regions, and the openings in the walls are present only towards the ground floor. The upper floor area is characterized by a reduced mass around the perimiter. The lack of material around the window opening on the south seems to have been compensated on the north face of the building. Once more, the loaded zones remain completely unchanged.

3.4.3 Complex house

The complex house is imagined as the most elaborate problem of the three. It is formed as an expansion to te previous 3D problem. On the west side a double height space was added, along with new architectural elements such as a balcony on the north side and an external staircase on the east. The balcony is represented by a large overhang and the staircase is represented by an inclined load surface. There are a total of 4 load zones: roof, 1st floor slab, balcony, and staircase. A simplified foorplan is given in Figure 68. The input parameters are identical to the previous problem in all aspects. An overview of the setup data is given in Table 6, while the graphical representation of the Grasshopper output is given in Figure 69.

	Dimensions [m]	Load [kN/m^2]	supports	voxel size [cm]	Material properties		
					E [kN/cm^2]	Cross section	Yield strength
Single story house	8.5x5.5x7	4	fixed	25x25x 25	21000	10x10cm	23.5 kN/cm^2

Table 6: overview of inputs used for the complex house

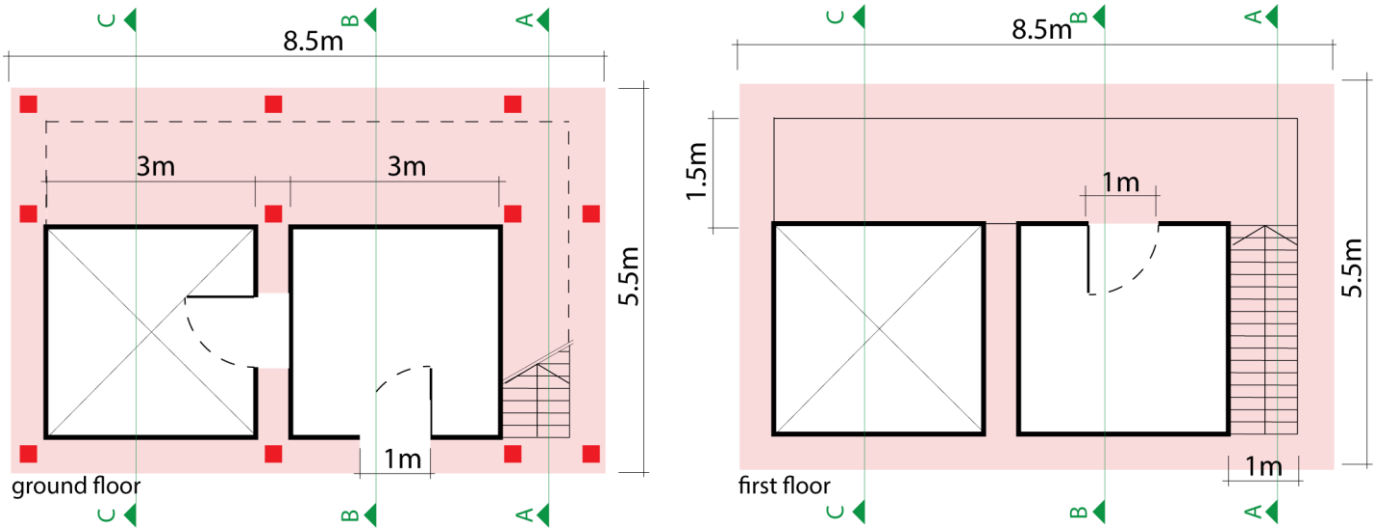

Figure 68. Floorplans of the complex house. Red squares are the supports, pink area is the design space

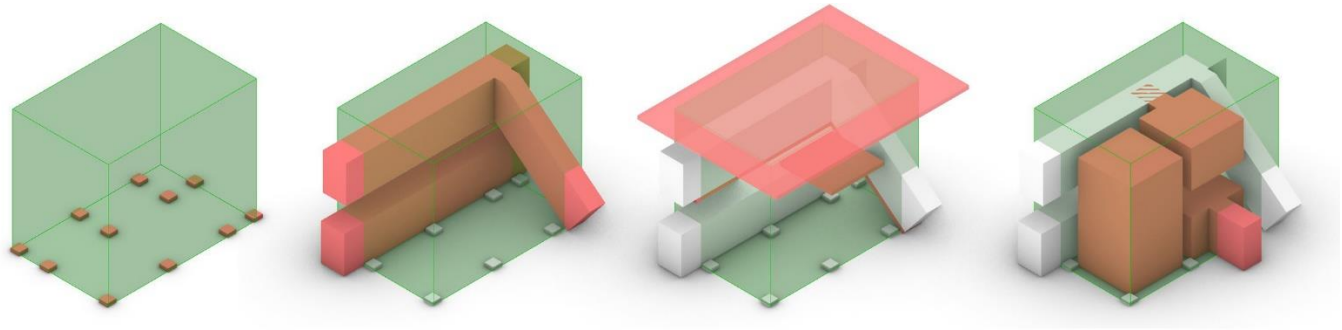

Figure 69. Floorplans of the complex house. Red squares are the supports, pink area is the design space

The results obtained after 50 iterations are presented in Figure 70. The culling threshold of 0.0015kN/cm^2 was used, which resulted in the retention of 46.5% of the original material within the design space. The optimization procedure yielded a structure of complex geometry. The resulting geometry has a large degree of discontinuity and a presence of threedimensional checkerboard pattern. Similarly to previous 3D cases, the walls have been perforated with arch-like openings, and the material has been removed from the roof and balcony slabs as well.

Two interesting elements can be observed in the obtained geometry. Firstly, the stairs on the east façade seem to have formed in a well organized manner. This could be an accidental result of the way in which the design space was constructed. In addition, the flight of stairs appears to be supported by an arch

or a diagonal block of material spanning from the support area to the middle of the staircase (Figure 71-a). A similar feature is noticeable in the results obtained by Ansys. A second element is located on the opposite façade in the form of a slender branch-like column. The element starts at one of the supports and slightly curves upwards before attaching to the roof slab (Figure 71-b). A slightly less pronounced element can be discerned in the optimization output of Ansys.

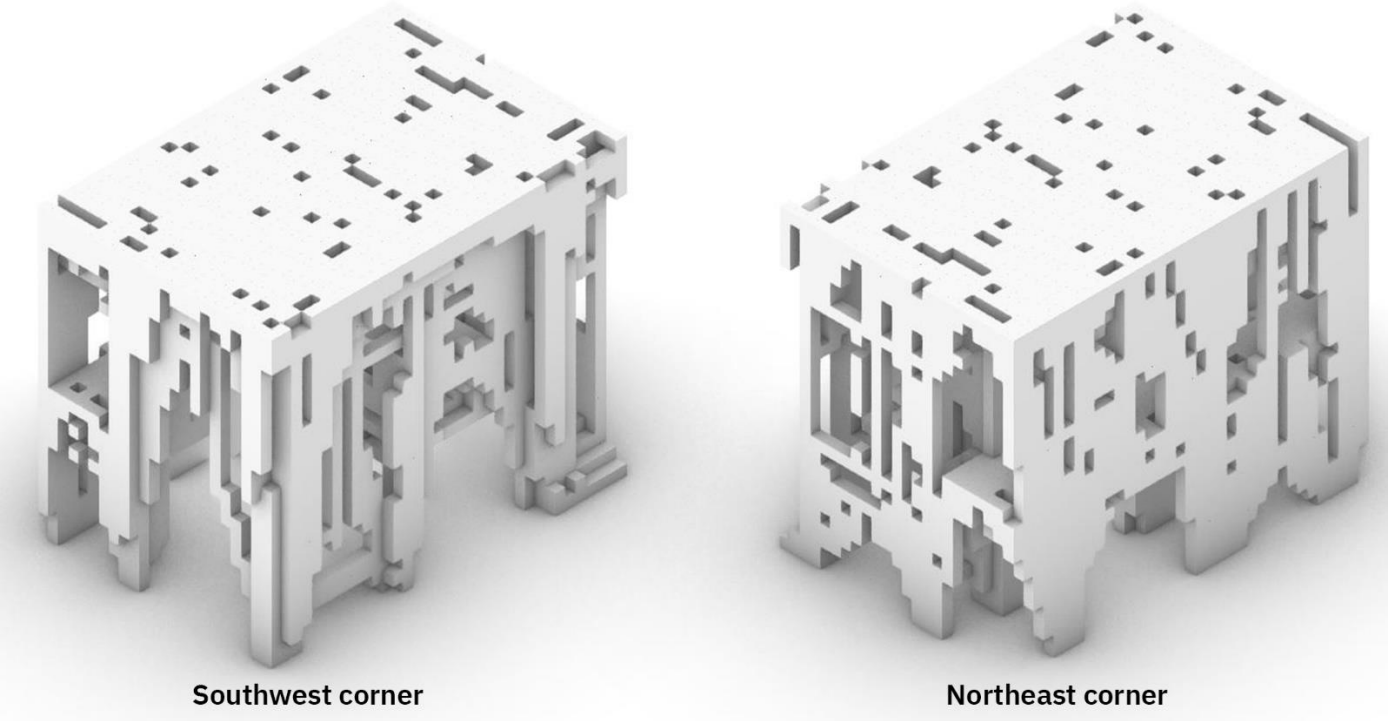

Figure 70: culling after **iteration 50:** min σ_{pr} /node=0/cm^2; max σ_{pr} /node=0.087kN/cm^2; avg σ_{pr} /node= 0.004kN/cm^2; Threshold= 0.0015 kN/cm^2 (46.5% of material remaining)

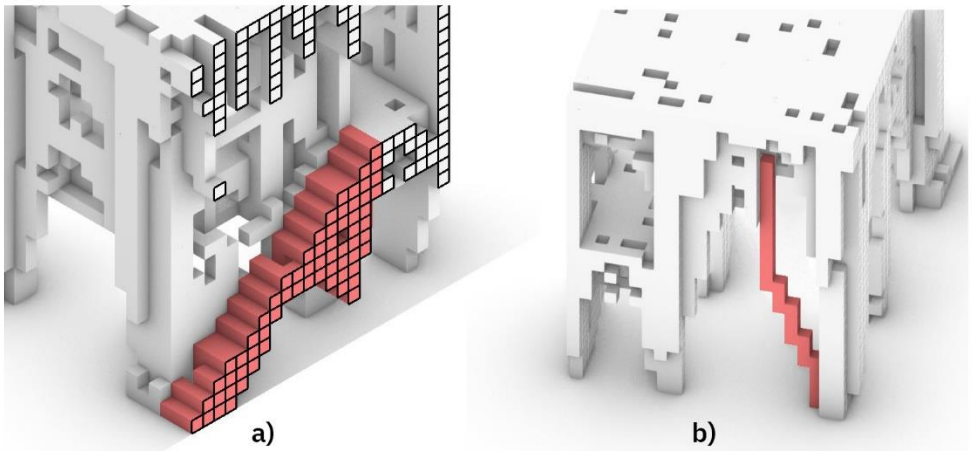

Figure 71. observed interesting features
a) staircase; b) branch-like columng

A visual comparison between the initial design space and the final result can be observed in Figure 72.

Figure 72. Relationship between the initial and final geometry; green-initial boundary of the design space; red-assigned voids.

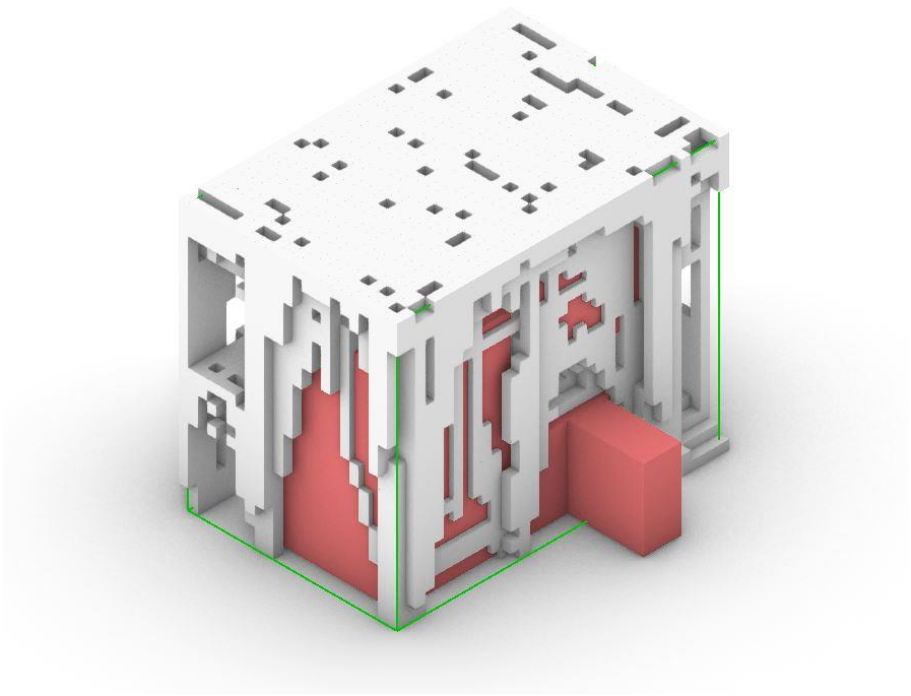

The following vertical and horizontal sections, and elevations provide a better overview of the obtained geometry. The horizontal sections have been taken at 1.5 meter intervals. The positioning of the vertical sections is illustrated in the floorplans (Figure 68).

Figure 73. vertical sections

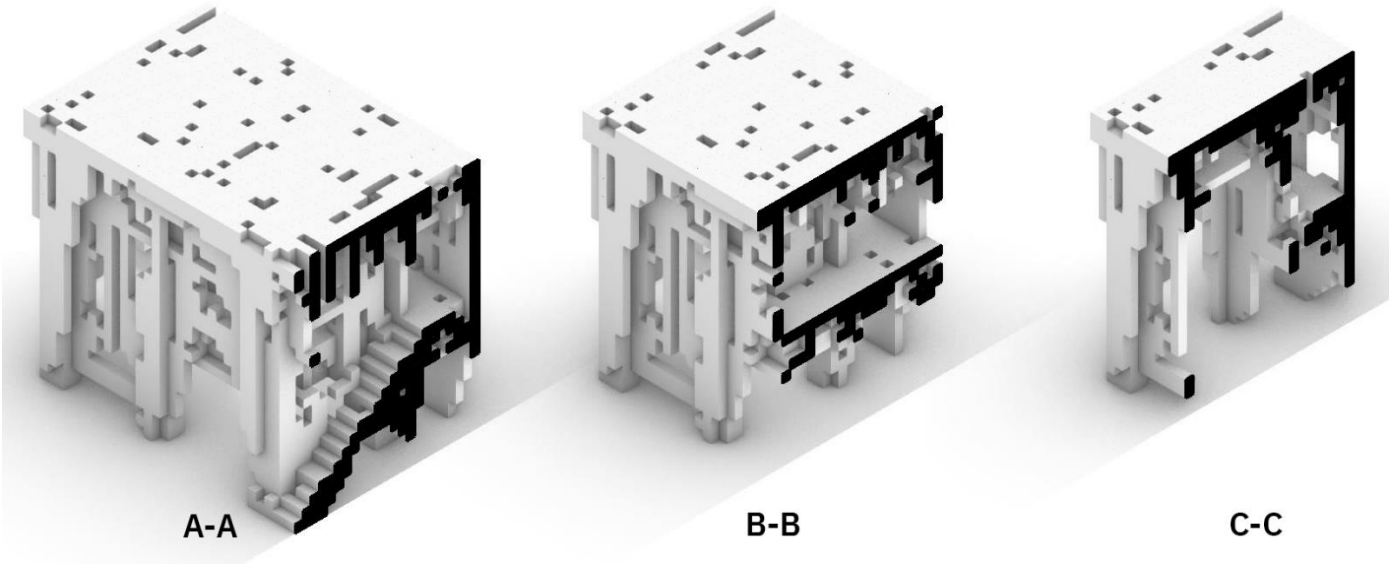

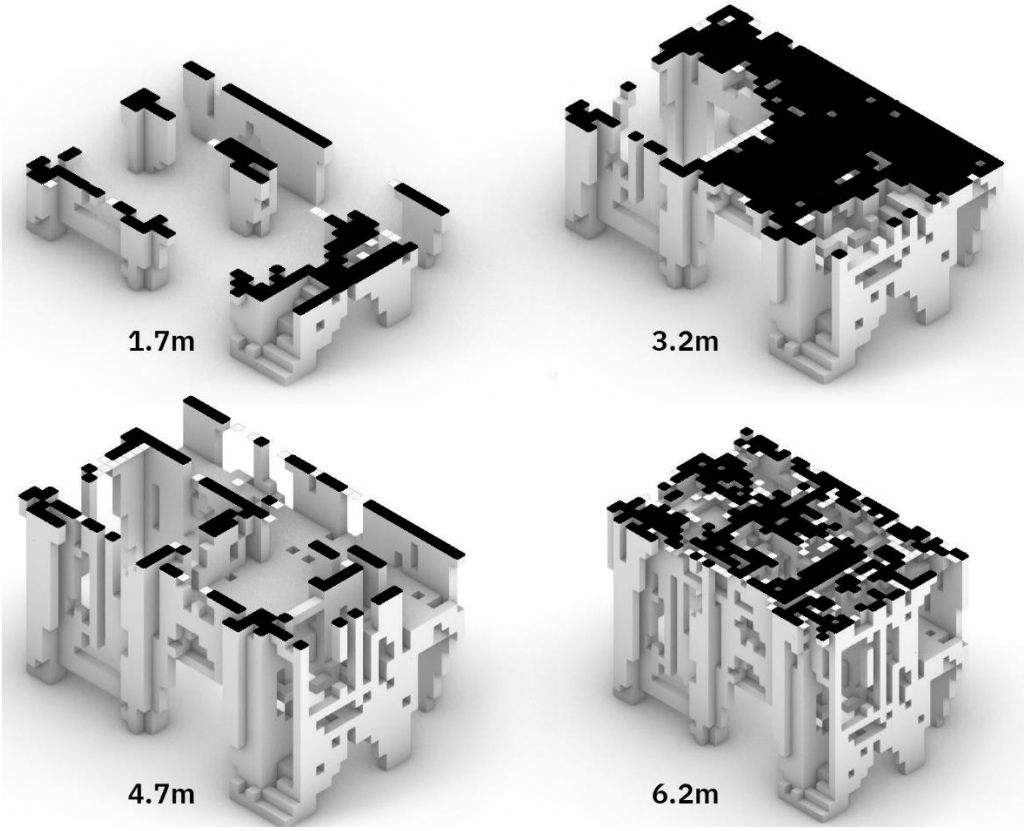

Figure 74. Horizontal sections through the topology optimization results for a complex house.

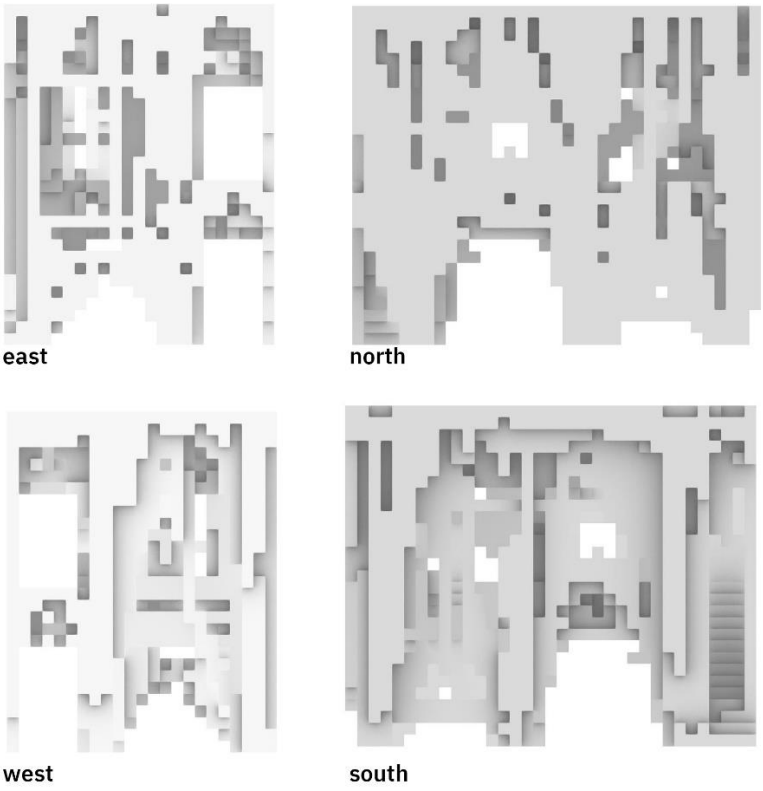

Figure 75. elevations of the complex house topology optimization results.

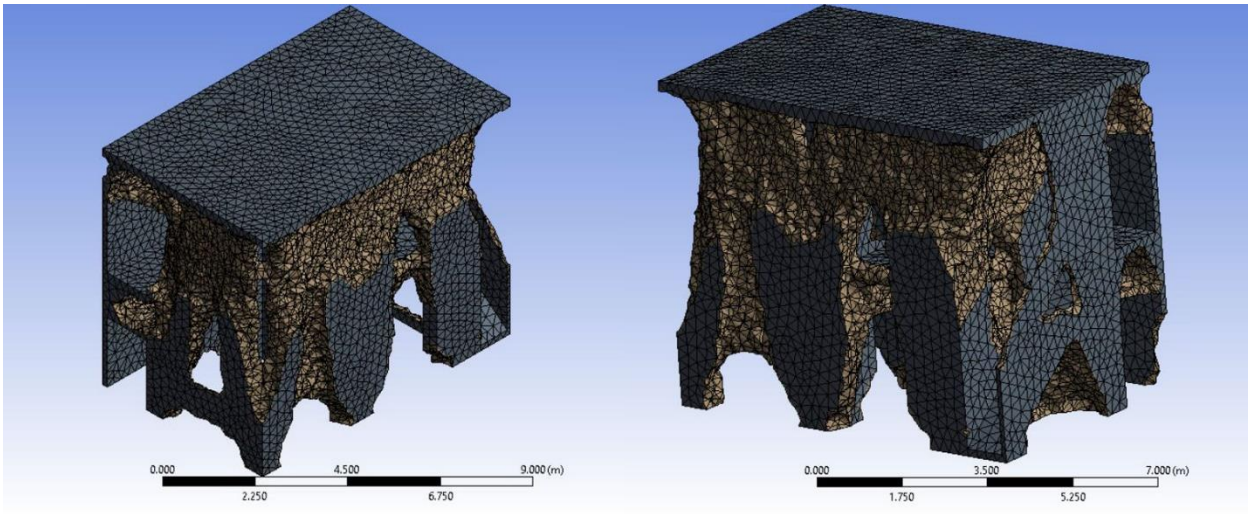

Figure 76. Ansys results for the case of a complex house. Left: southwest corner; Right: southeast corner

The design space was imported into ansys as a closed solid and was set up in the same way as the Grasshopper one. A topology optimization procedure was run using the SIMP method with the compliance minimization goal and 50% mass constraint. The obtained geometry bears some resemblances to the geometries obtained by the SKO method proposed by this research. The positions and sizing of the openings in the walls bear similarities between the two models. In contrast, the Ansys geometry does not have material removed from the roof area or the balcony area, which is not the case in the Grasshopper model. It would be beneficial to increase the resolution of the grasshopper model to gain a more detailed geometry, in order to gain a more detailed insight into the formal characteristics of the design.

04. CONCLUSIONS

"The more our world functions like the natural world, the more likely we are to endure on this home that is ours, but not ours alone". (Benyus, 2009, pp 20)

4.1 General conclusions

Research presented within this report is focused on the creation of a bio-inspired computational tool for early stage architectural form finding. The motivation behind proposing such a tool is the wish to help designers contribute to material savings within the construction industry, achieve sound structural performance design at an early stage and explore a different aesthetic of architecture. Towards achieving this goal several sub-objectives have been introduced.

The primary objective was the creation of a tool which brings biological postulates to the problem of designing stuctures. This objective has been met through the development a Grasshopper script which is based on the SKO and CAO methods for topology optimization proposed by Claus Mattheck. The algorithms for these methods were inspired by tree growth and adaptive bone mineralization, making them fall within the group of heuristic algorithms for topology optimization. These methods were chosen due to their intuitive nature and ease of application.

The Grasshopper script utilizes Rhino Grasshoper for the interface and geometry output. Integral to the script are Karamba3D and Hoopsnake componends which respectively play a role in performing the FEM analysis and creating a feedback loops which avoid Grasshoppers recursive loop avoidance checks. In addition, custom Python-scripted components were used for various mathematical calculations and manipulations of geometry. This allowed for achieving the research objective of creating a topology optimization method which would be integrated into the workflow of architectural designers.

A goal of creating a tool which would be intuitive for use was tackled by allowing the user to create the design space and input parameters through the manipulation of geometry rather than manual numerical input, as required by most commercial software. The usability of the tool with respect to time required is satisfactory. The time required for an optimization of a design space consisting of 33k elements is between 15-20 minutes. Based on this it can be noted that the tool can be used at a very early stage of the design process to produce a multitude of ‘sketch’ designs which would later be individually evaluated and taken into further development.

With respect to the objective of creating a method that works in both 2D and 3D cases several conclusions can be made. The three 2D TOY problems which were used for getting an understanding of the functionality of the tool produce results of satisfactory quality. Six different methods were tested on each of the TOY problems in order to gain insight into the settings and parameters that yield the

best results with respect to performance and apperel. By comparing the results with respect to their performance and appearance, as well as comparing with those obtained via a commercially available software Ansys, it can be concluded that the method yielding the best results is PR2. This method uses Principal Reference stress indicator and the local stress increment option for converting these reference stresses into the new distribution of the Young's modulus. The functionality of the method in 3D applications is still limited and unexplored. The results obtained for simple 3D problems like in the case of a ground floor house give valid indications about the behavior of the design space created by the user and provide reasonable solutions for more efficient use of material. For more complex problems the results become hard to interpret due to large discontinuations in geometry. These discontinuations in the form of checkerboard patterns are present in both 2D and 3D. The method can however still be greatly improved with respect to speed, accuracy, user experience etc. as will be elaborated in the recommendations section.

4.2 Applicability

This section of the conclusions is aimed towards answering the research question 'What kind of architectural design problems is the proposed method applicable to?' It should be noted that this question still remains open as this thesis did not explore the full range of application possibilities. Nevertheless, several possible directions can be suggested.

In the current state od development, the method proposed within this research can not be used for obtaining final designs which would be suitable for direct real life application. However several 2D and 3D design problems can be tackled.

For 2D design problems, the is applicable on a smaller and larger scale. Smaller scale application comes down to finding more befitting topologies for planar architectural elements such as walls, beams, slabs etc. much like other comercially available software. On a larger scale it could be used for architectural problems which could be abstracted into two-dimensional ones. A case in point would be the Akutagawa River Side office building from Takatsuki, Japan, where topology optimization has been used for coming up with a more materially efficient structural façade. This example hints towards a use in which building envelopes having a 0 Gaussian curvature could be developed and analyzed in twodimensional space onto which the load, and support conditions would be attached.

In 3D design challenges, a more refined and improved version of the tool could be used for form finding architecture which is constructed out of discrete modular elements or building blocks. These could include bricks, polymer boxes (Figure 77), readymade objects (Figure 78), or non cubic elements such as wooden pallets (Figure 79).

Figure 77. Serpentine Gallery Pavilion by BIG, London, UK, 2016. Constructed using GFRP boxes (source: dezeen.com)

Since bricks successfully carry only compressive loads, the method would have to be adjusted to prioritize compression only structures. Building blocks made from materials which could cake both compressive and tensile loads such as blocks created from GFRP or CFRP could be used in conjunction with the proposed method.

Figure 78. Recropolis by Refunc studio, Biddinghuizen, Netherlands, 2009. Structure constructed from 240 reused water tanks (source: refunc.nl)

Figure 79. Pallet temple by Refunc studio, Cairo, Egypt, 2017 (source: refunc.nl)

4.3 Recommendations

A number of recommendations could be suggested to both potential users of the tool and those interested in its further development.

Both groups should make note of the need to develop a better method for determining the appropriate values for the many variables such as the k, σ_{ref}, and the culling threshold. A more precise way which does not rely on trial-and-error testing would greatly increase the usability of the tool.

Currently, the proposed PR2 method produces results with visible checkerboard patterns. Therefore, introducing a logic for solving this phenomenon would greatly increase the functionality of the tool as it would ensure that the results are always a continuous structure and would require minimal post-processing.

Due to time constraints, the research did not get to a point at which the CAO method would be developed and tested. Development of the CAO method would yield even better results as it would solve the problem of local stress concentrations i.e. notch stresses.

As part of future development, the computational time should be adressed. This can partially be done by improving and cleaning up the code. Additionally, introducing a logic which would recognize symettrical design spaces could lead to a reduced calculation time as only half of the space could be analyzed. Alternatively, this would also allow for an increased resolution of the design, while retaining the same calculation time.

As concluded by the literature research, constrctability of topologically optimized designs plays a determining factor in their real-life application. Hence, it would be useful to further develop the method so that it takes constructability constraints into account.

Lastly, the current tool requires the design space to be discretized into a lattice of beams as a representation of a continuous space. This was done due to the fact that the FEM solver freely available only performs analysis on linear and shell elements. In this abstraction from continuous space to lattice the model looses on accuracy. It would be a great improvement if a custom volumetric FEM solver could be embedded directly within the Python code.

References:

Addis, B. (2016) In search of Some Principles of Bio-mimetics in Structural Engineering in Knippers et al. Biomimetic Research for Architecture and Building Construction(pp.90). Cham, Switzerland: Springer International Publishing

Altair Engineering, Inc. (2015) Danish Team Uses HyperWorks to Prove the Value of Topology Optimization for Concrete Architectural Structures. Retrieved from: https://www.altair.com/resource/detail/1195

ANSYS, Ansys 17.2 [Software]. Available from: ,http://www.ansys.com/., 2019 (accessed 15.09.19).

Baalen, V.S. (2017). Topology Optimised Pedestrian Bridge: A feasibility study in using Topology Optimisation as a design tool for bridge design (unpublished master's thesis). Retrieved from: repository.tudelft.nl/islandora/object/uuid:6184bd62-63d2-4929-ae94-7f549149f5a5?collection=education

Baumgartner, A., Harzheim, L., & Mattheck, C. (1992). SKO (soft kill option): the biological way to find an optimum structure topology. International Journal of Fatigue, 14(6), 387–393. https://doi.org/10.1016/0142-1123(92)90226-3

Bendsoe, M. P. (1995). Optimization of structural topology, shape, and material. Berlin : Springer (used in 2.5.3. Types of structural design optimisations)

Bendsoe, M.P. and Sigmund, O.(2003). Topology Optimization: Theory, Methods, and Applications. Springer, 2003. doi: 10.1007/978-3-662-05086-6.

Benyus, M. J. (2009). Biomimicry. Innovation inspired by Nature. New York City: Harper Collins Publishers L.L.C

Eggermont, M. ‘Interview with Julian Vincent’, Zygote Quarterly, Vol, 1, Spring 2012, p.26

Fuller, R. B. (1969). Operating manual for spaceship earth. New York: Simon and Schuster.

Gebisa, A.W., Lemu, H.G. (2017) A case study on topology optimized design for additive manufacturing. IOP Conf. Ser.: Material Science Eng. 276

Geyer P. and Rueckert K. (2005). Conceptions for MDO in Structural Design of Buildings. 6th World Congresses of Structural and Multidisciplinary Optimization, Rio de Janeiro, Brazil

Gosman, et al. (2013), Development of Cortical Bone Geometry in the Human Femoral and Tibial Diaphysis. The Anatomical Record., 296: 774-787. doi:10.1002/ar.22688

Grubor, P (2011). Biomimetics in Architecture:Architecture of Life and Buildings. Vienna: Springer Wien

Januszkiewicz, K., & Banachowicz, M. (2017). Nonlinear Shaping Architecture Designed with Using Evolutionary Structural

Vincent, J.F.V. (1997). Stealing ideas from nature. RSA Journal, Aug./Sept.,pp.36-43

Knippers J, Nickel K, Speck T (eds) (2016): Biomimetic research for architecture and building construction: biological design and integrative structures. Biologically-inspired systems, vol 9, Springer, Heidelberg, Berlin. https://doi.org/10.1007/978-3-319-46374-2Google Scholar

Mattheck, C. (1998). Design in Nature. Learning from Trees. Berlin: Springer-Verlag

Naboni, R., & Paoletti, I. (2018). Architectural Morphogenesis Through Topology Optimization. In D. D'Uva (Ed.), Handbook of Research on Form and Morphogenesis in Modern Architectural Contexts. Hershey, USA: IGI Global. https://doi.org/10.4018/978-1-5225-3993-3

Nagy, D (2017,Jan 24). Learning from Nature. Retrieved from http://medium.com/generative-design

Optimization Tools. *IOP Conference Series: Materials Science and Engineering*, *245*(8). https://doi.org/10.1088/1757-899X/245/8/082042

Ohmori, H., Iijima, T., Hasegawa, Y., Futai, H., & Muto, A. (2004). Structural Design of Office Building by Computational Morphogenesis. *International Journal of Technology and Design*, (20), 77–82. Retrieved from https://www2.le.ac.uk/offices/estates/information-for-estates-staff/dfp/downloads/Section15

Pawlyn, M (2016). Biomimicry in Architecture (2nd ed.). London: RIBA Publishing

Pohl, G., Nachtigall, W.(2015).Biomimetics for Architecture and Design. Springer International Publishing. ISBN 978-3-319-19119-5

Querin, O. M., Victoria, M., Alonso, C., Ansola, R., & Martí, P. (2017). *Topology Design Methods for Structural Optimization*. *Topology Design Methods for Structural Optimization* (1st ed.). Academic Press.

Rozvany G. I. N. (2009). A critical review of established methods of structural Topology Optimisation. Found in: Structural and Multidisciplinary Optimisation. DOI 10.1007/s00158-007-0217-0

Sigmund, O. (2001). A 99 line topology optimization code written in matlab. *Structural and Multidisciplinary Optimization*, *21*(2), 120–127. https://doi.org/10.1007/s001580050176

Sigmund, Ole. (2011). On the usefulness of non-gradient approaches in topology optimization. *Structural and Multidisciplinary Optimization*, *43*(5), 589–596. https://doi.org/10.1007/s00158-011-0638-7

Thompson, D. W. (1942). On Growth and Form. Cambridge: Cambridge University Press.

United Nations, Department of Economic and Social Affairs, Population Division (2017). World Population Prospects: The 2017 Revision, Key Findings and Advance Tables. Working Paper No. ESA/P/WP/248.

Vitruvius Pollio., & Morgan, M. H. 1. (1960). Vitruvius: The ten books on architecture. New York: Dover Publications. (used in 1.4.1

Wolff J.(1892). The Law of Bone Remodeling. Berlin Heidelberg New York: Springer, 1986 (translation of the German 1892 edition)

Xie, Y. M., Zuo, Z. H., Huang, X., Tang, J. W., Zhao, B., & Felicetti, P. (2011). Architecture and urban design through evolutionary structural optimisation algorithms. *Algorithmic Design for Architecture and Urban Design ALGODE TOKYO*, (November 2014).

Yang, X.S (2010). Nature-Inspired Metaheuristic Algorithms (2nd ed.). Frome: Luniver Press

Zuo, Z. H., & Xie, Y. M. (2015). A simple and compact Python code for complex 3D topology optimization. *Advances in Engineering Software*, *85*, 1–11. https://doi.org/10.1016/j.advengsoft.2015.02.006